Levelized Cost of Energy in Sustainable Energy Communities

A systematic approach for multi-vector energy systems

Miguel de Simón-Martín,

Stefano Bracco*,

Giorgio Piazza,

Luisa Carlotta Pagnini,

Alberto González-Martínez,

and Federico Delfino

*Corresponding author: stefano.bracco@unige.it

Foreword

Under preparation

Acknowledgments

We would like to express our special thanks to the following colleagues.

Jorge Blanes-Peiró, the head of the ERESMA (Energy Resources' Smart Management) Research Group from the University of León, who immediately supported the ERESMAGrid project and understood its potential in shaping the future as a living lab for the University of León and its technical studies portfolio.

Ana-María Diez-Suárez, Álvaro de la Puente-Gil and Enrique Rosales-Asensio, members of ERESMA, for their constant support, suggestions and general help in this and other related projects.

Luca Barillari and Paola Laiolo, members of the CenVIS Center, for their support in providing data about SPM and SEB facilities.

Giovanni Bianco and Mansueto Rossi, members of DITEN Department, for their suggestions about the operation of the SEB.

Levelized Cost of Energy in Sustainable Energy Communities

A systematic approach for multi-vector energy systems

Table of Contents

Levelized Cost of Energy in Sustainable Energy Communities

A systematic approach for multi-vector energy systems

INTRODUCTION

Introduction

0.1. Overview

The world is currently facing an energy revolution characterized by the paradigm change from a centralized and monodirectional energy system to a bidirectional one where distributed renewable and sustainable energy sources are more and more exploited. Moreover, stronger relations between different energy vectors, namely electricity, heat and cooling energy, are arising, contributing to more efficient and sustainable systems. Furthermore, energy communities are being promoted all around the world, especially in Europe, to lead the fight against the climate change by satisfying our energy needs in a sustainable and competitive way.

Although the "Energy Community" concept has been investigated for several decades, in order to provide energy to isolated or islanded systems, recently it has been presented as a sustainable way to provide energy in a more general context thanks to the massive introduction of distributed renewable power plants, energy storage devices and the improvement of monitoring and control systems, granting benefits to all the community members. Indeed, it is worth noting that microgrid and nanogrid installations are currently growing, due to their high flexibility and capability to be fed in a total or high amount, by Renewable Energy Sources (RES). This makes them a viable solution for the provision of sustainable energy at the urban, industrial and commercial levels. In the case of Europe, the Mediterranean countries, and in a prominent position, Spain and Italy, are taking a leading role in this paradigm change, although several steps must still be carried out to move in this direction.

0.2. Focus of the book

The success of the energy communities not only relies on technology development, where impressive improvements have been made in the last few years, but also in the economic feasibility. Otherwise, the sustainability of any project can be compromised.

It is well known that, in the power systems and energy management field, techno-economic decisions must be taken constantly. Therefore, decision tools are used to support project promoters, energy managers, policymakers, energy consultants and researchers to decide which systems are the most appropriate or in which systems the main investments should be made. One of the most reliable decision support tools is the Levelized Cost of Energy (*LCOEn*), as it provides realistic information on the costs involved in a certain energy system during its complete lifespan and allows the effective calculation of the investment sustainability.

Currently, the existing academic literature and technical reports on *LCOEn* are mainly focused on large power plants. Specific models for Energy Communities, i.e., microgrids and nanogrids, are not available yet. The *LCOEn* evaluation for microgrids and nanogrids sector must be considered with great attention and it will result of interest to both industry and academia.

0.3. Interest for readers

The main aim of this book is to provide a state of the art of the Levelized Cost of Energy calculation for energy communities from both a theoretical, defining a systematic analysis approach, and a practical point of view, providing results for three representative real case studies. To the authors' knowledge, the existing literature in this field does not address this issue yet. Then, **this book is intended for anyone interested in sustainability, energy projects design and RES integration**, but especially for:

- **Researchers and academics in energy economics, power systems and energy policies**, as it provides concise definitions of the *LCOEn* applied to the new emerging energy scenarios.

- **Energy projects promoters, power systems designers, energy companies' executives, facility managers and other related professionals**, as it presents practical examples of the *LCOEn* calculated for microgrids and nanogrids.

- **PhD and Master students in Electrical, Energy and Management Engineering courses**, as it includes a concise revision of the theoretical framework, up to date values for the main input parameters and an easy to understand methodology for calculating both the deterministic and probabilistic *LCOEn* in several scenarios.

0.4. Organization of the book

The book is organized into four main parts or chapters, which are briefly described here.

- **Chapter 1: The role of Energy Communities in the energy framework.** This chapter focuses the attention on the description and analysis of the energy communities both from the regulatory and technical points of view. The relevant role of microgrids and nanogrids to facilitate the spread of energy communities is highlighted, reporting the main definitions and types of microgrids and their parts. Moreover, the recent regulatory framework of energy communities in Europe and its implementation in Italy and Spain is analyzed in detail.

- **Chapter 2: The Levelized Cost of Energy indicator.** This chapter presents the definition of the *LCOEn*, its parameters, and its application to several energy systems, applying a systematic and rigorous approach. Then, the *LCOEn* and its variants (Levelized Cost of Electricity: *LCOE*, Levelized Cost of Stored Energy: *LCOS*, Levelized Cost of Heat: *LCOH*, Levelized Cost of Cooling: *LCOC* and Levelized Cost of Exergy: *LCOEx*) are presented, with special attention to the *LCOE* and the *LCOEx*. The *LCOE* has been widely used to compare utility-scale generation technologies but, in this chapter, its definition has been extended to combined generation and storage systems, polygeneration systems and electrical microgrids. Furthermore, to evaluate multi-vector energy systems, the concept of *LCOEx* is presented and defined.

- **Chapter 3: Application to real case studies.** The theoretical framework presented in the previous chapters is applied to three real existing case studies:

a thermal and electrical microgrid (the Smart Polygeneration Microgrid, in Italy), a thermal and electrical nanogrid (the Smart Energy Building, in Italy) and a pure electrical microgrid (the ERESMAGrid, in Spain). The three facilities are presented in detail and the *LCOE*, *LCOH*, *LCOC*, *LCOS* and *LCOEx* indicators are calculated according to the characteristics of each case, both for the integrated technologies individually and for the energy systems as micro/nanogrids. Moreover, a probabilistic approach has been adopted and a sensitivity analysis on the input parameters has been developed.

- **Chapter 4: Conclusions.** This chapter summarizes the general obtained conclusions, both from the analysis of the theoretical framework and the results of the analyzed case studies. Moreover, the main future research lines in this field are briefly depicted.

Finally, the appendix includes the used nomenclature, abbreviations and additional information for the interest of the reader.

0.5. About the authors

This book is the result of the active collaboration of the University of Genoa (Italy) and the University of León (Spain) in the field of sustainable and renewable microgrids. The authors have experience in the field of electrical engineering, microgrid design and operation, sustainability as well as civil infrastructures. The team of the University of Genoa has designed and currently manages the Smart Polygeneration Microgrid (SPM) and the Smart Energy Building (SEB) at the Savona Campus, whereas the team from the University of Léon operates the Laboratory on Electrical Systems and Smart Grids (ERESMAGrid) at the Vegazana Campus. Both microgrid projects are test-bed pilot facilities that constitute a reference point in the international scene. Thanks to the field experience, the two teams have carried out research activities on microgrids in collaboration with private companies and international research groups, acquiring competencies and know-how on the topic. Brief references of each author are presented next.

- **Miguel de Simón-Martín** is a Lecturer of Electrical Engineering at the University of León, Spain, and he has specialized in Power Systems, Energy Economics and Renewable Energy Sources. In 2011, he graduated cum laude in Industrial Engineering at the University of León and, since 2015, he holds an International PhD in Engineering from the University of Burgos, Spain. As a member of the Energy Resources' Smart Management (ERESMA) Research Group, he has joined and coordinated several R&D projects, both from public calls and private initiatives, and is the main author of several industrial patents and computer programs applied to the RES field.

- **Stefano Bracco** graduated cum laude in Management Engineering and received a PhD in Mechanical Engineering (Fluid Machinery and Energy Systems) at the University of Genoa, Italy, where he is currently an Associate Professor of Electrical Power Systems. He has been involved in many research projects in the energy sector at a national and an international level, funded by public authorities or private companies. He has been the technical officer of the University of Genoa for the project "Smart Energy Building" at the Italian Ministry for the Environment and Protection of Land and Sea.

- **Giorgio Piazza** is currently a PhD candidate of Electrical Engineering at the University of Genoa, working on the optimal design and operation of energy communities and microgrids. He is involved in national and European research projects and participates in the technical panel *Tariffs and smart charging* of MOTUS-E. He is an energy engineer with professional experience in designing small scale thermal and electrical power systems. In 2018, he graduated cum laude in Energy Engineering (M.Sc.) and was awarded the best M.Sc. thesis award "Ing. GB FERRARI" from the company ABB in the category *Smart grids, smart cities and sustainable mobility.*

- **Luisa Carlota Pagnini** graduated in Civil Engineering at the University of Genoa, received her PhD in Seismic Engineering at the Polytechnic of Milan (Italy) and

has been a Visiting Scholar at the Tokyo Institute of Polytechnics (Japan). She is a Tenured Professor in Structural Engineering at the University of Genoa and a member of the Giovanni Solari – Wind Engineering and Structural Dynamics Research Group (GS–WinDyn) that operates in interdisciplinary fields related to structural dynamics and wind engineering.

- **Alberto González-Martínez** graduated in Electrical Engineering from the Industrial Engineering School at the University of León and graduated in Industrial Engineering at the University of Valladolid, Spain. In 2016 he received his PhD in Engineering at the University of León, where he is a Lecturer of Electrical Engineering and member of the management board of the School of Mining Engineers since 2001 and 2007, respectively. He currently collaborates with the ERESMA Research Group, where he has joined and coordinated several projects from public calls and private initiatives related to Energy Savings, Energy Efficiency and Power Systems.

- **Federico Delfino** is a Full Professor of Power Systems Engineering at the University of Genoa where he is currently the Rector of the University. He has acted as Scientific Manager of several international and national innovation projects and committees dealing with the real demonstration of the concepts of Sustainable Energy and Smart City, in partnership with industry and institutional stakeholders. He is presently the Scientific Coordinator of the "Living Lab Microgrid" jointly operated by the Italian Electricity Company and the University of Genoa; the Scientific Coordinator of the demonstration project "Living Grid" within the Italian Technological Cluster on Energy (CTN Energia) and the President of the Scientific Research Committee of the Italian Association of Bank Foundations (ACRI).

0.6. Final remarks

The authors suggest as a general recommendation to have on hand the table of abbreviations and nomenclature for the readers help, although the nomenclature has

been chosen and applied in such a way it should be self-explicative. Readers interested only in the *LCOEn* calculation can omit chapter one. Finally, the authors apologize beforehand for the probable mistakes and misprints and will be grateful if they receive comments to improve this work.

Levelized Cost of Energy in Sustainable Energy Communities

A systematic approach for multi-vector energy systems

CHAPTER 1 – The role of energy communities in the energy framework

The role of energy communities in the energy framework

1.1. Introduction

In the present chapter the attention is focused on the role of the energy communities in the new energy scenarios. They are analyzed from the regulatory and technical point of view with a special attention to their implementation in Italy and Spain. Referring to technical aspects, the authors highlight the importance of microgrids and nanogrids to facilitate the spread of the energy communities. The chapter reports the main definitions and types of microgrids and describes the main subsystems which compose a microgrid, such as generation technologies or the operation and control systems.

1.2. Energy communities in Europe

"Energy Community" (EC) is a generic term indicating a set of consumers and producers which belong to the same legal entity (cooperative, consortium, association) with the aim of addressing together the energy supply process [1]. For historical reasons, energy communities have different shape and functionalities, according to the precise aim they were shaped upon. Minor islands, where the grid connection with the inland may not exist, are an intuitive example. In these cases, residents are likely to group together to address the energy supply process in a communitarian way, as shown in [2, 3], and renewables allow the residents to decrease their dependence from fossil fuels coming from the inland. In the same way, in mountain regions and rural areas, where for historical reasons the grid is not present, or unreliable, local communities can group together around a significant power plant located in the area, exploiting natural resources present in the region. Examples are reported in [4–6], where the exploitation of hydro and biomass resources allow satisfying electrical and thermal demands. All the previous cases have in common historical and geographical drivers to pursue a greater

energy reliability. All the members of the community are characterized by a physical proximity with one another and the energy distribution networks are often owned by these cooperatives.

In more recent years, a new form of energy cooperatives was born, the so called “virtual energy cooperative”, aided by a massive introduction of distributed renewable power plants and an improvement in IoT (Internet of Things) devices. The virtual cooperatives use the already existing distribution grid as a medium to operate as a unique entity, overcoming in this way the physical proximity constraints. In [7, 8], distributed renewable plants built in an associated way can grant benefits to all the community members. More information about ongoing energy cooperative initiatives around Europe can be obtained at the European federation of citizen energy cooperatives [9].

1.3. ECs from the regulatory point of view

In this section, ECs are analyzed from the regulatory point of view. The two main types of ECs introduced at the European level are described and some examples of how the concept of EC has been implemented in Italy and Spain are shown.

1.3.1. Renewable & Citizen Energy Communities

In this context, the European Union has decided to define and regulate two different declination of the energy community concept (Figure 1.1): the Renewable Energy Community (REC), regulated by the Renewable Energy Directive (RED II) [10] in 2018 and the Citizen Energy Community (CEC), regulated by the Electricity Market Directive (EMD II) [11] in 2019. These regulatory interventions aim to exploit energy communities as a driver to achieve the target of 55% of CO_2 emissions reduction by 2030, set in the Clean Energy Package for all European Citizens [12]. To reach this important goal, the renewable energy must reach 32% of the European energy mix in terms of final energy consumption [10], and the energy efficiency (generation, transmission, distribution, consumption) must reach 32.5% [13]. In this context, RECs and CECs can become significant contributors, increasing decentralized generation and enhancing the figure

of prosumers and active clients, representing therefore a source of system integration and high reliability.

Figure 1.1. EU Directives on Energy Communities.

RECs and CECs are based on open and voluntary participation of natural persons, small and medium enterprises (SMEs) and local authorities with the primary purpose to provide environmental, economic or social benefits for their shareholders or for the local areas where they operate. Although they both can produce, consume, share and store electricity, the main differences between the two definitions of EC are the energy vectors involved, the type of generation units accepted (RES or fossil), the proximity to the generation unit constraints and the activities which are allowed to perform, such as selling and buying energy, acting as a distributor or suppling Electrical Vehicles (EVs) charging services. In Figure 1.2, a scheme of the main differences between the two EC types are depicted.

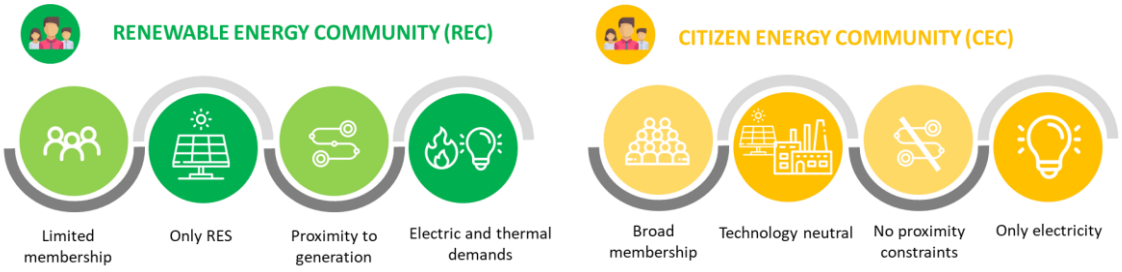

Figure 1.2. RECs vs CECs.

The EU directives define the general schemes, the aims and the most important constraints but leave the actual implementation to each Member State, which has to

implement within a specific time limit EU dispositions by means of national laws. In this way, the differences and peculiarities of each State are considered, but, at the same time, some discrepancies in the actuation rules may appear among different States. As an example, the EU Directive 2018/2001 states that every member of the community must be located in the proximity of the renewable energy projects that are owned and developed by the legal entity assumed by the REC. The concept of proximity is not further specified in the directive, thus leading to differences in the transposition into national laws. Several countries interpret proximity as a geographical distance, considering a maximum radius, the postal code or the cadastral reference, e.g. in France the peremeter to evaluate the collective self-consumption is 2 km radius [1]. Others, such as Spain, also refer to a "technical" or "electrical" distance, assuming two members to be in proximity if they are connected to the same secondary transformation substation of the national distribution grid.

In Figure 1.3 the timeline of implementation of the two directives for the different Member States is summarized. Belgium was the first to introduce the concept of "communautés d'énergie renouvelable" or renewable energy communities in the Decree of 30 April 2019 [14], followed by Portugal and France, the latter having introduced also the concept of CEC. Italy has followed with the national law 28/02/2020 n.8 [15] introducing the concepts of REC and the renewable energy collective self-consumers. For what concerns Spain, it was one of the first to define renewable energy collective self-consumers through the Royal Decree 244/2019 [16], which allows different customers of the same neighbourhood or industrial district to benefit from the generation of a renewable power plant located in their proximity. It must be also noted that the self-consumption was already mentioned in the Spanish Electricity Sector Law, Law 24/2013 [17], and included as a specific measure for the protection of electricity consumers by the Royal Decree-Law 15/2018 [18]. During 2020, the Spanish government in the "Plan Nacional Integrado de Energía y Clima 2021-2030" [19] has stated its willingness to introduce the appropriate national normative framework to juridically implement RECs and CECs and entrusted this responsibility to the Ministry of the Environment and IDAE (the energy authority of the Country). Moreover, in the recent

Royal-Decree Law 23/2020 a general REC definition has been introduced recalling the EU Directive 2018/2001.

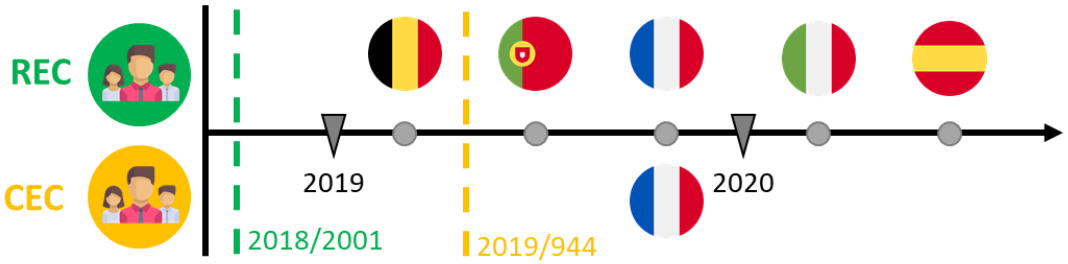

Figure 1.3. Timeline of the national implementation of the EU directives.

1.3.2. Italian provisional implementation of RECs

Focusing the attention on Italy, as mentioned, the concepts of renewable energy collective self-consumers and renewable energy communities were addressed by a national law [15] and by the publication of the technical rules [20] by the national energy authority (ARERA - Italian Regulatory Authority for Energy, Networks and Environment) in the last days of 2020. The defined rules are still provisional and it is expected that they will be confirmed or revised by the end of 2021. The renewable energy collective self-consumers are defined as a group of customers being in the same building, as depicted in Figure 1.4, able to share the energy coming from a RES plant with a peak power lower or equal than 200 kW_p[1] (peak power[2]). As an example, if a new photovoltaic plant is placed on the roof of the building and connected to the distribution grid of the condominium, the following quantities can be defined for every time interval:

[1] According to the Italian Legislative Decree of the 4th of November 2021, which reports the final implementation of 2018/2001/EU Directive, the maximum peak power of each plant belonging to an italian renewable collective self-consumption scheme has been increased from 200 kW_p to 1 MW_p.
[2] In solar photovoltaics (PV), peak power refers to the rated DC power provided by a PV field under standard test conditions (STC), which are characterized by an incident effective irradiance of 1 kW/m^2, an ambient temperature of 25 °C and an Air Mass index (AM) of 1.5.

- the renewable energy which is self-consumed, given by the minimum between the production of the photovoltaic plant (yellow flow) and the demand of the common services of the condominium (blue flow);

- the renewable energy which is collectively self-consumed, given by the minimum between the surplus of renewable energy which is injected into the grid (red flow) and the sum of all the consumptions of the renewable energy collective self-consumers (green flows).

It must be noted that there is a substantial difference between the renewable energy which is self-consumed and the one which is collectively self-consumed. In the first case the energy goes from the producer to the consumers using a proprietary internal network (blue line). This means that the energy which is self-consumed comes entirely from the renewable energy source production plant, thus not being subjected to any kind of taxations nor specific tariffs. On the other hand, the energy which is collectively self-consumed is actually retrieved by the distribution grid (black line) at different prices depending on the specific contract between each consumer and its energy seller company. Then, each consumer will retrieve a part of their cost thanks to the national incentive currently in force, set at € 100 /MWh of renewable energy collective self-consumed and valid for twenty years. Moreover, the collective self-consumers have the possibility to sell the surplus of renewable energy at the hourly zonal price to the national energy service manager (GSE) by means of the dedicated withdrawal scheme called “ritiro dedicato” (dedicated withdrawal). In Italy, the GSE acts as a national common and unique collector of energy coming from renewable plants, collecting the energy and selling it through the national electricity market. It remunerates the RES plant owners following a predetermined scheme, which may involve a fixed tariff or a variable one, depending on the results of the electricity market.

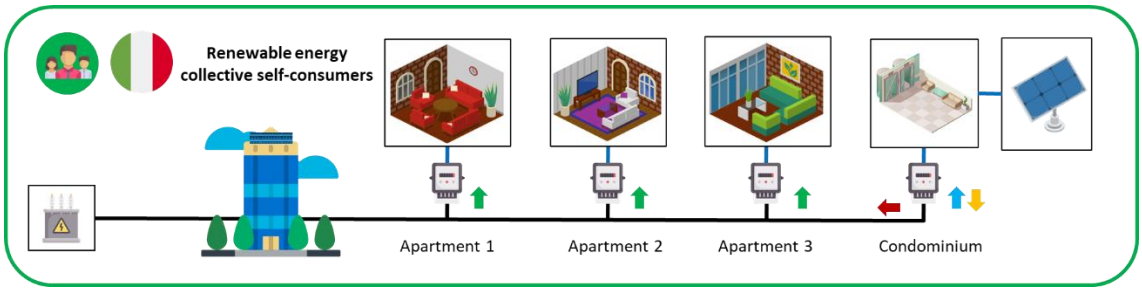

Figure 1.4. Italian scheme of the renewable energy collective self-consumers.

On the other hand, RECs must involve several subjects belonging to more than one building with the above-mentioned limitation of being connected to the same secondary substation[3]. In this way, the proximity constraints are also respected, but all the MV (medium voltage) customers are completely cut off from the possibility of joining the community. In Figure 1.5, an example of a simple Italian REC is depicted; as can be noted, the scheme is fairly similar to the previous one with some minor differences. In the case of an Italian REC, there can be several production plants with a peak power lower or equal than 200 kW_p[4] for each plant. As before, the following quantities can be defined for every time interval:

- the renewable energy which is self-consumed, given by the difference between the production of the photovoltaic plant (yellow flow) and the demand of the condominium (blue flow);

- the renewable energy which is shared by the community, given by the minimum between the energy which is injected into the grid (red flow) and the sum of all the consumptions of the renewable energy community (green flows).

As mentioned for the previous case, there is a substantial difference between the energy which is self-consumed and the energy which is shared within the community. The

[3] According to the Italian Legislative Decree of the 4th of November 2021, which reports the final implementation of 2018/2001/EU Directive, the proximity constraints for REC has been expanded from the secondary to the primary transformation cabin, therefore the MV users are now eligible to join an Italian REC.

[4] According to the Italian Legislative Decree of the 4th of November 2021, which reports the final implementation of 2018/2001/EU Directive, the maximum peak power of each plant belonging to an Italian REC has been increased from 200 kW_p to 1 MW_p.

shared energy is a fictious economic term and, analogously to the collective self-consumed energy, it is retrieved directly from the distribution grid (black line) at different prices, depending on the existing contract with the energy providers. Each consumer will then retrieve a part of the expenses through the incentive currently in force for the shared energy, currently set at € 110 /MWh and valid for a period of twenty years. As for the previous case, the possibility to sell the renewable energy at the hourly zonal price of the electricity market to the national energy service manager (GSE) still remains.

As it can be noted, both the Italian renewable energy collective self-consumers scheme and the REC one involve the use of the already existing distribution grid (black line). In this sense, the REC can neither distribute electricity to all its members nor collect the production from all its producers, being only the owner of the renewable generation power plants.

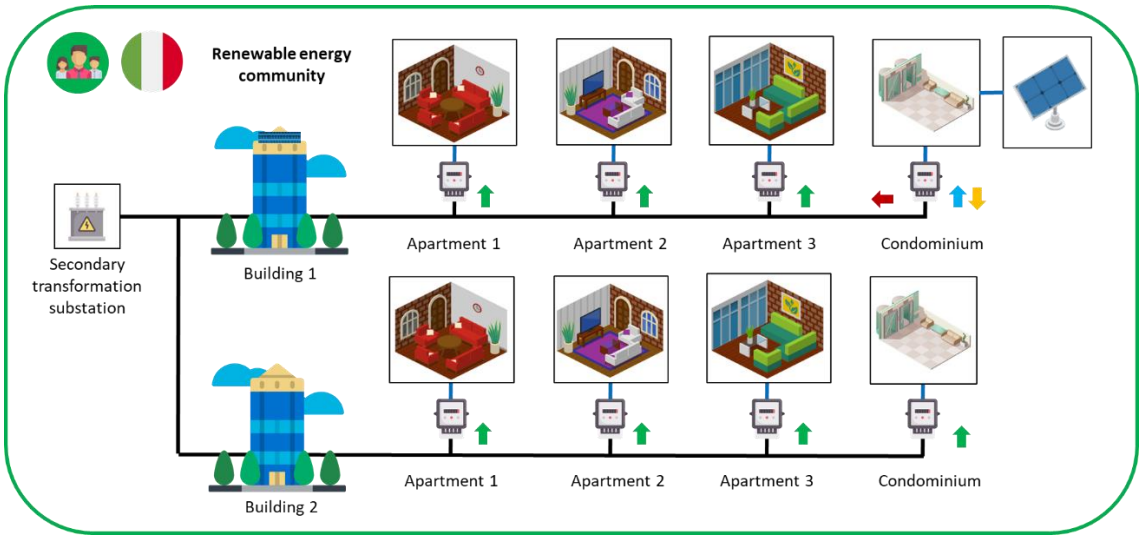

Figure 1.5. Italian scheme of a REC.

1.3.3. Spanish Implementation of RECs

Focusing the attention on Spain, as already mentioned, the Royal Decree 244/2019 [16] has defined the possibility to establish an “autoconsumo colectivo” when a number of several consumers are fed in an agreed manner by different renewable plants located

in their proximity. The connection among the collective consumers can be of two types: a direct connection using a proprietary internal grid, or using the already existing distribution grid. This second case is possible only if at least one of the following conditions is satisfied:

- the connection of all the collective consumers must be at low voltage level with the same secondary transformation substation;
- both generation plants and consumers must be located at a distance lower than 500 meters, measured in orthogonal plain projection between the equipments of measure;
- power units and associated consumers must be located in the same land registry reference, i.e., the first 14 digits coincide (with the exception of autonomous regions with their own land registry regulations).

The renewable collective self-consumers can join different schemes established in the RD 244/2019 and better detailed in the technical rules established by the IDAE guide for self-consumers [21], as follows:

- **Collective consumption without surplus**: in this configuration (Figure 1.6) the collective self-consumers own a system which blocks any kind of injection into the national distribution grid (black line). The consumers are linked by a proprietary internal grid (blue line). The collectively self-consumed energy is defined as the minimum between the hourly generation (yellow flow) and the sum of the individualized hourly self-consumption (green flows). When the PV production is higher than the overall consumption, the collectively self-consumed energy is equal to the overall consumption and the excess production is curtailed. On the other hand, when the PV production is lower than the overall consumption, the collectively self-consumed energy is equal to the PV production.

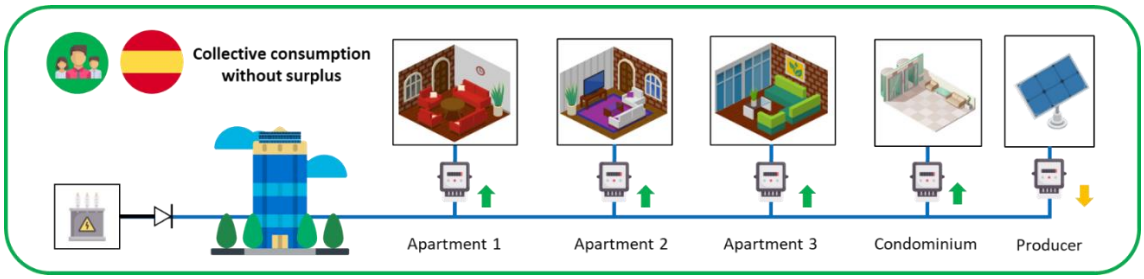

Figure 1.6. Spanish scheme for the collective consumption without surplus.

- **Collective consumption with compensation for the surplus**: the consumers must be connected through a proprietary internal grid (blue line) and, in case of excess of PV production, the energy which is not collectively self-consumed will compensate part of the energy obtained from the distribution grid (black line) at a later time by all the collective members at either an agreed tariff or at the average hourly market price minus the deviation costs ("PVPC autoconsumo"), as depicted in Figure 1.7. It must be noted that the maximum compensation is the cost of the energy purchased from the grid (negative compensations are not allowed). The collectively self-consumed energy is defined as in the previous case, but in this case the excess production (outgoing red flow) can be traded with the one coming from the distribution grid at a different time interval (incoming red flow). The compensation balances are set monthly. Moreover, the production plants must have a maximum power lower or equal than 100 kW[5].

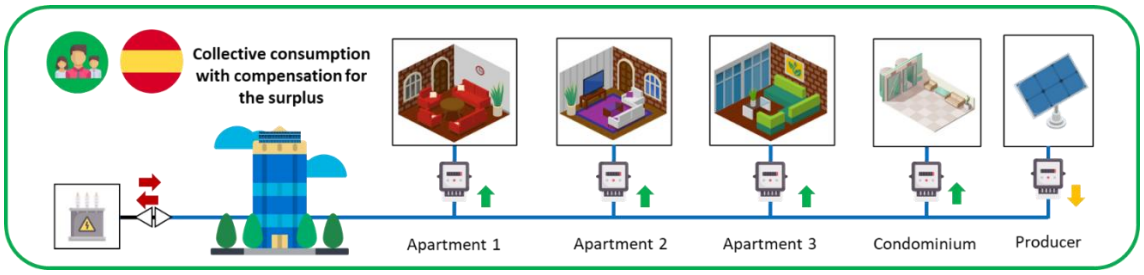

Figure 1.7. Spanish scheme for the collective consumption with compensation for the surplus.

- **Collective consumption with no compensation for the surplus**: the consumers must be connected through the distribution grid (black line in Figure 1.8) from

[5] It must be highlighted that the rated power for PV facilities in Spain is the maximum rated power of the power inverter, not the peak power of the PV field.

the same secondary transformation substation and in geographical proximity as stated before. The energy collectively self-consumed is the minimum between the hourly generation (yellow flow) and the sum of the individualized hourly self-consumptions (green flows). Furthermore, in this specific case the excess renewable production is owned by the producer who can sell it on the electricity market through an intermediary.

In all the Spanish configurations the collective self-consumed energy is equal to the self-consumed energy of the Italian case, thus not being subjected to any tariffs. This is a substantial difference between the two national approaches making the Spanish way more appealing to the collective self-consumers, who have greater economic advantages. On the other hand, the Italian approach is more conservative and aims to maintain, as much as possible, the revenues coming from taxes and system costs applied to the energy bills.

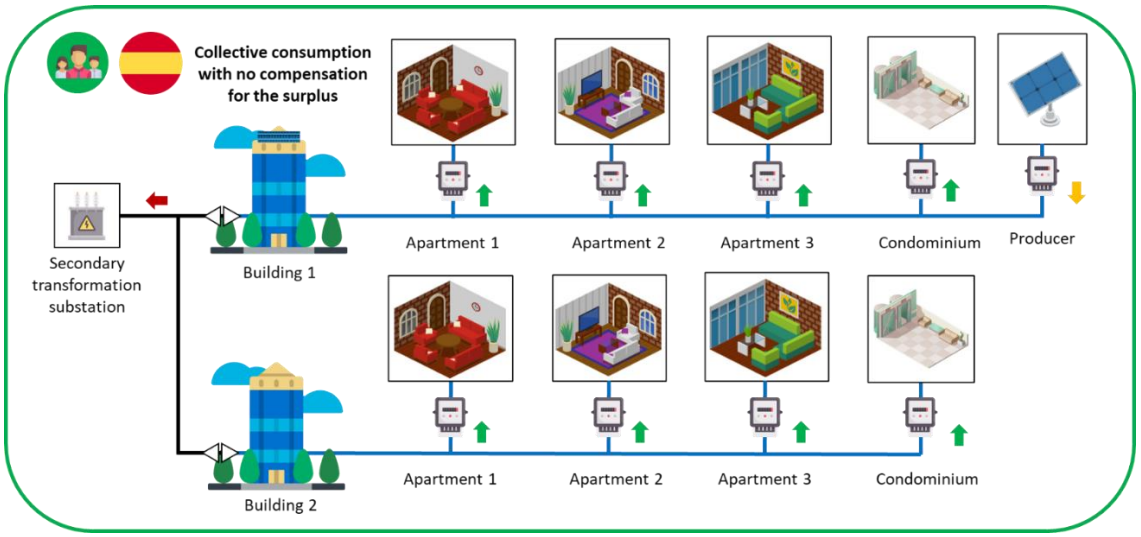

Figure 1.8. Spanish scheme for the collective consumption with no compensation for the surplus.

As can be deduced, the implementations considered by the two State Members present similarities and discrepancies, but the main direction is the same. Nevertheless, the regulatory framework is still developing in both countries and it will certainly change in the near future to better adapt to the practical problems which will arise during their implementation.

1.4. Microgrids and Nanogrids

The application of the EC concept is based on the implementation of microgrids and nanogrids, both characterized by the presence of energy prosumers and smart loads [22–25]. In this section, the most important technical aspects of the aforesaid technologies are analyzed and critically discussed.

1.4.1. Definitions and main characteristics

The spread of distributed generation facilities and the implementation of the microgrid concept has strongly facilitated the development of ECs. Indeed, an EC includes different dispersed power generation technologies and, sometimes, it consists of a group of microgrids which exchange energy. It follows the importance of defining what is a microgrid and when a microgrid can be considered a nanogrid.

Among the many existing definitions of the microgrid concept, the most representative one is reported by the U.S. Department of Energy (DOE) and cited in [26]. According to the DOE, a microgrid is "a group of interconnected loads and distributed energy resources within clearly defined electrical boundaries that acts as a single controllable entity with respect to the grid. It can connect and disconnect from the grid to enable it to operate in both grid-connected or island mode". This definition introduces several features which can be further discussed:

- In a microgrid we find both loads and generators. Loads can be either manageable or non-manageable, whereas power plants can be fed by either renewable sources (mainly solar, wind, biomass and hydro) or fossil fuels (above all natural gas). A microgrid can also include prosumers which are entities able to consume and locally produce energy; nowadays, Zero Energy Buildings (ZEBs) constitute a very interesting application of the concept of prosumer.
- A microgrid must be characterized by clearly defined physical boundaries, that is by a unique Point of Common Coupling (PCC) with the external grid, which is typically represented by the low or medium voltage public distribution network.

The PCC identifies the physical connection which permits to exchange energy in both directions with the public network managed by a specific Distribution System Operator (DSO). The microgrid can buy electricity when the local production is lower than the loads, and sell electricity when a surplus local production occurs. By this way, the microgrid can offer services to the electric system through the participation to Ancillary Service Markets (ASMs). It is important to remark that there are countries where the regulatory authority does not permit to inject power into the public grid under certain conditions, thus making the exchange at the PCC interface to be only monodirectional.

- A microgrid can be also operated in islanded mode, i.e. disconnected from the public grid. It is not simple to operate an islanded microgrid, since this needs to have devices able to control frequency and voltage, but it can lead to technical and economic advantages, especially when the main public grid presents criticalities and weakness points.

There are full electric microgrids with only electrical loads, electrical storage batteries and power plants producing and storing electricity, and multi-vector microgrids where electrical, thermal and cooling energy are produced, consumed and exchanged. Considering that the microgrid concept is more and more applied in residential and tertiary sectors, the presence of buildings to be also heated and cooled implies the need of installing multi-vector microgrids, often called « hybrid microgrids ». In these facilities, different energy vectors can be used: electricity, natural gas, hydrogen, warm and chilled water, etc. Moreover, with the increase of electric vehicles in our cities, in many cases microgrids host EV charging infrastructures (slow, quick and fast chargers) as well as vehicle-to-grid (V2G) technologies. With the application of V2G devices, EVs become non-stationary electrical storage systems and can be easily used to compensate the variable production of renewable sources and to smooth the load profile of buildings [27].

Polygeneration microgrids constitute complex systems where electrical and thermal devices interact to provide energy to different users with the goal of maximizing the use of renewable sources, and thus reducing the environmental impact of the energy supply.

Next to power generation and consumption technologies, a microgrid is also characterized by the presence of electrical networks (made of cables, substations, transformers, protection systems, etc.) and pipelines (the so called distributed heating and cooling networks) to convey warm and cold water and/or air to end-users. A complex ICT (Internet and Communication Technologies) infrastructure is adopted to control and manage a microgrid. This means a set of devices (smart meters, fiber-optic cables, remote terminal units, etc.) and sotware tools (SCADA system, Energy Management Systems, forecasting algorithms, etc.) used to real-time monitor, operate and control power plants, storage systems and loads. Consequently, in a microgrid, different domains coexist (mechanical, electrical, ICT, social, environmental, economic, etc.) and different skills are required to manage all the aforesaid components. Therefore the main components of a microgrid are:

- Generation plants (electrical/thermal/cooling energy, renewable/fossil sources);
- Loads (manageable/non-manageable, electrical/thermal);
- Storage systems (electrical/thermal);
- Networks (electrical/thermal/cooling);
- Power conditioning systems (inverters, etc.);
- Smart meters and ICT infrastructures;
- Optimization tools (EMS – Energy Management System);
- Smart appliances;
- Electric mobility systems (vehicles and charging infrastructures).

As far as the application of the microgrid concept is concerned, the main sectors where microgrids can be found are:

- Industrial sector (manufacturing companies, industrial parks);
- Commercial sector (malls);
- Residential sector (new districts);
- Tertiary sector (hospitals, ports, sports and leisure areas, office buildings, etc.);
- Public sector (schools, university campuses, military compounds, administrative headquarters, etc.).

All the aforesaid areas represent users characterized by the need of electrical and thermal energy which can be supplied in a sustainable way by a microgrid. Obviously, it is not simple to build a microgrid supplying a residential building in a historical centre (e.g. due to technical and regulatory constraints related to the installation of renewable power plants and pipelines). New districts (built in former industrial areas or green fields) constitute one of the best areas where a microgrid can be installed. This is due to the fact that, typically, a new residential district is composed of several buildings (condominiums and detached houses) and attains an electrical power demand of tens or hundreds of kW which best fits with the sizes of generation technologies available on the market. The installation of a microgrid in a critical facility, such as a hospital or a military compound, permits to increase the reliability of the energy supply, and when operated in islanded mode, guarantees the self-provision of energy even for long periods, if well designed. In schools and universities, microgrids can be also used for teaching and research purposes and the active participation of the final users in the microgrid daily operation can lead to increase the people awareness of this new technology, thus contribuiting to its spread also in the private sector. Many university labs develop research activities with private companies in order to test new devices and innovative control systems for their microgrids.

Mainly due to the still high capital costs of several components, nowadays, most of the microgrids are installed in remote areas with limited grid access, in places characterized by weak distribution networks and for R&D aims in research centres. However, new interesting microgrid projects are ongoing in renovated urban areas to increase the aggregation of distributed generation units and their combination with flexible demand, energy storage systems and electric mobility. Moreover, considering the widespread people's awareness on sustainability and the Digital Utility transformation (IoT and Big Data), microgrids are becoming one of the main pillars of smart cities.

To better understand the role of microgrids within power systems, some considerations can be drawn on Figure 1.9, which reports, in a very schematic way, the architecture of the electrical system of a developed country in a very near future [22]. There will be microgrids connected to MV distribution networks and installed in industrial and urban

districts as well as microgrids of smaller size connected to low voltage (LV) distribution networks. In the latter case new urban districts will be characterized more and more by the presence of smart buildings acting as energy prosumers. Renewable power plants could be connected to different voltage levels as a function of their size and location, whereas large size power plants, such as combined cycles, nuclear stations and hydro plants will transfer their production toward the high (HV) and very high (VHV) voltage transmission networks. Slow and quick charging points for EVs will be typically connected to LV networks while fast and ultra-fast charging stations will withdraw power from MV networks. Smart districts at urban level will be also equipped with district heating and cooling networks always present in multi-vector energy systems.

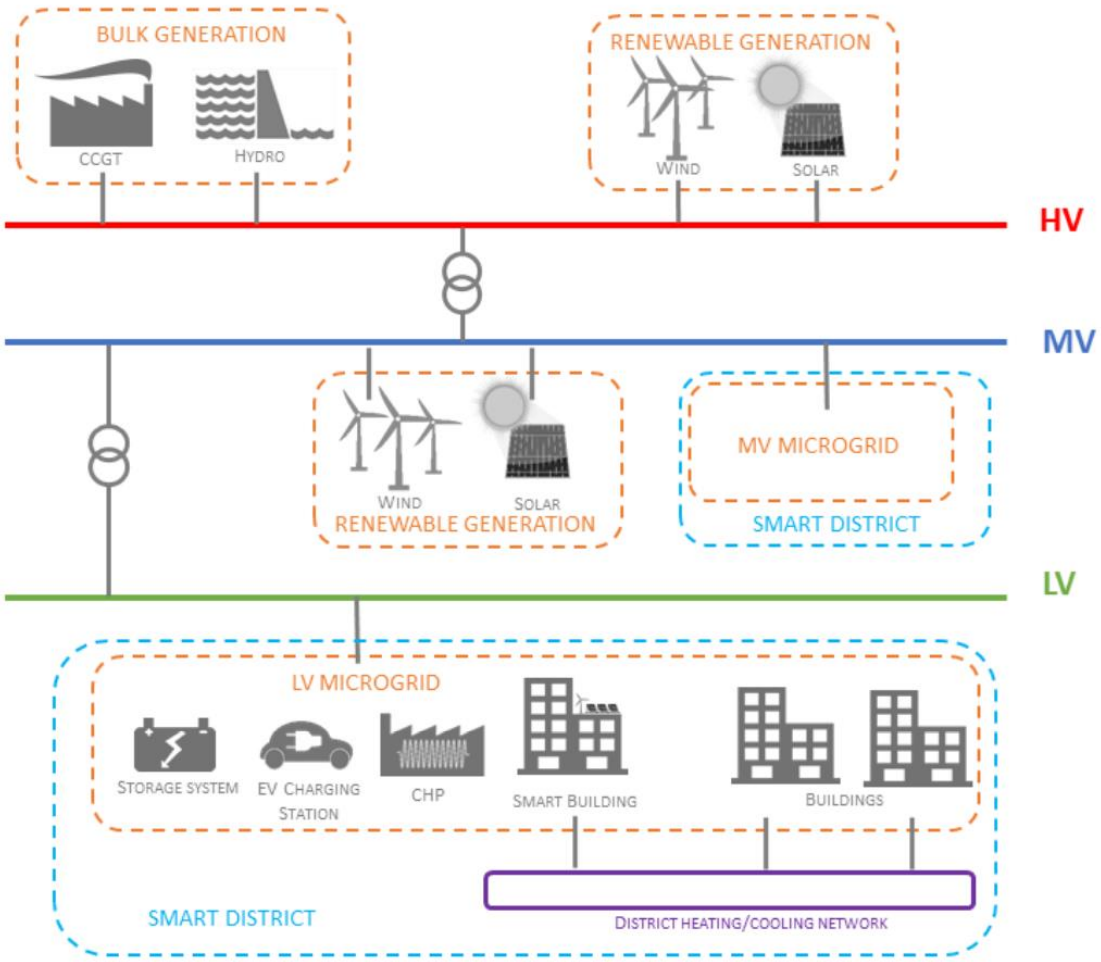

Figure 1.9. Current deployment of microgrids in developed countries.

When a microgrid is designed for a single building or a detached house it is better to name it "nanogrid" [28], even if the use of the term "microgrid" still remains valid. The main technologies installed in a nanogrid are: renewable power plants for electrical production (photovoltaic panels, micro wind turbines), thermal and cooling power production units (thermal solar collectors, heat pumps, boilers, electric heaters, absorption chillers), cogeneration engines and microturbines, and wall boxes for EV charging. On the other hand, as aforesaid, a microgrid is typically used to provide energy to several buildings, a factory and other wider areas. While in a nanogrid power plants are always integrated with the building (installed on the roof or inside utility rooms), in microgrids, power technologies can be either installed in the buildings (decentralized configuration) or within a dedicated area (centralized configuration). Considering the recent European regulations and targets on energy efficiency and the implementation of the EC concept, most of the new sustainable buildings in our cities will be energy prosumers in a near future and, in a certain way, could be considered nanogrids. However, it is important to highlight that to be a prosumer does not mean to be a nanogrid. Indeed, a bulding acting as a prosumer can be considered as a nanogrid when all the installed devices (loads and generation plants) are managed by a controller, specifically, a Building Management System (BMS), which operates as the EMS of a microgrid but with additional features, such as the control of the confort level inside the building and other functionalities [29].

1.4.2. Technologies for electrical energy production

The most common technologies used to produce electrical energy in microgrids are photovoltaic panels, micro and mini wind turbines (WTGs) and small size hydro power plants. In urban districts, solar and wind technologies prevail while in remote areas the exploitation of hydro resources also play a crucial role. On the other hand, in nanogrids PV installations are predominant.

PV power plants are mainly based on the use of Silicon wafers or “thin-film” technologies. Different structures of the semiconductor material can be adopted: “mono-crystalline”,

"multi-crystalline" (also known as "poly-crystalline") or "amorphous" material. As far as the installation is concerned, there exist rooftop PV systems mounted on residential buildings (3-20 kW_p), rooftop PV systems mounted on office or commercial buildings (also > 100 kW_p), PV systems on ground. In microgrids connected to the distribution network, PV plants act as grid-connected systems whereas in some remote installations (both in islanded microgrids and nanogrids) it is common to find stand-alone PV plants coupled with storage systems. The energy production of a PV field depends on many factors, such as: the surface area of PV modules and their orientation (azimuth and tilt angles), the solar irradiance (that is a function of the season, the time during the day, and the latitude of the site), the efficiency of the cells, the efficiency of the BoS (Balance of System), the ambient temperature, the cleanliness of the solar modules, shading effects, mismatch losses, etc. Nowadays on the market there are Silicon panels having a rated efficiency higher than 22% and a peak power around 400-500 W_p. New solutions based on transparent PV panels and flexible materials represent a valid choice when particular constraints on the building integration of PV arise.

International Electrotechnical Commission (IEC) Standards on the design requirements for small wind turbines [30] consider "small wind turbines" those with a rotor swept area smaller than 200 m^2; this means a diameter lower than 16 m and a rated power lower than 75 kW. WTGs typically installed in microgrids are characterized by a rated power lower than the aforesaid value, while in nanogrids we can find micro wind turbines with power output values of a few kW. As a function of the specific location (gusty conditions, available space, safety and maintenance requirements, etc.) it is possible to choose if it is more favorable to install a Vertical Axis Wind Turbine (VAWT) or a Horizontal Axis Wind Turbine (HAWT), taking into account not only capital and operating costs, but also evaluating the expected power production. HAWTs are more efficient, as the technology is the one in use for larger size ones. VAWTs have few movable parts and, therefore, lower maintenance costs; moreover, they have proved to be less exposed to gusts and wind fluctuations [31, 32]. However, the installation of small size wind turbines in the urban context often presents several criticalities [33]. They usually have lower performance in terms of efficiency and higher costs per unit of

installed power in comparison with large turbines. They are affected by atmospheric turbulence, gusty wind, as well as frequent downtime and damages; consequently, uncertainties in the prediction of power production are very high and their installation in urban environments is not yet cost-effective [34].

Regarding the exploitation of hydro resources in microgrids, it is worth mentioning the attention pointed on “small hydro”, defined as the sector of hydro power plants characterized by a rated power lower than 10 MW, typically between a few kW and hundreds of kW. Most of the small size hydro power plants are run-of-river plants, even if reservoir plants are also employed when the orography of the site shows suitable conditions. Small size hydro plants constitute one of the most cost-effective energy technologies for rural electrification in less developed countries, and they can be used to improve the grid stability and to mitigate to aleatority of intermittent other renewable sources, such as wind or solar. Different hydro turbines (impulse or reaction type) can be installed in microgrids: Turgo, Pelton, Francis, Propeller, Banki and Ossberger are some of the most widespread models [22]. Obviously, the design of a hydro power plant does not only consider the turbine with the generator but all the other components such as the control gate, the penstock, the draft tube, the powerhouse, etc. In the latest times, their capacity in some cases to be reversable (pump-generator) has become a very appreciated feature and some of them are also used for load shedding and energy storage. Finally, strict legal rights for water use and environmental requirements have to be taken into account during the design phase by planning compensatory measures, like fish passage structures or the minimum ecological flow guarantee of the river.

1.4.3. Technologies for thermal and cooling energy production

As aforementioned, polygeneration microgrids and nanogrids provide not only electrical energy but also thermal (heating and sanitary water) and cooling energy. Dedicated pipelines permit to convey warm and cold fluids from generation sources to end-users represented by buildings. Among the technologies used to produce thermal energy,

boilers, heat pumps, solar thermal collectors and electric heaters represent the main adopted solutions.

Solar thermal systems are used to heat buildings, to produce Domestic Hot Water (DHW), to heat swimming pools or to provide hot water to industrial processes, and to drive absorption chillers (solar cooling) [22]. We can find unglazed, flat plate, evacuated tubular or parabolic solar collectors. Flat plate and evacuated tubular collectors are the two main technologies employed for DHW production and space heating in buildings. The thermal energy production mainly depends on the solar irradiance and the ambient temperature. The main components of a solar thermal system are: the collectors (mounted on the roof of the building), the circuit of the fluid flowing into the collector, the storage tank, pumps and valves. Storage devices constitute components able to connect the solar system with other heat sources such as boilers and heat pumps, as well as with the loads (heating and DHW circuits).

Boilers, usually fed by natural gas or renewable fuels (biomass, biofuels, etc.), are typically used in microgrids to supply warm water in order to heat the buildings and to produce DHW. When microgrids are installed to provide energy to an industrial site, boilers (fire-tube or water-tube type) often produce steam which becomes an energy vector for the industrial process. The use of heat recovery boilers, fed by the exhaust gas coming from a prime mover or an industrial process, is also very widespread. Rated thermal powers range from hundreds of kW to some tens of MW. Moreover, in the majority of cases, boilers are coupled with thermal storage systems and cogeneration units. In these installations they act as slack devices, being switched on when high performance cogeneration microturbines and engines are not able to fully satisfy the thermal loads. In the domestic sector, and thus in nanogrids, condensing boilers are more and more installed since they are characterized by a higher efficiency. Typical rated power values in the residential and tertiary sectors range from a few kW to several tens of kW.

Heat pumps are used to heat buildings and to produce DHW. In electrically-driven heat pumps, electricity is used to lift low exergetic heat (taken from ambient air, water or

ground) to a higher temperature level by running a vapour compression cycle. As a consequence, heat pumps represent electrical loads. When supplied by electrical energy coming from renewable power plants they become a green technology to produce thermal energy. In the residential and tertiary sectors, geothermal heat pumps represent a green solution which permits to couple the building thermal inertia with that one of the ground [35]. Furthermore, the smartest heat pumps available on the market permit to be operated in a flexible way acting as manageable loads within demand response strategies.

The two main technologies to produce cooling energy in microgrids and nanogrids are electrically-driven heat pumps (also called compression chillers) and absorption chillers. Compression chillers are reversible heat pumps which are able to produce both thermal and cooling energy as a function of the season and the required final use. Absorption chillers are thermally activated since they are fed by thermal power to give a cooling effect. They can be indirect-fired (heated by warm water coming from a cogeneration plant or derived from an industrial process) or direct-fired (heated by the combustion of a fuel). A greener solution is represented by solar cooling installations, where an absorption chiller is fed by the fluid heated by solar thermal collectors. On the market there are single-effect and multi-effect absorption chillers with different working fluids (typically lithium bromide/water or water/ammonia). We can generalize by saying that when green electricity is locally produced, compression chillers are preferred over absorption chillers, while the latter use to be installed where there is the availability of a free heat source.

1.4.4. Cogeneration technologies

Combined Heat and Power (CHP) units are power plants able to produce electrical and thermal energy simultaneously. On the other hand, Combined Cooling, Heat and Power (CCHP) units are characterized by three useful effects, being also able to provide cooling energy. The use of CHP and CCHP units, instead of the separate production (of each useful effect in a separate plant), guarantees primary energy saving and CO_2 emission

reduction, as set by the Directive 2012/27/EU [36] related to high performance cogeneration. In order to properly design a cogeneration/trigeneration plant, it is necessary to develop an energy audit of the user to define electrical and thermal (heat and cooling energy) load profiles in order to verify if the simultaneous need of electrical and thermal energy occurs and that justifies the installation of a cogeneration/trigeneration system.

The most used small-size technologies in the cogeneration sector are microturbines and internal combustion engines. As reported in [22], to design a cogeneration plant different aspects have to be considered: technical (thermal/electric load ratio of the end-user, desired temperature values of fluids, capacity factor of the plant, characteristics of the installation site, etc.), environmental (limits on emissions, soil occupation constraints, etc.), economic (capital cost and operating costs, financing options, etc.), regulatory (feed-in-premium or feed-in-tariff incentives, tax policies on fuels, grid connection code requirements, etc.). Microturbines are very compact machines which can be installed individually or in multi-pack assembly. The are characterized by limited weight, low emissions and reduced noise. When coupled with smart power conditioning systems, they can operate in islanded-mode or grid-connected. However, their performance stongly depends on external ambient conditions (temperature and pressure) and on the installation site elevation; moreover, their electrical efficiency diminishes at partial loads [37]. Microturbines produce thermal energy (warm water or steam) by extracting heat from the exhaust gas at the exit of the turbine. On the other hand, spark and compression ignition internal combustion engines use three different sources (exhaust gas, jacket water and lube oil circuits) to produce thermal energy. Compared to microturbines, internal combustion engines are characterized by lower capital costs, higher electrical efficiency, lower dependence on ambient temperature, higher maintenance costs, emissions, noise and vibrations; moreover, they are less suitable for steam production. In CHP applications, microturbines and engines are often coupled with boilers and thermal storage systems, whereas in CCHP plants they thermally drive absorption chillers. On the market it is possible to find engines smaller than microturbines, since the smallest microturbines

present rated electrical power values around 30 kW, while there are engines for domestic application with a few hundreds of kW of electrical power. Consequently, cogeneration engines can be also used in single-family dwellings whereas microturbines are more suitable for buildings having more than 10 apartments (each one typically characterized by load peaks of 3-6 kW in Europe). In the aforesaid cases, cogeneration plants are more and more employed to provide thermal energy for space heating and DHW production. Furthermore, when coupled with absorption chillers, they substitute traditional compression chillers to cool buildings during summer.

1.4.5. Energy Storage Systems

Electrochemical batteries represent the most preferrable technology of electrical storage in microgrids and nanogrids [38, 39]. Different types of batteries are available on the market (Li-ions, Na/S, Na/$NiCl_2$, Ni/Cd, etc.), each one characterized by specific technical features and operating modes. The main quantities which describe a battery storage system are the nominal capacity, the energy density, the rated voltage and current values, the minimum/maximum charging and discharging power, the minimum State of Charge (SoC), the maximum number of life cycles, the temperature operating range and the self-discharge rate. Typical performance curves of batteries show the voltage profile as a function of the charged or discharged energy, and the capability curve in the active/reactive power plane. Moreover, it is important to consider that both charging and discharging efficiencies, as well as the maximum charging and discharging power, can be affected by both the operating temperature and the SoC.

The increased installation of battery storage systems in the recent decade derives from the need of adopting storage devices able to compensate the fluctuation of the electricity production from renewable sources (mainly wind and solar). Indeed, in microgrids, battery packs are usually coupled with PV plants and micro WTGs, permitting to increase self-consumption and to flatten the daily load curve of end-users. Battery storage systems can provide/absorb active power to control frequency and reactive power for voltage control. In grid-connected microgrids, storage systems can contribute

to solve grid congestions and to defer investments in presence of the increase of loads. In nanogrids, a typical configuration of a smart house includes PV panels, some batteries, smart loads and an EV wall box which all interact in order to maximize self-consumption, reduce the energy bill and limit the environmental impact. Through a precise estimation of the daily domestic load profiles and a correct evaluation of the numerous cost items it is possible to optimally size the nanogrid, in terms of number of PV panels and batteries, with the aim of better exploiting the available renewable resources [28].

In polygeneration microgrids and nanogrids we can also find thermal energy storage systems which permit to accumulate thermal energy when the production exceeds the load [40]. Thermal energy can be stored at different temperatures by exploiting sensible heat, latent heat or chemical energy of different fluids and materials. Sensible thermal energy storage systems typically consist in the installation of insulated tanks where hot water produced by CHP units, heat pumps, boilers or solar thermal systems is stored, and then used for heating or DHW production purposes. It is also possible to store chilled water produced by compression and absorption chillers. Through water stratification and the use of an effective thermal insulation it is possible to guarantee a thermal reserve even for very long periods. In urban districts, very large systems are often installed to provide a seasonal storage service and some of them are based on underground thermal energy storage technologies. On the other hand, more innovative projects deal with the application of phase change materials for thermal energy storage [41]; these systems enable higher storage capacities and target-oriented discharging temperatures.

1.4.6. Electric mobility infrastructures

In microgrids and nanogrids the main electric mobility infrastructures consist of charging points for electric vehicles (bikes, scooters and cars) [42]. These devices can be simple wall boxes (wall-mounted), pole stations or more complex chargers. The complexity of chargers mainly depend on the charging power and the supply type (AC – Alternate Current or DC – Direct Current). The main characteristics in terms of power values of AC

chargers currently available on the Italian and Spanish markets can be summarized as follows:

- Wall boxes: single phase (3.7-7.4 kW) or three-phase (≤ 22 kW);
- Pole stations: single phase (3.7 kW) or three-phase (≤ 22 kW);
- Fast chargers: three-phase (≤ 43 kW).

The most used connectors available on AC chargers are Type 2, Type 3C and Type 3A, while the main ones installed on EVs are Type 1 and Type 2 [43].

As far as DC charging is concerned, the main adopted connectors are CHAdeMO and CCS Combo 2. In the first case, the typical maximum transferrable power is around 62 kW (125 A, 500 V) but with CHAdeMO 2.0 and ChaoJI it will be possible to reach values of 900 kW. With CCS Combo 2 typical values of charging power around 100 kW are currently used, but there are advanced installations which permit to attain higher values (> 400 kW). DC chargers are more complex and expensive than AC chargers since they contain AC/DC power conversion devices (inverters, etc.); on the other hand, AC chargers can be seen as smart sockets.

In microgrids and nanogrids we can find traditional monodirectional chargers (from the station to the vehicle) and bidirectional chargers (the vehicle can be discharged to provide power to the network). In the latter case we talk about vehicle-to-grid (V2G), vehicle-to-building (V2B) and vehicle-to-home (V2H) technologies, as a function of which system the EV interact with. More in general, we deal with V2X technologies that represent a challenging solution to open the ancillary services market to electric mobility. By using V2X technologies, EVs can behave as wheeling storage systems and thus can be used to compensate the aleatory production of renewables and the variability of loads.

1.4.7. Operation and management

As described in the previous sections, a microgrid can represent a very complex system made of different subsystems (generation plants, loads, storage systems, electrical and

thermal networks, ICT infrastructure, smart meters, etc.). In Figure 1.10 a general scheme of a microgrid is reported with the aim of showing the main aforesaid subsystems together with their interactions. In accordance with the DOE's definition of microgrid, there is a unique PCC with the distribution grid, in this case modeled as the MV network. The reported microgrid is characterized by five buses: one AC - MV bus, two AC - LV buses and two DC buses. This indicates that, in general, a microgrid can include both AC and DC parts. Power conditioning devices permit the inteconnection of AC and DC sections as well as between DC buses. There are DC and AC loads, while PV plants and storage systems can be connected to both AC and DC buses. A quick charging station for EVs is connected to one of the two AC - LV buses, while a V2G station is present on one of the two DC buses. The generator indicates a cogeneration microturbine equipped with a high-speed permanent magnet generator and connected to the corresponding AC - LV bus through a power conditioning system.

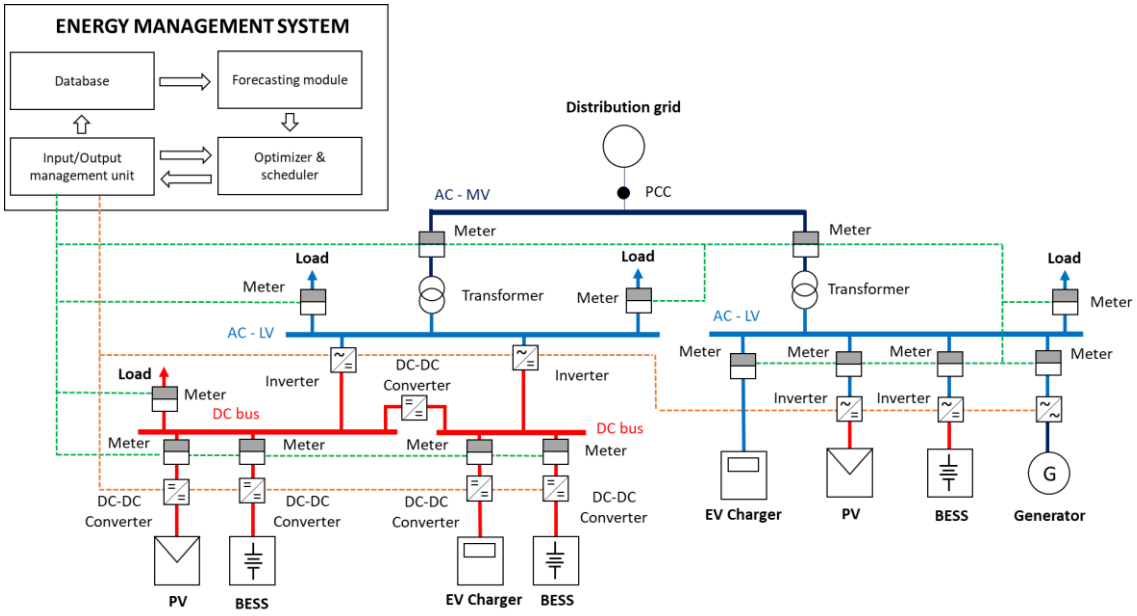

Figure 1.10. Scheme of a representative advanced microgrid.

As far as the operation and management of the microgrid, it is important to distinguish different levels:

- **The field:** where several smart meters and ICT devices (remote terminal units, etc.) are installed in order to acquire real operating data and send them to the SCADA system (through communication links and protocols, e.g. IEC 61850 protocol);
- **The SCADA system:** that gathers information from the field and sends commands or set-points (given by the EMS) to the devices (power inverters, etc.) and real measures to the EMS;
- **The EMS:** which is the "brain" of the microgrid concerning the power dispach and schedule of power loads [22, 44]. Its main function is that of determining the optimal schedule of dispatchable power plants (e.g. CHP units, boilers, etc.), storage systems and EV charging infrastructures with the goal of minimizing operating costs and/or carbon dioxide emissions. The core of the EMS is typically a software tool based on an optimization mathematical model whose main inputs are: cost items (fuel and electricity prices, maintenance unitary costs, etc.), technical and environmental constraints related to the performance of power plants (minimum and maximum power output of generation sources, minimum state of charge of storage systems, power lines capacity, acceptable voltage ranges, etc.), electrical and thermal load forecasts, estimation of power production from renewable sources. This indicates the importance of coupling the optimizer with a forecasting tool able to estimate loads and renewable energy production, usually based on weather forecast and historical data stored in a large database.

  When developing an EMS of a microgrid different approaches can be considered: day-ahead, real-time or Model Predictive Control (MPC). In the first case, the optimizer determines at day *d* the optimal schedule of technologies for day *d*+1 (24-h time horizon) by considering as input data the estimated daily load and renewable production profiles. A real-time optimizer determines optimal set-points of plants at time *t*+1 based on real measures gathered at time *t* but without looking forward, thus showing a short-sighted vision. On the other hand, the MPC approach is a sort of day-ahead algorithm which is performed more

times during the day which it refers to, since a great part of input data are real-time updated and the determined optimal set-points are not applied to the whole time horizon but to a limited time window after which the algorithm is executed again.

1.5. Summary and chapter conclusions

This first chapter has described the new configuration of the electric power system characterized by the presence of microgrids, nanogrids and energy communities. The main features of the aforesaid entities have been described mainly focusing on the analyisis of regulatory and technical aspects. The main electrical and thermal energy production technologies, as well as storage systems and electric mobility infrastructures, have been briefly described together with the definition of the most important characteristics of operation and management tools.

1.6. References

1. Robert Schuman Centre for Advanced Studies (European University Institute), Verde SF, Rossetto N, et al (2020) The future of renewable energy communities in the EU: an investigation at the time of the clean energy package. Publications Office of the European Union, LU

2. Aerovind (Energy cooperative initiative in a minor island in Denmark). https://www.aeroevind.dk/. Accessed 20 Oct 2021

3. SIFNOS (Energy cooperative initiative in a minor island in Greece). https://www.sifnosislandcoop.gr/. Accessed 20 Oct 2021

4. SEM - Società Elettrica in Morbegnov (Energy cooperative initiative in a mountain region in Italy). https://www.sem-morbegno.it/ChiSiamo.html. Accessed 20 Oct 2021

5. CEDIS - La nostra storia. In: Cedis - Consorzio Elettrico di Storo. https://www.cedis.info/chi-siamo/la-storia/. Accessed 20 Oct 2021

6. Business concept of Eno Energy Cooperative | Enonenergia.fi (Energy cooperative initiative in a mountain region in Finland). http://www.enonenergia.fi/Business_concept_of_Eno_Energy_Cooperative. Accessed 20 Oct 2021

7. Interreg Europe (Virtual energy cooperative initiative in Malta). https://www.interregeurope.eu/policylearning/good-practices/item/86/solar-photovoltaic-communal-farm-scheme/. Accessed 20 Oct 2021

8. Condivisione energetica da fonti rinnovabili | Energia Positiva (Virtual energy cooperative initiative in Italy). https://www.energia-positiva.it/la-cooperativa/. Accessed 20 Oct 2021

9. REScoop (European Federation of citizen energy cooperatives). https://www.rescoop.eu/. Accessed 20 Oct 2021

10. European Parliament (2018) Directive (EU) 2018/2001 of the European Parliament and of the Council of 11 December 2018 on the promotion of the use of energy from renewable sources

11. European Parliament (2019) Directive (EU) 2019/944 of the European Parliament and of the Council of 5 June 2019 on common rules for the internal market for electricity and amending Directive 2012/27/EU

12. European Commission (2020) Communication from the commission to the european parliament, the council, the european economic and social committee and the committee of the regions Stepping up Europe's 2030 climate ambition Investing in a climate-neutral future for the benefit of our people

13. European Parliament (2018) Directive (EU) 2018/844 of the European Parliament and of the Council of 30 May 2018 amending Directive 2010/31/EU on the energy performance of buildings and Directive 2012/27/EU on energy efficiency

14. Energy communities report – JRC (Joint Research Center of European Union). https://publications.jrc.ec.europa.eu/repository/bitstream/JRC119433/energy_communities_report_final.pdf. Accessed 20 Oct 2021

15. Gazzetta Ufficiale Conversione in legge, con modificazioni, del decreto-legge 30 dicembre 2019, n. 162, recante disposizioni urgenti in materia di proroga di termini legislativi, di organizzazione delle pubbliche amministrazioni, nonche' di innovazione tecnologica

16. Ministerio para la Transición Ecológica (2019) Real Decreto 244/2019, de 5 de abril, por el que se regulan las condiciones administrativas, técnicas y económicas del autoconsumo de energía eléctrica

17. Jefatura del Estado (2013) Ley 24/2013, de 26 de diciembre, del Sector Eléctrico

18. Jefatura del Estado (2018) Real Decreto-Ley 15/2018, de 5 de octubre, de medidas urgentes para la transición energética y la protección de los consumidores

19. IDAE - Instituto para la Diversificación y Ahorro de la Energía (2020) Plan Nacional Integrado de Energía y Clima (PNIEC) 2021-2030 | IDAE

20. Gruppi di autoconsumatori e comunità di energia rinnovabile GSE (Italian technical rules for the renewable energy collective self-consumer and renewable energy community). https://www.gse.it/servizi-per-te/autoconsumo/gruppi-di-autoconsumatori-e-comunita-di-energia-rinnovabile/documenti. Accessed 20 Oct 2021

21. Guía profesional de tramitación del autoconsumo | Idae. https://www.idae.es/publicaciones/guia-profesional-de-tramitacion-del-autoconsumo. Accessed 25 Oct 2021

22. Delfino F, Bracco S, Brignone M (2018) Microgrid Design and Operation: Toward Smart Energy in Cities. Boston

23. Perez-DeLaMora DA, Quiroz-Ibarra JE, Fernandez-Anaya G, Hernandez-Martinez EG (2021) Roadmap on community-based microgrids deployment: An extensive review. Energy Reports 7:2883–2898. https://doi.org/10.1016/j.egyr.2021.05.013

24. Hirsch A, Parag Y, Guerrero J (2018) Microgrids: A review of technologies, key drivers, and outstanding issues. Renewable and Sustainable Energy Reviews 90:402–411. https://doi.org/10.1016/j.rser.2018.03.040

25. Cagnano A, De Tuglie E, Mancarella P (2020) Microgrids: Overview and guidelines for practical implementations and operation. Applied Energy 258:114039. https://doi.org/10.1016/j.apenergy.2019.114039

26. Ton DT, Smith MA (2012) The U.S. Department of Energy's Microgrid Initiative. The Electricity Journal 8:84–94. https://doi.org/10.1016/j.tej.2012.09.013

27. Bracco S, Delfino F, Piazza G, de Simón-Martín M (2020) V2G technology to mitigate PV uncertainties. In: 2020 Fifteenth International Conference on Ecological Vehicles and Renewable Energies (EVER). pp 1–6

28. Bracco S, Delfino F, Piazza G, et al (2019) Nanogrids with Renewable Sources, Electrical Storage and Vehicle-to-Home Systems in the Household Sector: Analysis for a Single-Family Dwelling. In: 2019 IEEE Milan PowerTech. pp 1–6

29. Bianco G, Bracco S, Delfino F, et al (2020) A Building Energy Management System Based on an Equivalent Electric Circuit Model. Energies 13:1689. https://doi.org/10.3390/en13071689

30. International Electrotechnical Commission (2013) IEC 61400-2:2013 - Wind turbines - Part 2: Small wind turbines

31. Orlando A, Pagnini L, Repetto MP (2021) Structural response and fatigue assessment of a small vertical axis wind turbine under stationary and non-stationary excitation. Renewable Energy 170:251–266. https://doi.org/10.1016/j.renene.2021.01.123

32. Liu J, Lin H, Zhang J (2019) Review on the technical perspectives and commercial viability of vertical axis wind turbines. Ocean Engineering 182:608–626. https://doi.org/10.1016/j.oceaneng.2019.04.086

33. Kc A, Whale J, Urmee T (2019) Urban wind conditions and small wind turbines in the built environment: A review. Renewable Energy 131:268–283. https://doi.org/10.1016/j.renene.2018.07.050

34. Pagnini LC, Burlando M, Repetto MP (2015) Experimental power curve of small-size wind turbines in turbulent urban environment. Applied Energy 154:112–121. https://doi.org/10.1016/j.apenergy.2015.04.117

35. Gabrielli P, Acquilino A, Siri S, et al (2020) Optimization of low-carbon multi-energy systems with seasonal geothermal energy storage: The Anergy Grid of ETH Zurich. Energy Conversion and Management: X 8:100052. https://doi.org/10.1016/j.ecmx.2020.100052

36. European Parliament, Council (2012) Directive 2012/27/EU of the European Parliament and of the Council of 25 October 2012 on energy efficiency, amending Directives 2009/125/EC and 2010/30/EU and repealing Directives 2004/8/EC and 2006/32/EC

37. Bracco S, Delfino F (2017) A mathematical model for the dynamic simulation of low size cogeneration gas turbines within smart microgrids. Energy 119:710–723. https://doi.org/10.1016/j.energy.2016.11.033

38. Bracco S, Delfino F, Trucco A, Zin S (2018) Electrical storage systems based on Sodium/Nickel chloride batteries: A mathematical model for the cell electrical parameter evaluation validated on a real smart microgrid application. Journal of Power Sources 399:372–382. https://doi.org/10.1016/j.jpowsour.2018.07.115

39. Lagrange A, de Simón-Martín M, González-Martínez A, et al (2020) Sustainable microgrids with energy storage as a means to increase power resilience in critical facilities: An application to a hospital. International Journal of Electrical Power & Energy Systems 119:105865. https://doi.org/10.1016/j.ijepes.2020.105865

40. IRENA (2013) Thermal energy storage: Technology brief

41. Pielichowska K, Pielichowski K (2014) Phase change materials for thermal energy storage. Progress in Materials Science 65:67–123. https://doi.org/10.1016/j.pmatsci.2014.03.005

42. Piazza G, Bracco S, Delfino F, Siri S (2021) Optimal design of electric mobility services for a Local Energy Community. Sustainable Energy, Grids and Networks 26:100440. https://doi.org/10.1016/j.segan.2021.100440

43. Falvo MC, Sbordone D, Bayram IS, Devetsikiotis M (2014) EV charging stations and modes: 2014 International Symposium on Power Electronics, Electrical Drives,

Automation and Motion, SPEEDAM 2014. 2014 International Symposium on Power Electronics, Electrical Drives, Automation and Motion, SPEEDAM 2014 1134–1139. https://doi.org/10.1109/SPEEDAM.2014.6872107

44. Zia MF, Elbouchikhi E, Benbouzid M (2018) Microgrids energy management systems: A critical review on methods, solutions, and prospects. Applied Energy 222:1033–1055. https://doi.org/10.1016/j.apenergy.2018.04.103

Levelized Cost of Energy in Sustainable Energy Communities

A systematic approach for multi-vector energy systems

CHAPTER 2 – The Levelized Cost of Energy indicator

The Levelized Cost of Energy indicator

2.1. Introduction

In this chapter, the concept and fundamentals related with the Levelized Cost of Energy (*LCOEn*), and its variants (Levelized Cost of Electricity: *LCOE*, Levelized Cost of Stored Energy: *LCOS*, Levelized Cost of Heat: *LCOH*, Levelized Cost of Cooling: *LCO*C and Levelized Cost of Exergy: *LCOEx*) will be presented. Firstly, this chapter pretends to provide a brief introduction to the calculation of the *LCOEn*, including the main definitions and formulations, the involved parameters and its advantages and limitations. Then, its application to electricity, thermal energy and exergy domains are presented, including the case of polygeneration and energy multi-vector systems. The theoretical part here presented will be then applied in the following chapter to some case studies.

2.2. The promoters' perspective of energy projects

Many governments and public organizations encourage the development of renewable energy sources to combat climate change, but the investors or promoters' decision depends on the estimated profitability of an energy project [1]. Before presenting the fundamentals of the *LCOEn*, the typical financial indicators used for energy projects are briefly introduced. It must be remembered that an energy generation project is not only a facility to solve a technical problem (the provision of energy to end-users), but also an economic asset which provides benefits, or at least savings, to its promoters. Unless an external obligation (in order to guarantee the provision of energy or other circumstances), an energy project will not be even considered if it does not achieve the desired "financial performance".

2.2.1. Economic feasibility of an energy project

In order to measure the financial performance of an energy project, some meters or financial indicators are calculated and compared in order to help the promoters to

choose their best investment option. Typically, when evaluating the financial feasibility of an energy generation project, the following financial indicators are usually evaluated:

- **Payback Period:** this metric evaluates the period needed to return the initial investment costs or capital expenditures at year 0 ($CAPEX_0$) considering the estimated annual cash flow. It is usually measured in years and it can be "Simple" – *SPP* - (see Equation 2.1) or "Discounted" – *DPP* - (see Equation 2.2).

$$SPP = \frac{CAPEX_0}{Cash\ flow}.$$

Equation 2.1

In contrast with the *SPP*, which just considers the nominal annual cash flow of the project without determining the present value of future cash flows through discounting, the *DPP* also considers when the cash flows occur and the prevailing rate or return in the market, i.e., the discounted values of the cash flows. To discount a cash flow, a discount rate *d* that accounts for the capital and the risk costs must be considered. Thus, it depends on how the project is being financed (using internal or external resources) and on the accepted risk level of the promoters.

The *DPP* represents the number of years to return the initial expenditure by discounting future cash flows occurred in the plant lifespan. It is obtained by solving Equation 2.2:

$$-CAPEX_0 + \sum_{i=1}^{DPP} \frac{Cash\ flow_i}{(1+d)^i} = 0.$$

Equation 2.2

In Equation 2.2, as well as in the following ones, the subscript *i* indicates that the term is related to *i*-th year. Therefore, the *DPP* calculation cannot be done directly but involves an iterative procedure, as the calculation of the discounted cash flows depends on the considered *i*-th period.

Moreover, it must be considered with caution if the inflation rate has been already accounted for when evaluating the cash flows or not. If the cash flows include the inflation effect, the real discount rate (d_{real}) must be used, while if the cash flows are nominal (they do not include the inflation rate), the nominal discount rate (d_{nom}) must be used in the calculation. The relationship between the real and the nominal discount rates can be seen in Equation 2.3, where *k* is the inflation rate:

$$d_{real} = \frac{1 + d_{nom}}{1 + k} - 1,$$

Equation 2.3

- **Net Present Value (*NPV*):** this financial metric evaluates the sum of the cash flows of the project during its whole life span (*n* years) and discounts them according to an estimated discount rate. It is given by Equation 2.4:

$$NPV = -CAPEX_0 + \sum_{i=1}^{n} \frac{Cash\ flow_i}{(1+d)^i}.$$

Equation 2.4

If the cash flows are considered constant along the life span of the project, Equation 2.4 can be simplified to the following expression:

$$NPV = -CAPEX_0 + Cash\ flow \cdot \frac{1 - (1+d)^{-n}}{d},$$

Equation 2.5

where the term multiplying the cash flow is the inverse of the capital recovery factor (*CRF*), which represents the ratio of a constant annuity to the present value of receiving that annuity for a given time span.

- **Internal Rate of Return (*IRR*):** this metric is calculated as the discount rate that makes the *NPV* of the project equal to zero (see Equation 2.). Consistently, it can be calculated in nominal or real terms.

$$-CAPEX_0 + \sum_{i=1}^{n} \frac{Cash\ flow_i}{(1+IRR)^i} = 0.$$

Equation 2.6

- **Cost of Energy (*COEn*):** in contrast with the above-mentioned metrics, this financial indicator is exclusive of energy projects, as it is related with the unitary costs of the product, which in this case is the energy produced by the generation plant or system. It is evaluated as the ratio of the sum of all the involved yearly costs along the life span of the project ($Costs_i$) and the sum of the energy produced in each year (En_i), without discounting, as it can be seen in Equation 2.7. It can be applied to electricity, heat, cooling, etc.

$$COEn = \frac{\sum_{i=0}^{n} Costs_i}{\sum_{i=1}^{n} En_i}.$$

Equation 2.7

The involved costs in all time periods include (see Equation 2.8) capital expenditures, operation and maintenance expenditures (*OPEX*), Fuel or input costs (herein referred to as *Fuel costs*) and possible other costs (herein referred to as *Other Costs*), such as externalities, intended as indirect societal costs and/or other indirect costs connected with the energy system.

$$Costs_i = CAPEX_i + OPEX_i + Fuel\ costs_i + Other\ costs_i$$

Equation 2.8

where *OPEX*, *Fuel costs* and *Other costs* are usually zero for *i*=0 (i.e., at the construction and installation year).

2.2.2. Why do we need the Levelized Cost of Energy indicator?

The above presented metrics to analyze the economic feasibility of a project present an intrinsic limitation as they are size and location dependent, i.e., they are typically used to compare different investment options but only for the same site. Therefore, they do not provide a suitable estimation method for carrying out a comparative analysis among different projects. To overcome these limitations, the Levelized Cost of Energy (and its specific applications) is a common metric, especially in the electricity sector (*LCOE*), widely used by policy makers for estimating and comparing the costs of generating technologies [2]. It considers the full life-cycle costs (fixed and variable) of a generating

technology per unit of energy, thus allowing comparison among different generation technologies independently of size, costs structure and useful life [2, 3].

The *LCOEn* supplies a simple and quick procedure to measure the competitiveness of energy projects; it is widely used both for conventional and renewable power sources investments. It differs from the classical *COEn* metric in the way that it includes the present value of the total cost of building and operating a generation system over an assumed financial life time and duty cycle, converted to equal annual payments, in real terms [4]. *LCOEn* models are widely applied at national and regional levels for the energy systems design, energy generation projections and technology assessments [5].

On the other hand, the *LCOEn* is strictly related to the quantities accounted for and the assumptions made. It may therefore give rise to incomplete or misleading evaluations when used to make absolute assessments [2, 6]. It is, therefore, advisable that this metric is used appropriately, especially when comparing non-dispatchable energy technologies with conventional plants. In the case of renewable energy systems, the generated energy has not a homogeneous value as it depends on the resource availability ad it is especially affected by the intermittent nature of the source (currently, the adoption of energy storage systems still represents a costly solution). Hence, the value of the produced energy depends on the time when it is produced and, thus, the *LCOEn* is related with its variability patterns that determine its generation profile. The *LCOEn* might not adequately consider the temporal heterogeneity of the energy generation [2, 7]. Furthermore, other aspects, such as the renewable sources' location, grid-related costs and other intrinsic aspects are hardly accounted for in the classical definition of the *LCOEn*.

2.3. Definitions of the Levelized Cost of Energy (*LCOEn*)

The basic *LCOEn* formula can be derived from the following relationship that it is considered to be hold in competitive energy markets:

$$\sum_{i=1}^{n}\left[\frac{En_i \cdot p_i}{(1+d)^i}+\frac{Revenues_i}{(1+d)^i}\right] \geq \sum_{i=0}^{n}\left[\frac{CAPEX_i}{(1+d)^i}+\frac{OPEX_i}{(1+d)^i}+\frac{Fuel\ costs_i}{(1+d)^i}+\frac{Other\ costs_i}{(1+d)^i}\right],$$

Equation 2.9

where p_i denotes the annual average wholesale price, or the price at which the produced energy is sold or must be purchased from an alternative provider. $Revenues_i$ are the possible yearly benefits that may reduce the costs. They include incentives, internalities, intended as indirect benefits, avoided externalities, as well as other indirect benefits for a third party (that are classified in the following as beneficial externalities).

The left-hand side of Equation 2.9 represents the total discounted revenues for the whole lifetime of the project, while the right-hand side shows the total discounted cost of the plant. Thus, the total annual discounted revenues must cover, at least, the total annual discounted costs, including capital expenditures, operation and maintenance, fuel costs and other costs related to the energy supply system. This approach can be also called “discounted cash flow” analysis, where the cost of a generation technology is based on discounting financial flows to a common basis.

2.3.1. Basic definition

Based on the previous stated hypotheses, the *LCOEn* can be calculated as the average energy price over the whole lifespan of the facility that covers the sum of the annual discounted net costs, as it is expressed in Equation 2.10, where the costs term includes all the costs already described by Equation 2.8:

$$LCOEn = \frac{\sum_{i=0}^{n}\left[\frac{Costs_i}{(1+d)^i}-\frac{Revenues_i}{(1+d)^i}\right]}{\sum_{i=1}^{n}\frac{En_i}{(1+d)^i}}.$$

Equation 2.10

It represents the unitary production cost of energy, including the construction and operating costs of the power generation system, for unit of produced energy averaged over an assumed financial life and duty cycle. Therefore, it provides the value of the average energy price which makes the discounted revenues compensate for the total discounted costs after considering other possible revenues [4].

Typically, the *LCOEn* is calculated over an expected lifetime of 20 to 40 years (depending on the expected useful lifespan of the project), and it is given in units of currency per kWh or per MWh.

The expression shown in Equation 2.10 can be simplified when cash flows are considered constant over the evaluation time horizon. Thus, if we consider that i) the capital expenditures different from those at time 0 (initial investment), which are commonly related with equipment replacement, can be divided uniformly along the lifespan of the project and included in the *OPEX*, ii) the yearly *OPEX* and other periodic costs and revenues are the same in nominal terms during the lifespan and are called *Periodic Costs* and *Periodic Revenues*, respectively, and iii) the yearly energy production is constant along the complete useful life span (degradation effects or unavailabilities are not considered in the first place), and is called *En*. Then the *LCOEn* formula can be simplified to that shown in the following Equation 2.11.

$$LCOEn = \frac{CAPEX_0 + (Periodic\ Costs - Periodic\ Revenues) \cdot \frac{1-(1+d)^{-n}}{d}}{En \cdot \frac{1-(1+d)^{-n}}{d}} = \frac{CAPEX_0 \cdot d}{En \cdot [1-(1+d)^{-n}]} + \frac{Periodic\ Costs - Periodic\ Revenues}{En}.$$

Equation 2.11

2.3.2. Parameters of the LCOEn

The *LCOEn* value can be taken as a reference metric to compare the competitiveness across different generation technologies. However, when comparing *LCOEn* values for alternative systems, it is important to define in a proper manner the boundaries of the

system, the specific cost for the technology in use, the included internalities and externalities, such as transmission and distribution costs, R&D, tax, environmental impact studies, impacts on public health and environmental damage or government subsidies, among others and, in general, the criteria used to quantify costs and revenues. Key inputs for calculating the simplified *LCOEn* include capital expenditures, variable operation and maintenance costs, financing costs and an assumed utilization rate, capacity factor or equivalent hours for the system depending on its type [4].

In the following, all costs and revenues are grouped into direct costs, that are mainly given by capital expenditures, operation, maintenance, energy supplies; direct revenues and internalities, that include possible benefits for the stakeholder not directly related with the amount of produced energy; externalities, given by societal costs or benefits originating from the power plant. Costs and revenues adopted, as well as the inclusion or not of externalities, even if not directly translated into charges, must be clearly identified and declared when comparing the *LCOEn* of different facilities.

Direct costs

The *CAPEX* includes the total capital expenditures inside the plant boundaries, such as the generator, the civil engineering or any wiring, piping or other auxiliaries installed within the plant. The operation and maintenance costs, or *OPEX*, represent an annualized estimate of the total operating costs over the project design life, including both the cost escalation with ageing. Moreover, the *OPEX* also includes several other ongoing costs, such as insurance costs or land payments [8]. In [9], the cost of decommissioning of the plants is also taken into consideration, while in [10] the costs related to environmental taxes are considered.

The time value of money (inflation) can be included or not, depending on whether the discount rate does it or not. If the *OPEX* includes the inflation, then the real discount rate must be used in the formulation, otherwise, the nominal discount rate must be adopted (see Equation 2.3 at this concern).

Fuel costs are one of the main sources of costs in traditional generators. However, renewable energy sources (RES), such as the solar PV or wind, do not involve significant input and fuel costs and have typically low operation and maintenance costs. In this case, the capital cost represents the key quantity ruling the *LCOEn* evaluation. On the other hand, for those technologies with significant fuel costs, such as nuclear power plants or gas-fired power plants, both fuel and overnight costs affect significantly the *LCOEn* value.

Finally, precise estimations of the *LCOEn* should also consider other costs, such as the integration costs of the generation technology which are especially relevant (and difficult to calculate) in renewable energy systems. These costs can be defined as those additional costs of accommodating some generation technologies [11], or costs induced by a generation technology that are not directly related to the generation costs [2] and are included in the term of other costs in the above presented equations. They can be divided into:

- **Balancing costs:** due to the uncertainty or variability of power generation, such as the need to hold and use more operating reserves, the increase of ramping thermal power plants, cycling and others.
- **Grid-related costs:** due to the need to extend and reinforce the power network, including occasional benefits of lower grid needs and lower network losses.
- **Adequacy costs:** those deriving from the reduced deployment or utilization of old, low efficient, non-renewable or conventional power plants, which might imply a lack of conventional capacity providing backup services.

It has been observed in several studies that renewable energy sources, especially wind and solar, cause significant integration costs at penetration levels higher than 10% [12]. Moreover, apart from the cost definition and the adopted methodology, the size and composition of the integration costs of renewable energy sources are location-specific and tend to increase with growing penetration rates, while they tend to decrease over time, depending on the adaptation of the power systems.

Direct revenues and internalities

The *LCOEn* calculation through Equation 2.10 also accounts for revenues that compensate for the effect of the costs. Possible direct revenues are the availability of incentives, subsidies or the remuneration of the operation of the energy system due to side effects. For instance, in the calculation of the *LCOE* of a cogeneration plant (CHP), the remuneration of the produced thermal energy, which is a side effect of the production of electricity, must be considered (properly discounted) in the numerator of the formulation. In a similar manner, if calculating the *LCOH* of the same cogeneration plant, the remuneration for the production of electricity must be properly accounted.

On the other hand, internalities are long-terms benefits in monetary terms for the owner that are not directly related with the amount of the produced energy. Some examples of internalities are the benefits coming from the increase of the resilience due to polygeneration microgrids, from the increase in the energy quality, measured by the avoided blackouts, from the possibility of managing intermittent sources more efficiently as well as the attractiveness for investments and loans or the avoided costs related to the health issues supported by the owners (such as private insurances).

Externalities

Externalities are those indirect costs and benefits deriving from the impact of power generation on a community or on a third party to which no financial consideration is assigned. They are mainly due to negative effects on the environment, on the health and well-being of individuals. The fact that these costs are outside the logic of the market and the difficulty to translate them into economic value has often left aside their monetization. However, as long as they are not monetized, they determine the so called “market failure” [13], that is the inability of the free market to efficiently allocate goods and resources, increasing the well-being of some groups without reducing that of anyone else.

Since the 90s, growing attention has been paid in the evaluation of the externalities related to atmospheric emissions. Soon after, specific models for the estimation of

concentration of pollutants have been defined, together with suitable models for the estimation of impacts. The joint use of these tools and suitable monetization functions has allowed the economic estimation of damages by a series of subsequent steps that implies the assessment of emission, dispersion or impact. The damage cost is finally supplied in terms of cost per kilogram of emitted pollutant, or per kWh of produced energy. In this context, the European Environment Agency (EEA) has supplied a simplified modelling approach assessing in monetary terms the cost of damage to health and environment from selected air pollutants emitted by industrial facilities located in European Nations [14].

The available methodologies, however, cannot be all-inclusive, as other effects on the environment as well as other non-environmental externalities are inevitably left out. Moreover, large uncertainties exist, both in emission rates and damages [15]. Especially, uncertainties exist in costs associated with climate change, being its impact a long-term, global externality [16].

Externality costs can weight directly on the owner, and thus they must be considered in the *LCOEn* calculation, both through taxes and charges or benefits. A typical cost related to a negative externality is the carbon tax to compensate for the damage to the environment due to carbon dioxide and other greenhouse gases emission. In any case, a complete comparative analysis between different production units cannot ignore the quantification of externalities.

The main studies dealing with external costs of traditional and renewable power generation, such as [17–19], generally recognize that costs per kWh are worst for coal and lignite, quantified in around € 80 /MWh and oil, around € 66 /MWh. Natural gas is cleaner, quantified in around € 30 /MWh, while lowest costs are obviously found in renewable sources. Hydro power externalities are quoted around € 1.3 /MWh, while for solar, thermal, and wind power they are less or much less than € 1.0 /MWh (data from [20]). At this purpose, some criticisms may arise from the fact that hydropower, PV and wind energy affect the landscape, and these local externalities can create much discomfort in a small group of people.

Positive externalities can be defined as societal benefits that are infeasible to charge. Information about the quantification of positive externalities is practically absent, or they are evaluated in terms of avoided negative externalities from other technologies [21]. Positive impacts could be the social and occupational repercussions that can give new impetus to rural communities or areas of industrial crisis, also avoiding housing concentration in large urban centers. For instance, the presence of green energy infrastructures inside university campuses in decentralized locations may become an attractor for students and visitors, repopulating small towns and becoming "scientific tourist" attractors. In this sense, both the Campus of Savona from the University of Genoa (Italy) and the test-bed pilot facility of the Campus of Vegazana from the University of León (Spain) are good examples where sustainable energy research infrastructures gave birth to a number of innovation projects, making the campuses "open-air" demonstrators [22, 23]. In this context, a number of courses have been established on the topic of smart energy production and management. Benefits in monetary terms might come from the appeal for students who populated the small neighborhood making it a university district, as well as in attracting EU fundings and new collaborations for the research community. Population can also benefit from the creation of a comfortable green space open to the community, where people can work, study, spend free time and play sport experiencing a healthy lifestyle, but these benefits are difficult to quantify and add in the *LCOEn* formulation.

Discount rate

The discount rate is often expressed as the Weighted Average Cost of Capital (*WACC*). This represents the required average return of the combination of equity and debt to make a project an attractive investment opportunity, where each category of capital (equity and debt) is proportionately weighted. It is usually evaluated after taxes and it is, therefore, assumed that interest on debt serves as a tax reduction. Moreover, the equity returns are indicative of the required threshold return after payment of taxes [8]. The WACC is calculated as shown in Equation 2.12:

$$WACC = Equit\ costs \cdot \%\ Equity + \ [Debt\ costs \cdot \ \ \%\ Debt \cdot (1 - Tax\ rate)],$$

Equation 2.12

where *% Debt* = *debt/capital amount* and *% Equity* = *equity costs/capital amount*.

In practice, the *WACC* may be defined in after-tax or pre-tax terms and either in real or nominal terms (i.e. including or not the inflation rate). On the other hand, taxes can be adjusted including the present value of depreciation, which for the *LCOEn* calculation is commonly stated at 0.5% per year [8].

Utilization rate or equivalent operation hours

The capacity factor, or utilization rate, of a generation system is a crucial quantity for the *LCOEn* evaluation because it directly provides the produced energy. Its careful assessment is therefore essential for having reliable estimates of the cost of energy, especially when RES systems are involved. In this case, most of the costs are related with the size of the plant, rather than with the provided energy (e.g. fuel costs) and differences among plants of the same sizes are due to their different capacity factors, for example due to the availability of the primary energy source, or to its variability. Equation 2.13 shows the relation among two systems, A and B that have the same size and costs, but different equivalent operating hours (*EOH*) or full load hours. The discount rate is taken constant during the system lifespan and the same for both systems.

$$LCOEn^B = \frac{\sum_{i=1}^{n} \frac{EOH_i^A}{(1+d)^i}}{\sum_{i=1}^{n} \frac{EOH_i^B}{(1+d)^i}} LCOEn^A.$$

Equation 2.13

2.3.3. Other calculation models and approaches

The above-presented definition of the *LCOEn* is considered as the "simplified *LCOEn*" or "*sLCOEn*". The presented approach is relatively simplistic, given the fact that the model needs to be applied to a wide range of technologies in different countries and regions. This has the advantage, moreover, of producing a systematic, transparent and easy-to-

understand analysis. However, several different *LCOEn* models are available, as well as extended definitions.

The literature supplies variegated formulae of the *LCOEn*, with slight changes in the definition of its parameters and originated by different approaches in the model construction, to ensure that it matches research tasks and data availability [5]. The most widely spread *LCOEn* models are the U.S. DOE *LCOEn model* [24], the California Energy Commission Cost of Generation Model [25], the Department of Energy and Climate Change electricity costs model [26] and the Bureau of Resources and Energy Economics Australia Energy Technology Assessment model [27].

In [24], the levelized costs are calculated in three modes: the normalized mode, where a single discount rate and lifetime are used for all the compared technologies; the market mode, where it is used different discount rates, lifetime and other costs for each technology according to the DOE Program Estimates of 2011; or user defined. Moreover, in this model, the capital expenditures are turned into annual payments through a *CRF* which depends on the discount rate (7%) and the lifetime of the investment (30 years for generation plants). Then, the *LCOEn* is calculated in cents per kWh by the following equation:

$$LCOEn = \frac{CAPEX \cdot CRF \cdot (1 - T \cdot D_{PV})}{8760 \cdot CF \cdot (1 - T)} + \frac{Fixed\ OPEX}{8760 \cdot CF} + \frac{Variable\ OPEX}{1{,}000\,\frac{kWh}{MWh}} + \frac{Fuel\ price \cdot Heat\ Rate}{1{,}000{,}000\,\frac{BTU}{mmBTU}},$$

Equation 2.14

where *CF* is the capacity factor (the yearly average percentage of power as a fraction of capacity), *T* the tax rate paid (applied after depreciation credits) and D_{PV} the present value of depreciation, depending on the MACRS schedule (Modified Accelerated Cost Recovery System).

On the other hand, the model presented in [25] considers a variable set of fixed and variable cost components depending on whether the project is a merchant facility or

owned by an investor-owned utility (IOU) or a publicly owned utility (POU). In addition, the costs can vary with location because of differencing costs of land, fuel, construction, operations and environmental licensing. Then, as fixed costs are considered the total cost of capital and financing (at the point of interconnection with the existing transmission system), insurance costs, property taxes (*Ad Valorem*), fixed *OPEX* and corporate taxes (state and federal taxes). As variable costs, the report authors consider the fuel cost, the cap-and-trade allowance costs (GHG cost) and variable *OPEX* (as a function of the operating hours).

The approach reported in [26] considers only those costs accruing to the owner or operator of the generation asset and neglects wider costs that may in part fall to others, such as the full cost of system balancing and network investment, or air quality impacts. Moreover, the authors do not consider revenue streams available to generators (e.g. from sale of electricity or revenues from other sources), with the exception of heat revenues for CHP plants which are included so that the estimates reflect the cost of electricity generation only. It must be highlighted that the authors include, apart from the already mentioned costs, pre-development costs, carbon transport and storage costs and decommissioning fund costs. They also evaluate the expected availability, efficiency and load factor to calculate the expected generation capacity by assuming always a baseload.

Finally, in [27], the *LCOEn* is defined as the equivalent to the long-run marginal cost of energy (electricity) at a given point in time because it measures the cost of producing one extra unit of energy (electricity) with a newly constructed generation plant. It includes the operation and maintenance expenditures for each year and the authors open the possibility to include other costs such as a carbon price. However, they exclude the effects of taxation, the degradation effects for output from each technology, the plant decommissioning costs and the plant residual cost.

Among possible extended definitions, the “Financial Model Approach” (FMA) calculates the *LCOEn* as the required revenue to achieve a certain internal rate or return. It is

therefore suited to capture more complex financial assumptions, such as revenue requirements and the impacts of taxes and depreciation.

On the other hand, the *LCOEn* can also be defined in multiple ways, including the "Real *LCOEn*", the "inflation adjusted Real *LCOEn*" and the "Nominal *LCOEn*". The Real *LCOEn* is defined as a constant stream of values denoted in today's currency, the inflation adjusted Real *LCOEn* is defined as a nominal path that keeps a constant real value, while the Nominal *LCOEn* is defined as constant stream of values in nominal currency [28].

The Real *LCOEn* is preferred by Governments and policy makers as it uses real discount rates and removes the inflation effects associated with inputs and Operation and Maintenance (O&M) costs, or *OPEX*. On the other hand, promoters and project owners prefer to use the Nominal *LCOEn* as it includes assumptions regarding inflation. Moreover, when using a nominal discount rate, the nominal *LCOEn* can be analogous to a PPA (Power Purchase Agreement) or a FiT (Feed-in-Tariff) price which is flat across the economic life of the project [28].

2.4. Levelized Cost of Electricity (*LCOE*)

The Levelized Cost of Electricity, or *LCOE*, represents the *LCOEn* when considering power electricity generation sources. All the fundamentals stated before can be applied in this case and, actually, it represents the most common application case.

2.4.1. LCOE particularities for RES

Several foundations and organizations have carried out studies to estimate the potential for electricity production from renewables, identifying a clear disadvantage in terms of costs with respect to fossil fuels [29, 30]. It is widely known that renewable energy sources are extremely vulnerable to competing technologies. As long as it was possible to produce electricity at low costs, with little regard to pollution, the effects on the environment or other externalities, renewable energy sources were often less competitive than conventional technologies [4]. Even today, in those situations where

the negative impact on the climate and the environment is disregarded, conventional technologies may seem more cost-effective.

In the next paragraphs a brief description of the *LCOE* trends and particularities for the main renewable energy sources, based mainly on [2, 31], are depicted to put them in correlation with the *LCOE* calculation in more sophisticated systems, such as polygeneration systems and multi-vector energy systems and microgrids.

LCOE of solar PV systems

The global weighted-average *LCOE* of utility-scale PV plants declined from € 381/MWh in 2010 to € 57/MWh in 2020, which means an 85% drop. Moreover, the range of LCOE costs continues to narrow in these last years. This fact can be explained due to the rapid decline in total installed costs, increasing capacity factors and lower O&M costs. In the last decade, the solar PV industry has experienced various technological developments that have contributed to decrease costs along the whole solar PV value chain. Just the decline in the solar module cost is estimated to contribute to a 46% reduction of the *LCOE* at utility-scale when comparing 2010 and 2020. Together, cost reduction in power inverters, racking and mounting and other BoS (Balance of System) hardware is estimated to contribute another 18% to the *LCOE* reduction during that period. This decreasing trend has also been observed in residential PV systems. Assuming a 5% *WACC*, the *LCOE* of residential PV systems in the markets declined from approximately € 400/MWh in 2010 to € 200/MWh in 2020 (50% drop). Other markets, such as Japan, Italy or Australia have shown even higher drops in costs. Furthermore, between 2010 and 2020, the *LCOE* of commercial PV up to 500 kW declined between 50% and 79% in these markets showing a minimum value of around € 60/MWh (China).

LCOE of concentrating solar systems

With the reduction in total installed costs and O&M costs, increasing capacity factors and falling financing costs, the *LCOE* for Concentrating Solar Power (CSP) projects fell significantly between 2010 and 2020. In the last year, the global weighted-average *LCOE* of newly commissioned CSP plants is around € 108/MWh, which means a reduction of

the 68% with respect to 2010. This reduction is explained by the strong decrease of the installed costs and the increase in the capacity factors (from 30% to 42% on average). Moreover, reductions in the O&M costs and in the *WACC* are also found.

Several factors have contributed to reduce the *LCOE* of this technology since 2013. On the one hand, the broadening of the market and a larger gained experience. On the other, and with higher impact, the deployment to areas with higher DNIs (Direct Normal Irradiances), such as China, Morocco or South Africa. Furthermore, improvements in technology and cost reductions in thermal energy storage has led to an improvement in capacity factors, and has contributed to a 28% reduction in the *LCOE* over the 2010-2020 period. In the absence of a strong policy support for CSP, however, the market remains small and the pipeline for new projects meagre.

CSP and its low-cost thermal storage systems are often overlooked in favor of battery storage, given its rapid cost reductions. This is unfortunate, as CSP remains, along with pumped hydro storage, the only low-cost long-duration storage option available today. As the share of variable renewables grows, the possibility of adding low-cost long-duration storage will only grow in value.

LCOE of onshore wind energy

The interest in wind power generation has increased dramatically in the last years, and the technology of large size wind turbines is now well established. Common commercial machines are rated 2-5 MW on average and the tendency is to up scaling [29, 32]. On the contrary, small size wind turbines are, at present, less competitive, as construction and operating costs are often too high with respect to the power production [33, 34]. Notwithstanding this, they represent the appropriate technology to develop the strategic aim of small-scale distributed wind power generation in standalone, or grid connected configurations, integrated with other renewable sources.

The *LCOE* of an onshore wind farm is determined by the total installed costs, the lifetime capacity factor, O&M costs, the economic lifetime of the project, and the cost of capital. The cost of the turbines and towers makes up the most significant component of total

installed costs. On the other hand, with no fuel costs, the capacity factor and the cost of capital also have a significant impact on the *LCOE* calculation. Starting from this premise, the monitoring of costs and production of wind energy shows very high differences between the generation cost of small size wind turbines and that of large plants.

As far as large size applications are concerned, since 1983, the global weighted-average *LCOE* has declined approximately an 87%, achieving approximately € 41/MWh in 2019 at utility-scale. Consequently, onshore wind energy competes with hydropower as the most competitive renewable technology, without financial support.

The significant reduction of the LCOE for this technology can be explained mainly due, on the one hand, to the latest turbine technology improvements, especially in the optimization of the rotor diameter and turbine ratings, allowing a better exploitation of the sites. On the other hand, it can be found that economies of scale impact the costs of manufacturing, installation and O&M. Moreover, the O&M cost has been reduced thanks to the digitalization and improved practices. Finally, competitive auctions are leading to further cost reductions as it drives higher competitiveness.

Concerning small wind turbines, the *LCOE* is much higher and difficult to quantify, due to the huge variations the cost of installation, maintenance and of the *EOH*. As an example, an average value for Italy can be quantified in € 330/MWh in the target power ranging between 0-20 kW [35], but what is most impressive is the enormous variability of this value, with many prototypes with very low production, but also over-performing units, mainly related to turbines with generous rotor diameter with respect to the nominal rated power.

LCOE of offshore wind energy

In the latest years, increasing experience and competition, advances in wind turbine technology (seeking to increase efficiency and lower costs, several 8-8.8 MW wind turbines have been installed, and 14-20 MW units are currently under development), the establishment of optimized local and regional supply chains, and strong policy and

regulatory support schemes have resulted in a steady pipeline of offshore wind energy projects that have been increasingly competitive, i.e., with a lower *LCOE*.

From 2010 to 2020, the global weighted-average *LCOE* of offshore wind fell 48%, from € 162/MWh to € 84/MWh. Year-on-year, in 2020, weighted-average *LCOE* fell 9% from its 2019 value of € 93/MWh. From its peak in 2007, the global weighted-average *LCOE* of offshore wind fell by 53%. In this sense, the Netherlands had the lowest weighted-average *LCOE* for projects commissioned in 2020, at € 67/MWh, being followed by China, Denmark and Belgium.

LCOE of hydropower

Hydropower has historically provided the backbone of low-cost electricity in a significant number of countries around the world. However, it must be highlighted that hydropower projects can be designed to perform very differently from each other, and thus, it makes difficult to compare them. The strategy adopted in a hydropower project depends on the characteristics of the site inflows and the needs of the local market. Moreover, recently, hydropower systems with significant reservoir storage are increasing their value as they help to facilitate the growing share of variable renewable energy.

In 2020, the global weighted-average cost of electricity from hydropower was € 44/MWh, up 16% from the € 38/MWh recorded in 2010. Despite these increases through time, however, 99% of the hydropower projects commissioned in 2020 had an *LCOE* within or lower than this range. Moreover, 56% of the hydropower projects commissioned in 2020 had an *LCOE* lower than the cheapest new fossil fuel-fired cost option.

LCOE of geothermal systems

Geothermal power plants require continuous optimization throughout the lifetime of the project, which impacts directly on its *LCOE* results. The average *LCOE* for this technology varies from as low as € 40/MWh for second stage development of an existing

field to as high as € 170/MWh for small greenfield developments in remote areas, showing just a slight increase in the last decade.

O&M costs in these plants are high relative to other RES technologies, because over time the reservoir pressure around the production can decline if remedial measures are not taken.

LCOE of bioenergy

A wide range of *LCOE* values is observed for bioenergy-fired power plants due to the wide range of technologies, installed costs, capacity factors and feedstock costs. The global weighted-average *LCOE* of biomass-fired electricity generation for projects commissioned in 2020 was € 76/MWh, which is a similar figure than that of 2010. However, bioenergy can provide very competitive and dispatchable electricity where capital costs are relatively low and low-cost feedstocks are available, achieving an *LCOE* as low as around € 40/MWh. The most competitive projects take advantage of agricultural or forestry residues, already available at industrial processing sites. Furthermore, projects relying on municipal waste come with high capacity factors and are generally an economic source of electricity. However, their *LCOE* is usually higher than the average, especially in North America (given that these projects have been developed mostly to solve waste management issues, a slightly high *LCOE* is not necessarily an impediment to their viability).

In the case of bioenergy, the feedstock availability influences significantly the economic performance, and thus, the *LCOE*. The availability of a continuous stream of feedstock allows for higher capacity factors, but it is no necessarily more economical, as it can mean the need of more expensive feedstocks. Thus, the access to low cost feedstock offsets the impact on *LCOE* of lower capacity factors.

2.4.2. LCOE and grid parity

From the *LCOE* calculation the notion of competitiveness among generation technologies can be derived. One of the most common used indicators is the grid parity. Grid parity is the term given when the *LCOE* of a generation technology or energy system

is compared with the cost of acquiring electrical energy from the electricity market (Weighted Average energy wholesale Price: *WAP*) [4], as it is expressed in Equation 2.15.

$$Grid\ parity = \frac{LCOE}{WAP_{GRID}}.$$

Equation 2.15

It is usually applied to analyze the economic feasibility and competitiveness of distributed energy generators, which must compete with the supply from the electrical grid. When the grid parity, calculated as expressed in Equation 2.15, is equal or lower than 1, it means that the proposed energy generation project can compete effectively with the external power grid. Otherwise, the economic feasibility of the project is conditioned by the existence of subsidies. As an example, in [36] a temporal analysis of the solar PV grid parity in Europe is presented. The authors observe that the solar PV technology can achieve grid parity without subsidies for 2030 in a wider area in Europe, even with low availability of solar radiation, due to the reduction of costs, the increase of the technology efficiency and the rise of the electricity costs. Nevertheless, the grid parity depends on the energy mix of the market, and whether the calculation of the *LCOE* includes or not externalities.

It must be noticed that the grid parity approach, when the energy wholesale price is not correctly weighted (e.g., the solar *LCOE* of a PV power plant is compared with the yearly mean value of the electricity price instead of comparing with the daylight hours weighted average value of the electricity), can tend to overvalue the generation from some types of technologies. A classical example, electricity from WTGs is more heavily weighted to off-peak periods when electricity prices are usually lower, while can undervalue power production from others, such as solar PV, as this technology usually generates more electricity during peak-price periods [4]. Therefore, the energy generation time profile must be considered to properly get the weighted average price of the wholesale energy to get the appropriate conclusions when comparing with the *LCOE* of the energy systems.

2.4.3. LCOE of single generator systems

Figure 2.1 represents a typical generation unit connected to the power grid. In this case, a solar PV generator is shown, but the analysis can be extended to any other generator. The generator transforms the primary energy from an energy source (En_G^{PRIM}), in this case the solar radiation, into power energy (E_G). The effective power produced by the system is, indeed, the result of its maximum generation capacity (E_G^{MAX}) minus the energy curtailed or limited (E_G^{CURT}). In the case of power plants connected to the power grid, as they are remunerated by the total amount of energy injected to the grid, the curtailed energy is minimized. On the other hand, the maximum generation capacity can be constant, such as in some fossil fuel power plants, or variable in time, such as in a solar PV power plant where the maximum power capacity depends on the available resource. In any case, the net generated energy can be expressed as the product between the rated capacity (P_G) and its equivalent operating hours (EOH_G).

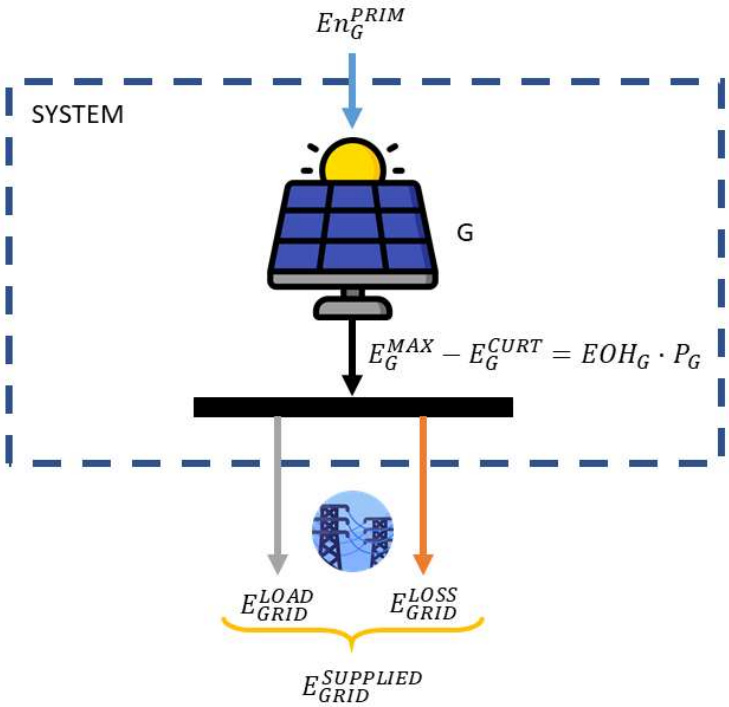

Figure 2.1. Representation of a single generation device system.

If a single-bus model is applied to represent the system, it can be concluded that the total energy produced by the power plant is supplied to the power grid to which it is connected ($E_{GRID}^{SUPPLIED}$). This energy includes both the power load (E_{GRID}^{LOAD}) and the

power losses due to transport and distribution (E_{GRID}^{LOSS}). Then, the energy balance of the system, applying a single-bus model analysis, is expressed in Equation 2.16:

$$E_G = E_G^{MAX} - E_G^{CURT} = E_{GRID}^{LOAD} + E_{GRID}^{LOSS} = E_{GRID}^{SUPPLIED}.$$

Equation 2.16

The *LCOE* of the generator represented in Figure 2.2 indeed is referred to the energy served or provided to the power grid. On the other hand, the costs associated to the served energy are related to the system itself (costs associated with the generator, the infrastructure for coupling to the PCC and the operation and management) and the inputs of the system (costs associated with the consumed primary energy). Thus, the *LCOE* for a single generator system can be deduced from Equation 2.9:

$$\sum_{i=1}^{n}\left[\frac{E_i^{SUPPLIED}\cdot p_i}{(1+d)^i}+\frac{Revenues_i}{(1+d)^i}\right] \geq \sum_{i=0}^{n}\left[\frac{CAPEX_i}{(1+d)^i}+\frac{OPEX_i}{(1+d)^i}+\frac{Fuel\ costs_i}{(1+d)^i}+\frac{Other\ costs_i}{(1+d)^i}\right],$$

Equation 2.17

$$LCOE_G = \frac{\sum_{i=0}^{n}\left[\frac{CAPEX_i}{(1+d)^i}+\frac{OPEX_i}{(1+d)^i}+\frac{Fuel\ costs_i}{(1+d)^i}+\frac{Other\ costs_i}{(1+d)^i}-\frac{Revenues_i}{(1+d)^i}\right]}{\sum_{i=1}^{n}\frac{E_i^{SUPPLIED}}{(1+d)^i}}.$$

Equation 2.18

In this case, as the served energy equals the generated energy (see Equation 2.16), and recalling the definition of costs given by Equation 2.8, Equation 2.18 can be simplified, considering the net costs NC_i (costs - revenues[1]) for the *i*-th time period:

[1] In the *LCOE* evaluation, revenues are only considered when there exist side effects of the generation, such as subsidies, externalities, internalities or benefits due to cogeneration. It also must be noted that, in the *LCOE* evaluation, costs are considered positive, while revenues are negative. Taxes are not included.

$$LCOE_G = \frac{\sum_{i=0}^{n} \frac{NC_i^G}{(1+d)^i}}{P_G \cdot \sum_{i=1}^{n} \frac{EOH_i^G}{(1+d)^i}}.$$

Equation 2.19

It must be highlighted that the equivalent operating hours of the generator may vary for each period of its lifespan, but in any case, $EOH_i^G \leq 8760$ h/year, i.e., the capacity factor of the generator cannot be higher than 1.

2.4.4. LCOE of combined generation and storage systems

Energy Storage Systems or ESS devices store surplus energy, i.e., not served energy, and shifts it to another period. An ESS can be modelled as a generator working in parallel with the others, with the difference that it is not fed by an external input of primary energy source, but by the energy from the system, as represented in Figure 2.2, where E_{ESS}^{CH} and E_{ESS}^{DCH} are, respectively, the energy charged and discharged by the storage device.

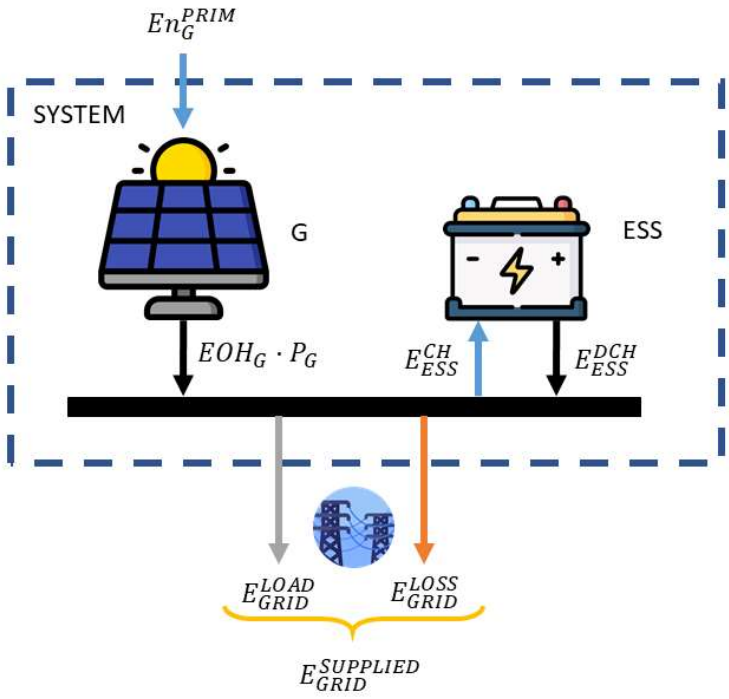

Figure 2.2. Representation of a combined generation and energy storage system.

Analogously to the analysis performed in the previous case, the energy balance of the system, applying a single-bus model analysis, is expressed in Equation 2.20:

$$E_G + E_{ESS}^{DCH} = E_{GRID}^{SUPPLIED} + E_{ESS}^{CH}.$$

Equation 2.20

Applying again Equation 2.9 to the case, the *LCOE* for this combined system is also referred to the served energy, that in this case does not coincide with the generated energy E_G. It can be deduced that the equivalent operating hours of the generator can increase (i.e., its curtailed energy can be reduced) because of the ESS presence, although there are some losses (difference between the discharged and the charged energy) due to the charging and discharging efficiency. Moreover, in this case, the total costs include not only those related with the generator (described in the previous section), but also those related with the ESS. The *LCOE* of combined generation and storage systems, $LCOE_{G+ESS}$, can be calculated by Equation 2.21:

$$LCOE_{G+ES} = \frac{\sum_{i=0}^{n} \frac{NC_i}{(1+d)^i}}{\sum_{i=1}^{n} \frac{E_i^{SUPPLIED}}{(1+d)^i}} = \frac{\sum_{i=0}^{n} \left[\frac{NC_i^G}{(1+d)^i} + \frac{NC_i^{ESS}}{(1+d)^i} + \frac{Costs_i^{SYST}}{(1+d)^i}\right]}{\sum_{i=1}^{n} \left[P_G \cdot \frac{EOH_i^G}{(1+d)^i} + \frac{(E_{ESS}^{DCH} - E_{ESS}^{CH})_i}{(1+d)^i}\right]},$$

Equation 2.21

where NC_i^G, NC_i^{ESS} are the yearly capital and operating costs related to the generator and the storage, respectively, and $Costs^{SYST}$ is an extra cost term that represents the costs of integrating and coordinating of the generator and the ESS, that cannot be associated to the individual devices. It must be also observed that, in this setting, the lifespan of the project (n) can differ from the expected useful lifespan of each device (n_G and n_{ESS}, respectively). The lifespan to be considered is represented by the useful lifespan of the generation unit ($n = n_G$), as without the generation unit, the ESS device cannot work. Then, if $n_G > n_{ESS}$, two approaches can be considered: (i) when the lifespan of the ESS ends, no storage capacity is available until the end of the lifespan of the project, with a consequent negative impact on the *EOH* of the generator; (ii) when the lifespan of the ESS ends, the old device is replaced by a new one. In this case, additional $CAPEX_i$ must be considered at the replacement time and, in a strict analysis, an economic

valorization of the new device at time period *n* (if its useful lifespan has not ended) must be included as a revenue[2]. However, an intermediate third approach, although less precise, is usually adopted, according to which the replacement costs are prorated among the lifespan of the project and included in the *OPEX* of the ESS. In all the presented cases, the adopted strategy should be clearly indicated.

Equation 2.21 can be rewritten reordering the terms in the denominator and splitting the terms in the numerator:

$$LCOE_{G+ESS} = \frac{\sum_{i=0}^{n} \frac{NC_i^G}{(1+d)^i} + \sum_{i=0}^{n} \frac{NC_i^{ESS}}{(1+d)^i} + \sum_{i=0}^{n} \frac{Costs_i^{SYST}}{(1+d)^i}}{\sum_{i=1}^{n} \left[\frac{(P_G \cdot EOH_G - E_{ESS}^{CH})_i}{(1+d)^i} + \frac{(E_{ESS}^{DCH})_i}{(1+d)^i}\right]},$$

Equation 2.22

If the first approach is adopted (the second approach will be presented in the next section applied to a polygeneration system), i.e., there is no replacement of the devices $(n \geq n_G \geq n_{ESS})$, Equation 2.22 can be expressed as a function of the *LCOE* of the generator, the *LCOS* of the stored energy and a virtual *LCOE* related to the integrating and coordinating costs:

$$LCOE_{G+ESS} = f_G \cdot LCOE_G + f_{ESS} \cdot LCOS_{ESS} + LCOE'_{SYST},$$

Equation 2.23

where f_G and f_{ESS} are the participation factors of the generator and the ESS, respectively, the $LCOE_G$ is the Levelized Cost of Electricity for the generator with energy curtailment, i.e., considering it produces $E_G^{MAX} - E_G^{CURT} = P_G \cdot EOH_G - E_{ESS}^{CH}$, and the $LCOS_{ESS}$ is the Levelized Cost of Storage of the ESS, defined in Equation 2.26, while $LCOE'_{SYST}$ indicates the virtual *LCOE* of the system costs, as defined in Equation 2.27.

[2] Several approaches can be considered to estimate the remaining value of an asset. Commonly, it is estimated considering a linear amortization of the *CAPEX* (see Equation 2.36).

$$f_G = \frac{\sum_{i=1}^{n_G} \frac{(P_G \cdot EOH_G - E_{ESS}^{CH})_i}{(1+d)^i}}{\sum_{i=1}^{n} \left[\frac{(P_G \cdot EOH_G - E_{ESS}^{CH})_i}{(1+d)^i} + \frac{(E_{ESS}^{DCH})_i}{(1+d)^i}\right]}.$$

Equation 2.24

$$f_{ESS} = \frac{\sum_{i=1}^{n_{ESS}} \frac{(E_{ESS}^{DCH})_i}{(1+d)^i}}{\sum_{i=1}^{n} \left[\frac{(P_G \cdot EOH_G - E_{ESS}^{CH})_i}{(1+d)^i} + \frac{(E_{ESS}^{DCH})_i}{(1+d)^i}\right]}.$$

Equation 2.25

$$LCOS_{ESS} = \frac{\sum_{i=0}^{n_{ESS}} \frac{NC_i^{ESS}}{(1+d)^i}}{\sum_{i=1}^{n_{ESS}} \frac{(E_{ESS}^{DCH})_i}{(1+d)^i}},$$

Equation 2.26

$$LCOE'_{SYST} = \frac{\sum_{i=0}^{n} \frac{Costs_i^{SYST}}{(1+d)^i}}{\sum_{i=1}^{n} \left[\frac{(P_G \cdot EOH_G - E_{ESS}^{CH})_i}{(1+d)^i} + \frac{(E_{ESS}^{DCH})_i}{(1+d)^i}\right]},$$

Equation 2.27

It must be observed in Equation 2.24 that the participation factor of the generator G is defined according to the curtailed equivalent operating hours, i.e. the energy provided by the generator in case it does not account with an ESS. Then, the $LCOE_G$ considering the generator working alone must be used in Equation 2.23 [3]. Moreover, in Equation 2.26, it must be recalled that the *LCOS* is defined with reference to the discharged energy of the ESS, independently of the needed charged energy on the device. Finally, the *LCOE* associated with the system integration is referred to the total supplied energy to the grid by the combination of the generator and the ESS.

[3] In Equation 2.23, the $LCOE_G$ refers to that calculated for a curtailed generation capacity, i.e., $P_G \cdot EOH_G - E_{ESS}^{CH}$. If other $LCOE_G$ value is used, then the numerator of Equation 2.24 must be in accordance.

2.4.5. LCOE of polygeneration systems

Polygeneration systems have become increasingly popular in recent years along with the increasing attention devoted to integration of traditional and renewable energy sources. Polygeneration means to use several generators and the same energy vector within a single integrated process (therefore differently with multi-vector energy systems, which will be analyzed in detail in Section 2.7). Figure 2.3 shows an example of a polygeneration system with two different generators, G1 and G2, these two-last used as subscripts for each analyzed quantity.

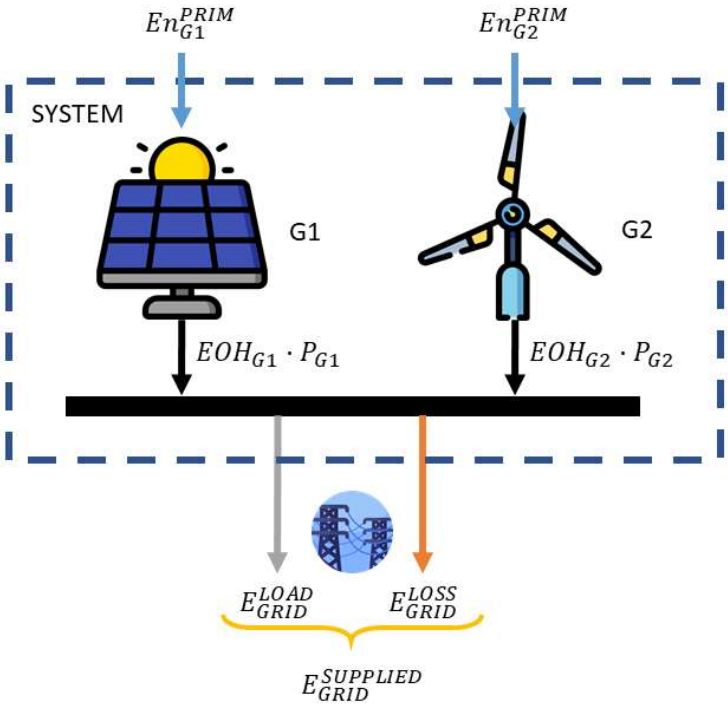

Figure 2.3. Representation of a polygeneration system.

In this case, the energy balance of the system is expressed as follows:

$$E_{G1} + E_{G2} = (EOH_{G1} \cdot P_{G1}) + (EOH_{G2} \cdot P_{G2}) = E_{GRID}^{SUPPLIED}.$$

Equation 2.28

Analogously to the combined generation and energy storage system, analyzed in the previous section, it is possible that the generation units have different lifespan values. Then, two approaches can be adopted:

a) The generation units are not replaced when their useful lifespan ends. Then the *LCOE* can be expressed as indicated in Equation 2.29:

$$LCOE_{G1+G2} = \frac{\sum_{i=0}^{n_{G1}} \frac{NC_i^{G1}}{(1+d)^i} + \sum_{i=0}^{n_{G2}} \frac{NC_i^{G2}}{(1+d)^i} + \sum_{i=0}^{\max(n_{G1},n_{G2})} \frac{Costs_i^{SYST}}{(1+d)^i}}{P_{G1} \cdot \sum_{i=1}^{n_{G1}} \frac{EOH_i^{G1}}{(1+d)^i} + P_{G2} \cdot \sum_{i=1}^{n_{G2}} \frac{EOH_i^{G2}}{(1+d)^i}}.$$

Equation 2.29

In this case, the integrating and coordinating costs of the different units ($Costs^{SYST}$) have been considered that persist until the last generator remains plugged to the system. However, running the system when a significant part of the generators decease is usually inefficient and thus, it can be set a lifespan of the system $n \leq \max(n_{G1}, n_{G2})$.

Similarly to Equation 2.22, Equation 2.29 can be expressed in terms of the individual *LCOE*s for each generation unit, as depicted in Equation 2.30:

$$LCOE_{G1+G2} = f_{G1} \cdot LCOE_{G1} + f_{G2} \cdot LCOE_{G2} + LCOE'_{SYST},$$

Equation 2.30

where f_{G1} and f_{G2} represent the participation factors of the generators G1 and G2 respectively, while the term $LCOE'_{SYST}$ represents the virtual Levelized Cost of the Electricity associated to the integration and coordination infrastructure.

$$f_{G1} = \frac{P_{G1} \cdot \sum_{i=1}^{n_{G1}} \frac{EOH_i^{G1}}{(1+d)^i}}{\sum_{i=1}^{n} \left\{ \sum_{j=1}^{2} \left[P_{Gj} \cdot \frac{EOH_i^{Gj}}{(1+d)^i} \right] \right\}}.$$

Equation 2.31

$$f_{G2} = \frac{P_{G2} \cdot \sum_{i=1}^{n_{G2}} \frac{EOH_i^{G2}}{(1+d)^i}}{\sum_{i=1}^{n} \left\{ \sum_{j=1}^{2} \left[P_{Gj} \cdot \frac{EOH_i^{Gj}}{(1+d)^i} \right] \right\}}.$$

Equation 2.32

$$LCOE'_{SYST} = \frac{\sum_{i=0}^{n} \frac{Costs_i^{SYST}}{(1+d)^i}}{\sum_{i=1}^{n} \left\{ \sum_{j=1}^{2} \left[P_{Gj} \cdot \frac{EOH_i^{Gj}}{(1+d)^i} \right] \right\}}.$$

Equation 2.33

b) The generation units are replaced when their useful lifespan ends. Then, a total lifespan of the system must be considered, which would be the maximum lifespan of all the devices, not greater than an overall maximum lifespan for the system, n_{lim}:

$$n = min[max(n_{G1}, n_{G2}), n_{lim}].$$

Equation 2.34

In this case, the generation units whose lifespan are lower than the most durable, must be replaced, adding capital costs in the replacement time period ($n_{Gj}+1$). Supposing that $n=n_{G1}$ and $n_{G2} < n_{G1}$, then the *LCOE* can be expressed as indicated in Equation 2.35:

$$LCOE_{G1+G2} = \frac{\sum_{i=0}^{n} \left[\frac{NC_i^{G1}}{(1+d)^i} + \frac{NC_i^{G2}}{(1+d)^i} + \frac{Costs_i^{SYST}}{(1+d)^i} \right] - \frac{RV_{G2}}{(1+d)^n}}{\sum_{i=1}^{n} \left[P_{G1} \cdot \frac{EOH_i^{G1}}{(1+d)^i} + P_{G2} \cdot \frac{EOH_i^{G2}}{(1+d)^i} \right]}.$$

Equation 2.35

The term RV_{G2} in Equation 2.35 refers to the residual value of the second generator in the case the new G2 unit installed at time n_{G2}+1 does not end its useful lifespan at the same time than that considered for the whole system. As stated in the previous section,

this residual value can be estimated through several methods. One of the most commonly used is to estimate a linear depreciation of the device, and thus, its residual value can be estimated as:

$$RV_{G2} = \left[ceil\left(\frac{n}{n_{G2}}\right) - \frac{n}{n_{G2}}\right] \cdot [CAPEX_0^{G2} \cdot \beta_{G2}],$$

Equation 2.36

β_{G2} being a reduction costs factor that accounts for the loss of the asset value (it should be defined as a function of time, as it must be evaluated at time step $z \cdot n_{G2} + 1$), regardless of its degree of wear and that is accounted at the last replacement time, $z \cdot n_{G2}$, where $z = floor\left(\frac{n}{n_{G2}}\right)$.

Equation 2.35 can be expressed as a function of the *LCOE* values of the generators, as it can be seen in Equation 2.37, keeping the assumption that $n = n_{G1} > n_{G2}$:

$$LCOE_{G1+G2} = f'_{G1} \cdot LCOE_{G1} + f'_{G2} \cdot LCOE'_{G2} + LCOE'_{SYST},$$

Equation 2.37

where $LCOE_{G1}$ is calculated according to Equation 2.19. As the lifespan of the generator G2 has been considered lower than the one of generator G1, its participation factor and *LCOE* values must be "normalized" to the considered lifespan of the system (n). Thus, Equation 2.38 shows the normalized participation factor for generator G2, while Equation 2.39 shows the definition of its normalized *LCOE*.

$$f'_{G2} = \frac{P_{G2} \cdot \sum_{i=1}^{n_{G2}} \frac{EOH_i^{G2}}{(1+d)^i}}{\sum_{i=1}^{n} \left\{\sum_{j=1}^{2} \left[P_{Gj} \cdot \frac{EOH_i^{Gj}}{(1+d)^i}\right]\right\}}.$$

Equation 2.38

$$LCOE'_{G2} = \frac{\sum_{i=1}^{n_{G2}} \frac{EOH_i^{G2}}{(1+d)^i}}{\sum_{i=1}^{n} \frac{EOH_i^{G2}}{(1+d)^i}} \cdot LCOE_{G2} + \frac{\sum_{z=1}^{floor\left(\frac{n}{n_{G2}}\right)} \left\{ \sum_{i=z\cdot n_{G2}+1}^{min[(z+1)\cdot n_{G2},n]} \left[\frac{NC_i^{G2}}{(1+d)^i} \right] \right\} - \frac{RV_{G2}}{(1+d)^n}}{P_{G2} \cdot \sum_{i=1}^{n} \frac{EOH_i^{G2}}{(1+d)^i}},$$

Equation 2.39

being $floor\left(\frac{n}{n_{G2}}\right)$ the number of times generator G2 is replaced during the lifespan of the system. It must be also noted that, for the replacement of the devices, the nominal $CAPEX_{0'}^{G2}$ might be reduced due to a reduction cost factor[4], as considered in the evaluation of the residual value of the asset, RV_{G2} (see Equation 2.36).

Moreover, it must be remarked that a polygeneration system can include one or several ESS devices. In this case, one should consider the economic modelling of the storage devices presented in Section 2.4.4 and the extension of Equations 2.30 or 2.37 for more than two devices. Equation 2.40 shows the *LCOE* calculation for a general polygeneration system with energy storage:

$$LCOE_{POLY} = \sum_{j=1}^{J} \left(f'_{Gj} \cdot LCOE'_{Gj} \right) + \sum_{k=1}^{K} \left(f'_{ESSk} \cdot LCOS'_{ESSk} \right) + LCOE'_{SYST},$$

Equation 2.40

where the normalized participation factors and *LCOE* values for both the generators and the ESS devices can be calculated as follows:

[4] *0'* refers to the initial time step of the replaced asset relative to its lifespan, which will be the $z \cdot n_{G2} + 1$ time step in the absolute time reference system. Then, $CAPEX_{0'}^{G2} = CAPEX_0^{G2} \cdot \beta_{G2}$.

$$f'_{Gj} = \frac{P_{Gj} \cdot \sum_{i=1}^{n_{Gj}} \frac{EOH_i^{Gj}}{(1+d)^i}}{\sum_{i=1}^{n} \left\{ \sum_{\gamma=1}^{\Gamma} \left[P_{G\gamma} \cdot \frac{EOH_i^{G\gamma}}{(1+d)^i} \right] + \sum_{\delta=1}^{\Delta} \frac{\left(E_{ESS\delta}^{DCH} - E_{ESS\delta}^{CH}\right)_i}{(1+d)^i} \right\}},$$

Equation 2.41

where Γ is the total number of generators and Δ the total number of ESS devices.

$$LCOE'_{Gj} = \frac{\sum_{i=1}^{n_{Gj}} \frac{EOH_i^{Gj}}{(1+d)^i}}{\sum_{i=1}^{n} \frac{EOH_i^{Gj}}{(1+d)^i}} \cdot LCOE_{Gj} + \frac{\sum_{z=1}^{floor\left(\frac{n}{n_{Gj}}\right)} \left\{ \sum_{i=z \cdot n_{Gj}+1}^{min[(z+1) \cdot n_{Gj}, n]} \left[\frac{NC_i^{Gj}}{(1+d)^i} \right] \right\} - \frac{RV_{Gj}}{(1+d)^n}}{P_{Gj} \cdot \sum_{i=1}^{n} \frac{EOH_i^{Gj}}{(1+d)^i}},$$

Equation 2.42

$$f'_{ESSk} = \frac{\sum_{i=1}^{n_{ESSk}} \frac{\left(E_{ESSk}^{DCH}\right)_i}{(1+d)^i}}{\sum_{i=1}^{n} \left\{ \sum_{\gamma=1}^{\Gamma} \left[P_{G\gamma} \cdot \frac{EOH_i^{G\gamma}}{(1+d)^i} \right] + \sum_{\delta=1}^{\Delta} \frac{\left(E_{ESS\delta}^{DCH} - E_{ESS\delta}^{CH}\right)_i}{(1+d)^i} \right\}}.$$

Equation 2.43

$$LCOS'_{ESSk} = \frac{\sum_{i=1}^{n_{ESSk}} \frac{(E_{ESSk}^{DCH})_i}{(1+d)^i}}{\sum_{i=1}^{n} \frac{(E_{ESSk}^{DCH})_i}{(1+d)^i}} \cdot LCOS_{ESSk} + \frac{\sum_{z=1}^{floor\left(\frac{n}{n_{ESSk}}\right)} \left\{ \sum_{i=z\cdot n_{ESSk}+1}^{min[(z+1)\cdot n_{ESSk}, n]} \left[\frac{NC_i^{ESSk}}{(1+d)^i} \right] \right\} - \frac{RV_{ESSk}}{(1+d)^n}}{\sum_{i=1}^{n} \frac{(E_{ESSk}^{DCH})_i}{(1+d)^i}},$$

Equation 2.44

Accordingly to the previous equations, the virtual *LCOE* of the integration and coordination infrastructure must be modified, as expressed in Equation 2.45.

$$LCOE'_{SYST} = \frac{\sum_{i=0}^{n} \frac{Costs_i^{SYST}}{(1+d)^i}}{\sum_{i=1}^{n} \left\{ \sum_{j=1}^{J} \left[P_{Gj} \cdot \frac{EOH_i^{Gj}}{(1+d)^i} \right] + \sum_{k=1}^{K} \frac{(E_{ESSk}^{DCH} - E_{ESSk}^{CH})_i}{(1+d)^i} \right\}}.$$

Equation 2.45

2.4.6. LCOE of a power grid costumer

In Figure 2.4 it is shown the case of a power costumer plugged to an external power grid. The power grid can be modelled as a generator which supplies power to the system by consuming a primary energy source, which is electrical energy, and null *CAPEX* and *OPEX* if the electrical connection infrastructure already exists and it is operated and maintained by the DSO.

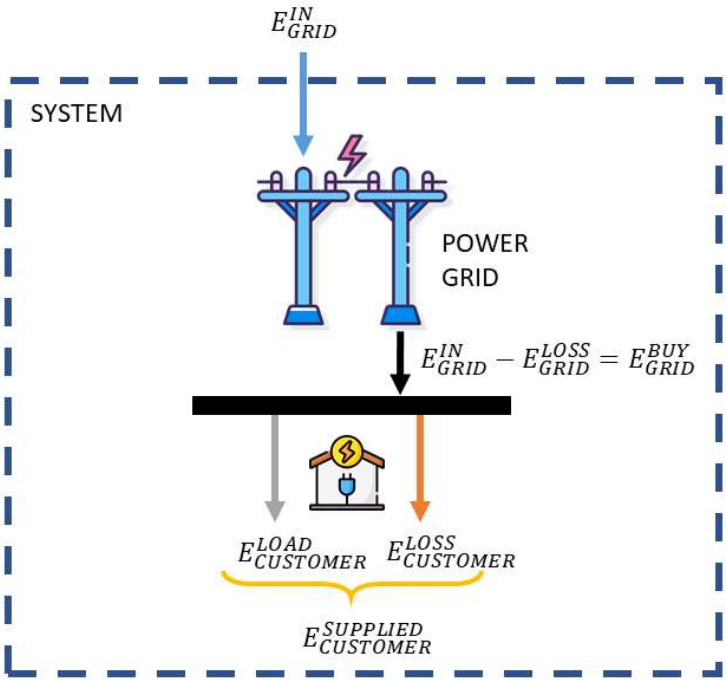

Figure 2.4. Representation of an electrical microgrid fed by the external power grid.

If a single-bus analysis is applied to the described system, the energy balance can be expressed as:

$$E_{GRID}^{IN} - E_{GRID}^{LOSS} = E_{GRID}^{BUY} = E_{CUSTOMER}^{LOAD} + E_{CUSTOMER}^{LOSS} = E_{CUSTOMER}^{SUPPLIED}.$$

Equation 2.46

Then, analogously to the previous conducted analysis, the *LCOE* of this system ($LCOE_{GRID\ CUSTOMER}$) can be defined as expressed in Equation 2.47. It must be noted that the *LCOE* is referred to the supplied energy to the customer. Moreover, if *CAPEX* and *OPEX* are considered null, costs are only related with the withdrawn electricity. In this case, the *LCOE* equals the weighted average price of the electricity purchased from the grid if this price remains constant for each time period.

$$LCOE_{GRID\ COSTUMER} = \frac{\sum_{i=0}^{n} \frac{Costs_i^{GRID}}{(1+d)^i}}{\sum_{i=1}^{n} \frac{(E_{GRID}^{BUY})_i}{(1+d)^i}} = \frac{\sum_{i=0}^{n} \frac{(p \cdot E_{GRID}^{BUY})_i}{(1+d)^i}}{\sum_{i=1}^{n} \frac{(E_{GRID}^{BUY})_i}{(1+d)^i}} = \bar{p}.$$

Equation 2.47

2.4.7. LCOE of electrical microgrids

As presented and defined in the first chapter, a microgrid is a set of interconnected loads and distributed energy resources within clearly defined electrical boundaries that acts as a single controllable entity with respect to the grid. Moreover, it is conceived to operate connected and disconnected to the power grid and accounts with generators and ESS devices. Figure 2.5 represents a simple microgrid that accounts with a power generator, such as a solar PV plant, and it is connected to the external power grid with the capability not only to purchase electricity from the grid, but also to inject (and sell) electricity, following the microgrid's EMS defined strategy.

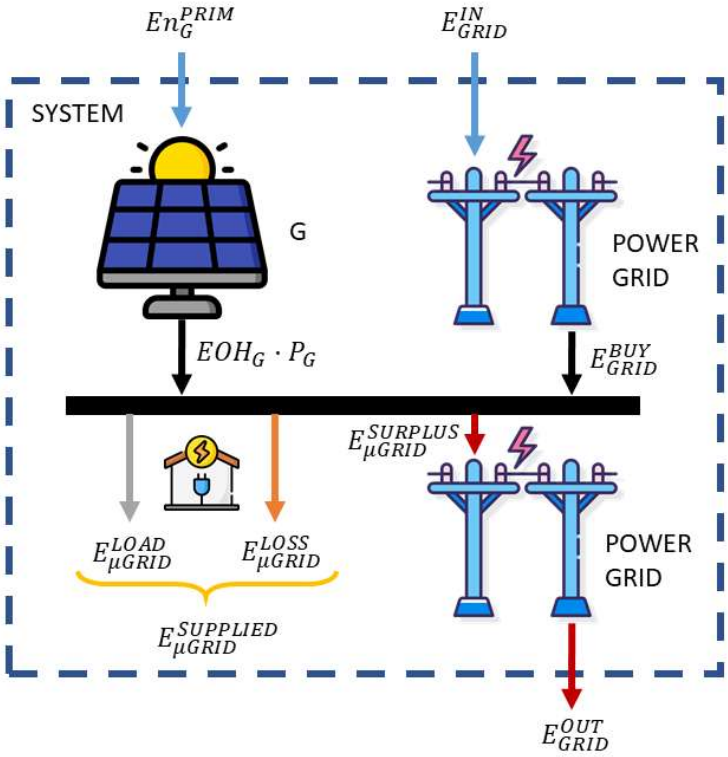

Figure 2.5. Representation of an electrical microgrid with a PV plant connected to the power grid.

Electrical microgrids manage and dispatch several generators which exploit different sources for several reasons, including the minimization of power delivery risks, the minimization of operation costs or the maximization of the exploitation of the local natural resources. The literature in this regard mainly generalizes the concept of the *LCOE* to the different existing units. By way of example, in [37], the *LCOE* evaluation includes the grid supplied energy through an additional cost term and considers the total

energy consumption, rather than the produced energy. On the other hand, [38] makes a step forward deriving *LCOE* from the total aggregated cost of the distributed energy resources and the total energy generated. However, integration costs, as well as auxiliary systems or benefits from the grid are not explicitly accounted for. In [39] proposes a new formulation of the LCOE for microgrids considering the sum of discounted costs and the sum of discounted energy demands of the site.

Focusing on the case of a pure electrical microgrid, such as the one represented in Figure 2.5, the energy balance of the system can be expressed as:

$$E_G + E_{GRID}^{BUY} = E_{\mu GRID}^{SUPPLIED} + E_{\mu GRID}^{SURPLUS}.$$

Equation 2.48

Applying again Equation 2.9 to the case, it can be observed that the *LCOE* for this system is still referred to the supplied energy (as expressed in Equation 2.47). However, this quantity does not coincide with the generated energy (E_G) because part of the electricity supply is provided by the external grid. Moreover, part of the generated energy is injected back to the power grid ($E_{GRID}^{OUT} = E_{\mu GRID}^{SURPLUS} - E_{GRID}^{LOSS}$). Then, the result can be expressed as shown in Equation 2.49:

$$LCOE_{\mu GRID} = \frac{\sum_{i=0}^{n} \left[\frac{NC_i^G}{(1+d)^i} + \frac{Costs_i^{GRID}}{(1+d)^i} + \frac{Costs_i^{SYST}}{(1+d)^i} - \frac{Revenues_i^{GRID}}{(1+d)^i} \right]}{\sum_{i=1}^{n} \left[P_G \cdot \frac{EOH_i^G}{(1+d)^i} + \frac{\left(E_{GRID}^{BUY} - E_{\mu GRID}^{SURPLUS}\right)_i}{(1+d)^i} \right]}.$$

Equation 2.49

In Equation 2.49, the term of costs associated with the grid ($Costs_{GRID}$) are those related with the purchase of electricity, or in other terms:

$$Costs_{GRID} = CAPEX_{GRID} + OPEX_{GRID} + E_{GRID}^{BUY} \cdot \bar{p}_{GRID}^{BUY}.$$

Equation 2.50

On the other hand, in Equation 2.49, the term of revenues associated with the grid ($Revenues_{GRID}$) are those related with the sale of surplus energy:

$$Revenues_{GRID} = E_{GRID}^{OUT} \cdot \bar{p}_{GRID}^{SALE}.$$

Equation 2.51

Accordingly to previous analysis, Equation 2.49 can be expressed as a function of the *LCOEs* of the connected devices to the microgrid:

$$LCOE_{\mu GRID} = f''_G \cdot LCOE'_G + f''^{BUY}_{GRID} \cdot LCOE_{GRID} + LCOE''_{SYST} - f''^{SURPLUS}_{\mu GRID} \cdot LROE_{GRID}.$$

Equation 2.52

In Equation 2.52, *f''* indicates the participation factor of each energy source referred to the energy served to the microgrid, as defined in Equations 2.53, 2.54 and 2.55, while *LROE* indicates the "Levelized Revenues of Electricity", which can be defined as the discounted revenues due to the electricity sold to the power grid and other revenues, such as the provision of ancillary services or increase of the system resilience.

$$f''_G = \frac{P_G \cdot \sum_{i=1}^{n} \frac{EOH_i^G}{(1+d)^i}}{\sum_{i=1}^{n} \left[P_G \cdot \frac{EOH_i^G}{(1+d)^i} + \frac{\left(E_{GRID}^{BUY} - E_{\mu GRID}^{SURPLUS}\right)_i}{(1+d)^i} \right]}.$$

Equation 2.53

$$f''^{BUY}_{GRID} = \frac{\sum_{i=1}^{n} \frac{(E_{GRID}^{BUY})_i}{(1+d)^i}}{\sum_{i=1}^{n} \left[P_G \cdot \frac{EOH_i^G}{(1+d)^i} + \frac{\left(E_{GRID}^{BUY} - E_{\mu GRID}^{SURPLUS}\right)_i}{(1+d)^i} \right]}.$$

Equation 2.54

$$f''^{SURPLUS}_{\mu GRID} = \frac{\sum_{i=1}^{n} \frac{\left(E_{\mu GRID}^{SURPLUS}\right)_i}{(1+d)^i}}{\sum_{i=1}^{n} \left[P_G \cdot \frac{EOH_i^G}{(1+d)^i} + \frac{\left(E_{GRID}^{BUY} - E_{\mu GRID}^{SURPLUS}\right)_i}{(1+d)^i} \right]}.$$

Equation 2.55

It must be noted in Equation 2.52 that the $LCOE'_G$ is used instead of the $LCOE_G$. This is due to the lifespan of the system (the microgrid), *n*, may not be the same than the

lifespan of the generator, n_G. Thus, the *LCOE* value for the generator must be normalized to the lifespan of the microgrid, by Equation 2.42. In the case that the lifespan of the microgrid coincides with that of the generator ($n = n_G$), the *LCOE* for the generation unit can be used.

The *LCOE* for the electricity purchased from the power grid is expressed in Equation 2.56, while the *LROE* of the electricity sold is shown in Equation 2.57.

$$LCOE_{GRID} = \frac{\sum_{i=0}^{n} \frac{Costs_i^{GRID}}{(1+d)^i}}{\sum_{i=1}^{n} \frac{(E_{GRID}^{BUY})_i}{(1+d)^i}}.$$

Equation 2.56

$$LROE_{GRID} = \frac{\sum_{i=1}^{n} \frac{Revenues_i^{GRID}}{(1+d)^i}}{\sum_{i=1}^{n} \frac{\left(E_{\mu GRID}^{SURPLUS}\right)_i}{(1+d)^i}}.$$

Equation 2.57

In the case the sale and purchase prices of electricity remain constant for each time period and the *CAPEX* and *OPEX* for the grid connection are not considered or neglected, then $LCOE_{GRID} = \bar{p}_{GRID}^{BUY}$ and $LROE_{GRID} = \bar{p}_{GRID}^{SALE}$.

Finally, Equation 2.58 shows the normalized *LCOE* of the integration and coordination infrastructure referenced to the supplied energy:

$$LCOE''_{SYST} = \frac{\sum_{i=0}^{n} \frac{Costs_i^{SYST}}{(1+d)^i}}{\sum_{i=1}^{n} \left[P_G \cdot \frac{EOH_i^G}{(1+d)^i} + \frac{\left(E_{GRID}^{BUY} - E_{\mu GRID}^{SURPLUS}\right)_i}{(1+d)^i} \right]}.$$

Equation 2.58

The previously analyzed case can be extended to other configurations. For instance, Figure 2.6 represents also a microgrid, but in this case includes a multi-vector energy

generator, such as a CHP unit. It is also connected to the external power grid and has the capability not only to purchase electricity from the grid, but also to inject it.

In this case, the only difference with respect to the microgrid presented in Figure 2.5 is that the CHP unit produces not only electricity but also heat to serve a heating demand. When calculating the *LCOE* of this system, the heating generation is not considered as a served or supplied product but a side effect of the electricity generation. Thus, this side effect must be accounted in the net costs of the generation unit, also with other externalities, internalities or other revenues linked to that generator, such as the avoided costs due to the fact that thermal energy is produced with the CHP unit instead of using a boiler. With this consideration, the set of Equations 2.52-2.58 also apply for this system.

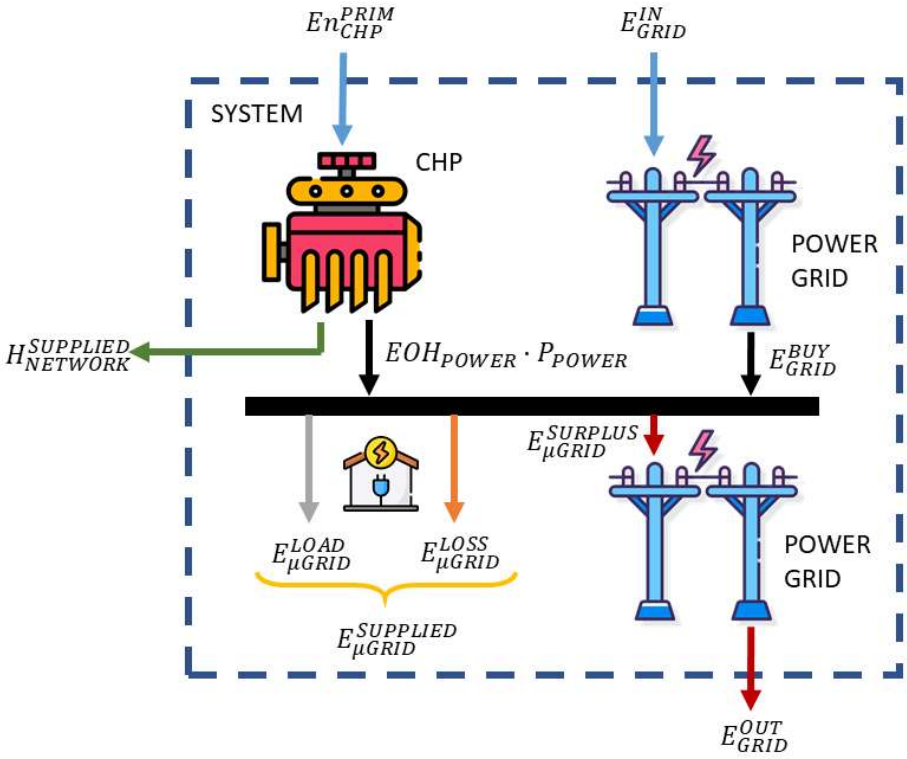

Figure 2.6. Representation of an electrical microgrid with a CHP unit and connected to the power grid.

Moreover, the presented approach for the *LCOE* evaluation of a microgrid can be generalized to a polygeneration system with several ESS devices, such that shown in Figure 2.7.

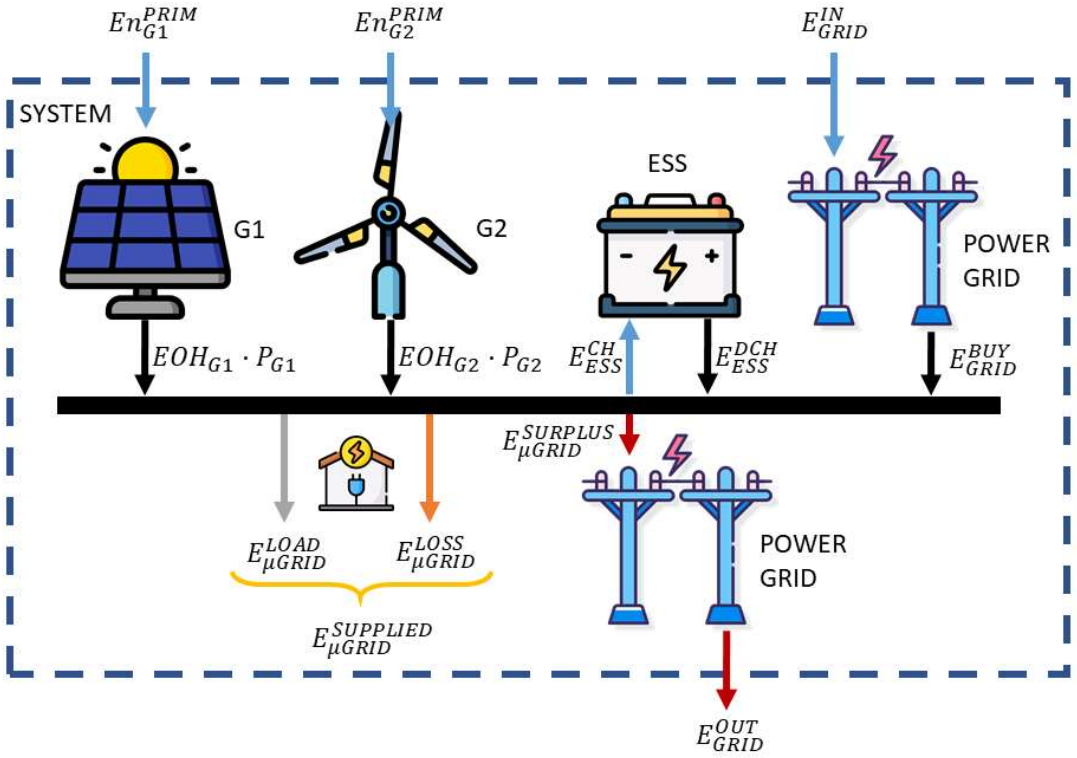

Figure 2.7. Representation of an electrical polygeneration microgrid with ESS devices connected to the power grid.

Equation 2.59 shows the generalized expression for the *LCOE* of an electrical microgrid with energy storage systems.

$$LCOE_{\mu GRID} = \sum_{j=1}^{J}\left(f''_{Gj} \cdot LCOE'_{Gj}\right) + \sum_{k=1}^{K}\left(f''_{ESSk} \cdot LCOS'_{ESSk}\right) + f''^{BUY}_{GRID} \cdot LCOE_{GRID} + LCOE''_{SYST} - f''^{SURPLUS}_{\mu GRID} \cdot LROE_{GRID}.$$

Equation 2.59

The participation factors and $LCOE''_{SYST}$ must be calculated as shown by the following expressions:

$$f''_{Gj} = \frac{P_{Gj} \cdot \sum_{i=1}^{n} \frac{EOH_i^{Gj}}{(1+d)^i}}{\sum_{i=1}^{n} \left\{ \sum_{\gamma=1}^{\Gamma} \left[P_{G\gamma} \cdot \frac{EOH_i^{G\gamma}}{(1+d)^i} \right] + \sum_{\delta=1}^{\Delta} \left[\frac{\left(E_{ESS\delta}^{DCH} - E_{ESS\delta}^{CH}\right)_i}{(1+d)^i} \right] + \frac{\left(E_{GRID}^{BUY} - E_{\mu GRID}^{SURPLUS}\right)_i}{(1+d)^i} \right\}}.$$

Equation 2.60

$$f''_{ESSk} = \frac{\sum_{i=1}^{n} \frac{(E_{ESSk}^{DCH})_i}{(1+d)^i}}{\sum_{i=1}^{n} \left\{ \sum_{\gamma=1}^{\Gamma} \left[P_{G\gamma} \cdot \frac{EOH_i^{G\gamma}}{(1+d)^i} \right] + \sum_{\delta=1}^{\Delta} \left[\frac{\left(E_{ESS\delta}^{DCH} - E_{ESS\delta}^{CH}\right)_i}{(1+d)^i} \right] + \frac{\left(E_{GRID}^{BUY} - E_{\mu GRID}^{SURPLUS}\right)_i}{(1+d)^i} \right\}}.$$

Equation 2.61

$$f''^{BUY}_{GRID} = \frac{\sum_{i=1}^{n} \frac{(E_{GRID}^{BUY})_i}{(1+d)^i}}{\sum_{i=1}^{n} \left\{ \sum_{\gamma=1}^{\Gamma} \left[P_{G\gamma} \cdot \frac{EOH_i^{G\gamma}}{(1+d)^i} \right] + \sum_{\delta=1}^{\Delta} \left[\frac{\left(E_{ESS\delta}^{DCH} - E_{ESS\delta}^{CH}\right)_i}{(1+d)^i} \right] + \frac{\left(E_{GRID}^{BUY} - E_{\mu GRID}^{SURPLUS}\right)_i}{(1+d)^i} \right\}}.$$

Equation 2.62

$$f''^{SURPLUS}_{\mu GRID} = \frac{\sum_{i=1}^{n} \frac{\left(E_{\mu GRID}^{SURPLUS}\right)_i}{(1+d)^i}}{\sum_{i=1}^{n} \left\{ \sum_{\gamma=1}^{\Gamma} \left[P_{G\gamma} \cdot \frac{EOH_i^{G\gamma}}{(1+d)^i} \right] + \sum_{\delta=1}^{\Delta} \left[\frac{\left(E_{ESS\delta}^{DCH} - E_{ESS\delta}^{CH}\right)_i}{(1+d)^i} \right] + \frac{\left(E_{GRID}^{BUY} - E_{\mu GRID}^{SURPLUS}\right)_i}{(1+d)^i} \right\}}.$$

Equation 2.63

$$LCOE''_{SYST} = \frac{\sum_{i=0}^{n} \frac{Costs_i^{SYST}}{(1+d)^i}}{\sum_{i=1}^{n} \left\{ \sum_{\gamma=1}^{\Gamma} \left[P_{G\gamma} \cdot \frac{EOH_i^{G\gamma}}{(1+d)^i} \right] + \sum_{\delta=1}^{\Delta} \left[\frac{\left(E_{ESS\delta}^{DCH} - E_{ESS\delta}^{CH}\right)_i}{(1+d)^i} \right] + \frac{\left(E_{GRID}^{BUY} - E_{\mu GRID}^{SURPLUS}\right)_i}{(1+d)^i} \right\}}.$$

Equation 2.64

2.5. Levelized Cost of Stored Energy (*LCOS*)

The *LCOEn* methodology can also be applied to domains others than the generation technologies so far, such as the energy storage or the demand response applications. As presented in the previous section by Equation 2.26 (recalled here for clearness), some academics and energy policy makers have introduced the "Levelized Cost of Storage" (*LCOS*) indicator [40]:

$$LCOS_{ESS} = \frac{\sum_{i=0}^{n_{ESS}} \frac{NC_i^{ESS}}{(1+d)^i}}{\sum_{i=1}^{n_{ESS}} \frac{(E_{ESS}^{DCH})_i}{(1+d)^i}} = \frac{\sum_{i=0}^{n_{ESS}} \left[\frac{CAPEX_i}{(1+d)^i} + \frac{OPEX_i}{(1+d)^i} + \frac{(p \cdot E_{ESS}^{CH})_i}{(1+d)^i} + \frac{Other\ costs_i}{(1+d)^i} - \frac{Revenues_i}{(1+d)^i} \right]}{\sum_{i=1}^{n_{ESS}} \frac{(E_{ESS}^{DCH})_i}{(1+d)^i}}.$$

Equation 2.26

It must be noticed that the *LCOS* indicator is referred to the energy discharged by the ESS, while the charged energy is considered in the numerator substituting the Fuel costs. Moreover, it must be considered potential revenues that reduce the *LCOS*, such as subsidies or the provision of ancillary services to the system. This metric aims to analyze the observed costs and revenue streams associated with commercially available energy storage technologies.

If the ESS is integrated in a combined system, such as with a generator or in a microgrid, it must be remembered to normalize the *LCOS* of the ESS device according to the considered lifespan of the system, *n*, as stated in Equation 2.44, to get the *LCOS'*.

In contrast with pure generation technologies, storage devices may have a significant different behavior between in-front-of-the-meter applications and behind-the-meter applications. For instance, in [40], six different applications (use cases) are identified. The main in-front-of-the-meter cases are:

- **Wholesale:** these are large-scale energy storage systems designed to replace peaking generation technologies, such as gas-fired turbines, with the aim to meet rapidly increasing demand for power peak and be quickly taken offline as power demand decreases.
- **Transmission and distribution:** the main purpose of these energy storage systems is to defer transmission and/or distribution upgrades. Then, they are placed at substations or distribution feeders controlled by utilities to provide flexible capacity while maintaining grid stability.
- **Utility scale:** these systems are designed to be paired with large solar PV facilities to improve the market price of solar generation, reduce solar curtailment and provide grid support when not supporting solar targets.

On the contrary, the main behind-the-meter cases are:

- **Commercial and industrial stand-alone:** these are energy storage systems designed for peak shaving and demand charge reduction services for commercial and industrial end-users. They can support different management strategies and provide grid services to a utility or the wholesale market.
- **Commercial and industrial self-consumption:** analogously to the previous case, these systems are designed to shave peaks in the energy demand but being paired with self-generation technologies, such as rooftop PV systems.
- **Residential self-consumption:** these systems aim to provide backup power, power quality improvements and extension of the usefulness of self-generation,

typically, solar PV. They are designed to regulate the power supply and smooth the amount of electricity sold back to the grid from distributed PV applications.

Depending on the application, the project parameters may change significantly, as it can be seen in Table 3.1 for reference.

Table 3.1. Project parameters of different case studies of storage systems. Data from [40].

Parameter	In-Front-of-the-Meter			Behind-the-Meter		
	Wholesale	**Transmission and Distribution**	**Utility Scale**	**Commercial and Industrial Standalone**	**Commercial and Industrial self-consumption**	**Residential self-consumption**
Project life [years]	20	20	20	10	20	20
Power rating [MW]	100	10	20	1	0.50	0.01
Capacity [MWh]	400	60	80	2	2	0.04
100% DOD Cycles / day	1	1	1	1	1	1
Days / year	350	250	350	250	350	350
Annual stored energy [MWh]	140,000	15,000	28,000	500	700	14
Feasible technologies	- Lithium-Ion - Flow Battery			- Lithium-Ion - Lead-Acid - Advanced Lead		

2.6. Levelized Cost of Thermal Energy

2.6.1. Levelized Cost of Heat (LCOH)

Analogously to the *LCOE* definition for electrical systems, it is possible to define a "Levelized Cost of Heat" (*LCOH*) for thermal energy. This indicator can be used in order to compare different thermal power technologies. According to the authors of [9, 10, 41, 42], the *LCOH* can be written in a similar manner to what is written for electricity by simply replacing *E*: electricity by *H*: provided heat. Furthermore, Figure 2.8 shows a thermal energy microgrid, which represents the analogous case to that presented in Section 2.4.6 for electrical microgrids.

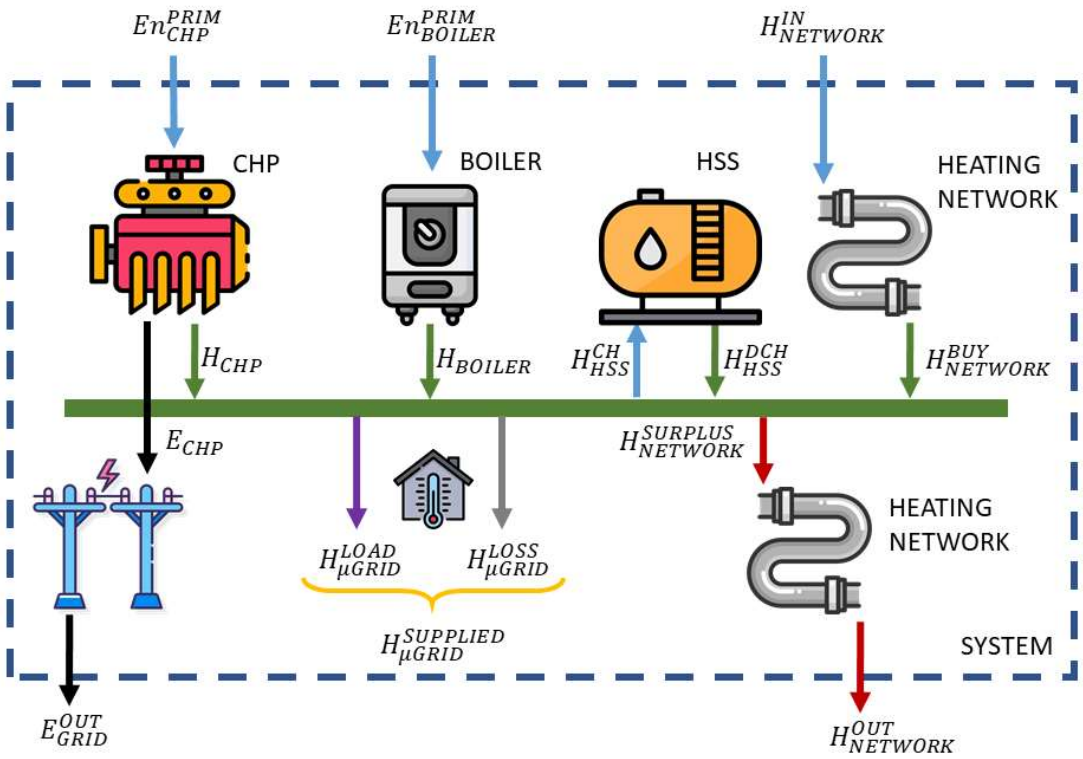

Figure 2.8. Representation of a thermal polygeneration microgrid with ESS devices connected to a heating network.

Then, the expressions to evaluate the *LCOH*, depending on the case are:

Single generator unit:

$$LCOH_G = \frac{\sum_{i=0}^{n} \frac{NC_i^G}{(1+d)^i}}{P_G^{th} \cdot \sum_{i=1}^{n} \frac{EOH_i^{G,th}}{(1+d)^i}},$$

Equation 2.65

where the super index *th* refers to the thermal capacity.

Normalized LCOH of a generator:

$$LCOH'_G = \frac{\sum_{i=1}^{n_G} \frac{EOH_i^{G,th}}{(1+d)^i}}{\sum_{i=1}^{n} \frac{EOH_i^{G,th}}{(1+d)^i}} \cdot LCOH_G + \frac{\sum_{z=1}^{floor\left(\frac{n}{n_G}\right)} \left\{ \sum_{i=z\cdot n_G+1}^{min[(z+1)\cdot n_G, n]} \left[\frac{NC_i^G}{(1+d)^i} \right] \right\} - \frac{RV_G}{(1+d)^n}}{P_G^{th} \cdot \sum_{i=1}^{n} \frac{EOH_i^{G,th}}{(1+d)^i}}.$$

Equation 2.66

Polygeneration system with thermal storage devices (HSS) and devices replacement:

$$LCOH_{POLY} = \sum_{j=1}^{J} \left(f'_{Gj} \cdot LCOH'_{Gj} \right) + \sum_{k=1}^{K} \left(f'_{HSSk} \cdot LCOS'_{HSSk} \right) + LCOH'_{SYST},$$

Equation 2.67

$$f'_{Gj} = \frac{P_{Gj}^{th} \cdot \sum_{i=1}^{n_{Gj}} \frac{EOH_i^{Gj,th}}{(1+d)^i}}{\sum_{i=1}^{n} \left\{ \sum_{\gamma=1}^{\Gamma} \left[P_{G\gamma}^{th} \cdot \frac{EOH_i^{G\gamma,th}}{(1+d)^i} \right] + \sum_{\delta=1}^{\Delta} \frac{\left(H_{HSS\delta}^{DCH} - H_{HSS\delta}^{CH} \right)_i}{(1+d)^i} \right\}}.$$

Equation 2.68

$$f'_{HSSk} = \frac{\sum_{i=1}^{n_{HSSk}} \frac{\left(H_{HSSk}^{DCH} \right)_i}{(1+d)^i}}{\sum_{i=1}^{n} \left\{ \sum_{\gamma=1}^{\Gamma} \left[P_{G\gamma}^{th} \cdot \frac{EOH_i^{G\gamma,th}}{(1+d)^i} \right] + \sum_{\delta=1}^{\Delta} \frac{\left(H_{HSS\delta}^{DCH} - H_{HSS\delta}^{CH} \right)_i}{(1+d)^i} \right\}}.$$

Equation 2.69

$$LCOH'_{SYST} = \frac{\sum_{i=0}^{n} \frac{Costs_i^{SYST}}{(1+d)^i}}{\sum_{i=1}^{n} \left\{ \sum_{\gamma=1}^{\Gamma} \left[P_{G\gamma}^{th} \cdot \frac{EOH_i^{G\gamma,th}}{(1+d)^i} \right] + \sum_{\delta=1}^{\Delta} \frac{\left(H_{HSS\delta}^{DCH} - H_{HSS\delta}^{CH}\right)_i}{(1+d)^i} \right\}}.$$

Equation 2.70

Thermal microgrid:

$$LCOH_{\mu GRID} = \sum_{j=1}^{J} \left(f''_{Gj} \cdot LCOH'_{Gj} \right) + \sum_{k=1}^{K} \left(f''_{HSSk} \cdot LCOS'_{HSSk} \right) + f''^{BUY}_{NETWORK} \cdot LCOH_{NETWORK} + LCOH''_{SYST} - f''^{SURPLUS}_{NETWORK} \cdot LROH_{NETWORK}.$$

Equation 2.71

$$f''_{Gj} = \frac{P_{Gj}^{th} \cdot \sum_{i=1}^{n} \frac{EOH_i^{Gj,th}}{(1+d)^i}}{\sum_{i=1}^{n} \left\{ \sum_{\gamma=1}^{\Gamma} \left[P_{G\gamma}^{th} \cdot \frac{EOH_i^{G\gamma,th}}{(1+d)^i} \right] + \sum_{\delta=1}^{\Delta} \left[\frac{\left(H_{HSS\delta}^{DCH} - H_{HSS\delta}^{CH}\right)_i}{(1+d)^i} \right] + \frac{\left(H_{NETWORK}^{BUY} - H_{NETWORK}^{SURPLUS}\right)_i}{(1+d)^i} \right\}}.$$

Equation 2.72

$$f''_{HSSk} = \frac{\sum_{i=1}^{n} \frac{\left(H_{HSSk}^{DCH}\right)_i}{(1+d)^i}}{\sum_{i=1}^{n} \left\{ \sum_{\gamma=1}^{\Gamma} \left[P_{G\gamma}^{th} \cdot \frac{EOH_i^{G\gamma,th}}{(1+d)^i} \right] + \sum_{\delta=1}^{\Delta} \left[\frac{\left(H_{HSS\delta}^{DCH} - H_{HSS\delta}^{CH}\right)_i}{(1+d)^i} \right] + \frac{\left(H_{NETWORK}^{BUY} - H_{NETWORK}^{SURPLUS}\right)_i}{(1+d)^i} \right\}}.$$

Equation 2.73

$$f''^{BUY}_{NETWORK} = \frac{\sum_{i=1}^{n} \frac{(H^{BUY}_{NETWORK})_i}{(1+d)^i}}{\sum_{i=1}^{n} \left\{ \sum_{\gamma=1}^{\Gamma} \left[P^{th}_{G\gamma} \cdot \frac{EOH_i^{G\gamma,th}}{(1+d)^i} \right] + \sum_{\delta=1}^{\Delta} \left[\frac{\left(H^{DCH}_{HSS\delta} - H^{CH}_{HSS\delta}\right)_i}{(1+d)^i} \right] + \frac{(H^{BUY}_{NETWORK} - H^{SURPLUS}_{NETWORK})_i}{(1+d)^i} \right\}}.$$

Equation 2.74

$$f''^{SURPLUS}_{NETWORK} = \frac{\sum_{i=1}^{n} \frac{(H^{SURPLUS}_{NETWORK})_i}{(1+d)^i}}{\sum_{i=1}^{n} \left\{ \sum_{\gamma=1}^{\Gamma} \left[P^{th}_{G\gamma} \cdot \frac{EOH_i^{G\gamma,th}}{(1+d)^i} \right] + \sum_{\delta=1}^{\Delta} \left[\frac{\left(H^{DCH}_{HSS\delta} - H^{CH}_{HSS\delta}\right)_i}{(1+d)^i} \right] + \frac{(H^{BUY}_{NETWORK} - H^{SURPLUS}_{NETWORK})_i}{(1+d)^i} \right\}}.$$

Equation 2.75

$$LCOH''_{SYST} = \frac{\sum_{i=0}^{n} \frac{Costs_i^{SYST}}{(1+d)^i}}{\sum_{i=1}^{n} \left\{ \sum_{\gamma=1}^{\Gamma} \left[P^{th}_{G\gamma} \cdot \frac{EOH_i^{G\gamma,th}}{(1+d)^i} \right] + \sum_{\delta=1}^{\Delta} \left[\frac{\left(H^{DCH}_{HSS\delta} - H^{CH}_{HSS\delta}\right)_i}{(1+d)^i} \right] + \frac{(H^{BUY}_{NETWORK} - H^{SURPLUS}_{NETWORK})_i}{(1+d)^i} \right\}}.$$

Equation 2.76

$$LROH_{NETWORK} = \frac{\sum_{i=1}^{n} \frac{Revenues_i^{NETWORK}}{(1+d)^i}}{\sum_{i=1}^{n} \frac{(H^{SURPLUS}_{NETWORK})_i}{(1+d)^i}}.$$

Equation 2.77

However, it must be highlighted that, when dealing with thermal energy, the temperature at which the energy is supplied can be an important factor, as reported in [41]. Thus, when comparing *LCOH* of different technologies can be crucial to consider

the same operating conditions for each technology. The evaluation of the exergy, as presented in Section 2.7 is recommended.

2.6.2. Levelized Cost of Cooling (LCOC)

Identically as defined for heat, the "Levelized Cost of Cooling" (*LCOC*) can be defined analogously to the *LCOE* by substituting *E* (electricity), or in the *LCOH* definitions *H* (heat), by *C* (cooling energy). Furthermore, the same considerations stated for heating regarding the framework boundaries and the "quality" (temperature) of the provided cooling energy must be considered.

2.7. Levelized Cost of Exergy (*LCOEx*)

Some particular energy systems, such as cogeneration plants or multi-vector energy microgrids providing power, heating, cooling and/or other services may be analyzed by specific economic and accounting approaches to separate the costs among the generated products (electricity, thermal energy, cooling energy or others). Otherwise, wrong conclusions about the efficiency of the systems can be drawn [43], for instance, if a cogeneration plant is only evaluated by its capacity to provide electricity dismissing its capacity to provide also thermal energy. However, this is not an easy task, mainly due to the different nature of the energy products, and several approaches can be adopted for this issue.

On the one hand, some researchers and policy makers prefer a physical or balance method of cost separation [43, 44]. According to this method, costs for heat production are calculated as if the heat was generated separately from the electricity [43]. The main advantages of this approach are that it provides transparent and accountable results, reduce initial assumptions and allows for seasonal fluctuations in output levels. On the other hand, the major disadvantage of this method is that any cost decreases due to cogeneration (i.e., a change in the working conditions to provide more heat instead of electricity) is accounted for electricity production only.

Another similar approach is the application of the so-called "heat credits" [44]. The heat credits can be defined as the revenue from heat generation in cogeneration systems, i.e. the value of heat produced by the cogeneration system calculated per unit of electricity generated by the system over its lifetime. This approach would be similar as defining thermal efficiency for electricity generation in cogeneration systems, targeting separation of fuel costs, or in other words, analyzing the fuel breakdown according to the final energy product (electricity or heat) and considering only the fuel costs associated with the product under analysis in the calculation.

In both cases, the electricity is assumed to be the main product. The incremental fuel is lower than the extra fuel amount that would be required if heat were produced separately [43] (it is considered a subtractive term indicating the thermal benefits, i.e., the avoided costs related to the thermal energy that is not needed to be produced in a separate plant, such as a boiler). However, one limitation that must be considered under this approach is that the heat credit rate still depends on the operation mode of the energy system (heat production vs. electricity production) and it is affected by the specific features of the generation technology [44].

In order to overcome the previous approaches' limitations, in [43] the application of the "Ginter triangle" is proposed as an alternative approach. Under this approach, a triangle is developed in the space between two axes (costs for electricity and heat). Thus, the triangle enables the estimation of the unit cost of the second product assuming the unit cost of the first one. The application of the Ginter method requires the use of coefficients to allow for separation of costs associated with combined generation. However, the determination of the separation coefficients for the cost components is complex due to the physical properties of simultaneous production. Thus, researchers, such as in [43], apply a risk analysis using a Monte Carlo simulation to determine cost ranges for energy products.

As an alternative to these approaches, we propose to evaluate the "Levelized Cost of Exergy" (*LCOEx*), which extends the *LCOEn* formulation to the total exergy produced by

the system, then including electricity, thermal energy or any other energy product together.

Exergy refers to *"the maximum theoretical amount of work that can be obtained from the interaction of the system under study with the reference ambient system"* [45]. The fraction of a given form of energy which can be fully converted in other forms is called "exergy", while the fraction which cannot be transformed is called "anergy" [46]. Thus, considering any form of energy, the bigger is its exergy, the higher is its technic and economic value. The First Principle of Thermodynamics establishes the equivalence between different forms of energy, while on the other hand, the Second Principle of Thermodynamics fixes the limits for the transformation of one form of energy into another. For instance, mechanical energy and electricity can be completely transformed into other forms of energy (useful work) while thermal energy cannot. Mechanical energy and electricity are pure exergy, on the other hand the exergy content of the thermal energy is higher dependent on the temperature at which it is supplied in respect to the reference temperature of the environment [47]. For this reason, the exergy of the thermal energy can be seen as the portion which can be transformed into useful work, which can be considered as proportional to the efficiency of the equivalent Carnot cycle between the temperature at which the heat is supplied/discharged and the reference one [48]. This relation is expressed in Equation 2.78, where the temperature at the numerator, T_C, refers to the cold source, while the one in the denominator, T_H, refers to that of the hot source. The cold source or the hot source can both refer to the ambient depending on the thermal application.

$$Ex = H \cdot \left(1 - \frac{T_C}{T_H}\right).$$

Equation 2.78

For a heating power plant, the exergy associated with the thermal energy produced can then be evaluated considering the temperature at which the heat is supplied as the higher temperature, while the reference temperature of the environment is the lowest one. On the other hand, for a cooling plant, the exergy associated with the cooling energy produced can be evaluated considering as the higher temperature the reference

temperature of the environment; and as the lower temperature the one of the technology used to extract heat from the environment. Considering a generic plant capable of producing both electricity and thermal energy, the exergy associated with the energy produced by the plant can be generally defined as reported in Equation 2.79, where T_a is the ambient temperature, T_s the temperature of the supplied thermal energy, and γ^{th} and γ^{co} represent the penalty factors associated to the Carnot cycle efficiency.

$$Ex = E + H \cdot \left(1 - \frac{T_a}{T_s}\right) + C \cdot \left(1 - \frac{T_s}{T_a}\right) = E + H \cdot \gamma^{th} + C \cdot \gamma^{co}.$$

Equation 2.79

From Equation 2.79 it is possible to notice that, for a generator which produces heat, the higher the temperature at which it supplies thermal energy, the lower its penalty factor; and thus, the higher the exergy associated to the produced thermal energy. Analogously, for a generator which produces cooling energy, the lower the temperature at which it provides it, the lower its penalty factor and thus, the higher the exergy associated to the produced cooling energy.

Once the concept of exergy has been properly defined, the *LCOEx* can be presented. As stated in Equation 2.80, this indicator measures the discounted cost of the exergy provided by a multi-vector system during its lifespan, i.e., the *LCOEx* is the average exergy price which makes the discounted revenues (related to the exergy content of final products) compensate the total discounted net costs.

$$LCOEx_G = \frac{\sum_{i=0}^{n_G} \frac{NC_i^G}{(1+d)^i}}{\sum_{i=1}^{n_G} \left\{ \sum_{m=1}^{M} \left[\frac{Ex_i^{G,m}}{(1+d)^i} \right] \right\}} = \frac{\sum_{i=0}^{n_G} \frac{NC_i^G}{(1+d)^i}}{\sum_{i=1}^{n_G} \left[\frac{E_i^G}{(1+d)^i} + \frac{(H^G \cdot \gamma^{th})_i}{(1+d)^i} + \frac{(C^G \cdot \gamma^{co})_i}{(1+d)^i} \right]},$$

Equation 2.80

where *m* refers to each source of exergy than the generator G can provide, up to *M*. For instance, in a pure electrical generator, such a solar PV plant, *M*=1, but in a CHP plant, *M*≥1.

If separated costs coefficients (α^E, α^{th} and α^{co}) can be defined for electricity, heat and cooling energy, respectively, Equation 2.80 can be rewritten as:

$$LCOEx_G = \frac{\sum_{i=0}^{n_G} \frac{(\alpha^E \cdot NC^G)_i}{(1+d)^i} + \sum_{i=0}^{n_G} \frac{(\alpha^{th} \cdot NC^G)_i}{(1+d)^i} + \sum_{i=0}^{n_G} \frac{(\alpha^{co} \cdot NC^G)_i}{(1+d)^i}}{\sum_{i=1}^{n_G} \left[\frac{E_i^G}{(1+d)^i} + \frac{(H^G \cdot \gamma^{th})_i}{(1+d)^i} + \frac{(C^G \cdot \gamma^{co})_i}{(1+d)^i} \right]},$$

Equation 2.81

where $\alpha^E + \alpha^{th} + \alpha^{co} = 1$. Then, the *LCOEx* of generator G can be expressed as a function of its *LCOE*, *LCOH* and *LCOC*:

$$LCOEx_G = f_G^E \cdot LCOE_G + f_G^{th} \cdot LCOH_G + f_G^{co} \cdot LCOC_G,$$

Equation 2.82

where:

$$f_G^E = \frac{\sum_{i=1}^{n_G} \frac{E_i^G}{(1+d)^i}}{\sum_{i=1}^{n_G} \left[\frac{E_i^G}{(1+d)^i} + \frac{(H^G \cdot \gamma^{th})_i}{(1+d)^i} + \frac{(C^G \cdot \gamma^{co})_i}{(1+d)^i} \right]}.$$

Equation 2.83

$$f_G^{th} = \frac{\sum_{i=1}^{n_G} \frac{H_i^G}{(1+d)^i}}{\sum_{i=1}^{n_G} \left[\frac{E_i^G}{(1+d)^i} + \frac{(H^G \cdot \gamma^{th})_i}{(1+d)^i} + \frac{(C^G \cdot \gamma^{co})_i}{(1+d)^i} \right]}.$$

Equation 2.84

$$f_G^{co} = \frac{\sum_{i=1}^{n_G} \frac{C_i^G}{(1+d)^i}}{\sum_{i=1}^{n_G} \left[\frac{E_i^G}{(1+d)^i} + \frac{(H^G \cdot \gamma^{th})_i}{(1+d)^i} + \frac{(C^G \cdot \gamma^{co})_i}{(1+d)^i} \right]}.$$

Equation 2.85

It must be noted that the exergy penalty factors for heat and cooling make that $f_G^E + f_G^{th} + f_G^{co} > 1$.

Finally, like for the *LCOE*, the *LCOH* or the *LCOC*, the *LCOEx* can be analyzed for combined systems, such a polygeneration plants or multi-vector energy microgrids. Following the same reasoning than that presented in Sections 2.4.4 to 2.4.6, the following results can be obtained:

Normalized *LCOEx* of a generator:

$$LCOEx'_G = \frac{\sum_{i=1}^{n_G} \left\{ \sum_{m=1}^{M} \left[\frac{Ex_i^{G,m}}{(1+d)^i} \right] \right\}}{\sum_{i=1}^{n} \left\{ \sum_{m=1}^{M} \left[\frac{Ex_i^{G,m}}{(1+d)^i} \right] \right\}} \cdot LCOEx_G + \frac{\sum_{z=1}^{floor\left(\frac{n}{n_G}\right)} \left\{ \sum_{i=z \cdot n_G+1}^{min[(z+1) \cdot n_G, n]} \left[\frac{NC_i^G}{(1+d)^i} \right] \right\} - \frac{RV_G}{(1+d)^n}}{\sum_{i=1}^{n} \left\{ \sum_{m=1}^{M} \left[\frac{Ex_i^{G,m}}{(1+d)^i} \right] \right\}}.$$

Equation 2.86

Polygeneration system with storage devices (EnSS)[5] and considering the replacement of the devices at the end of their lifespan:

$$LCOEx_{POLY} = \sum_{j=1}^{J}\left(f'_{Gj} \cdot LCOEx'_{Gj}\right) + \sum_{k=1}^{K}\left(f'_{ExSSk} \cdot LCOS'_{ExSSk}\right) + LCOEx'_{SYST},$$

Equation 2.87

$$f'_{Gj} = \frac{\sum_{i=1}^{n_{Gj}}\left\{\sum_{m=1}^{M}\left[\frac{Ex_i^{Gj,m}}{(1+d)^i}\right]\right\}}{\sum_{i=1}^{n}\left\{\sum_{\gamma=1}^{\Gamma}\left\{\sum_{m=1}^{M}\left[\frac{Ex_i^{G\gamma,m}}{(1+d)^i}\right]\right\} + \sum_{\delta=1}^{\Delta}\left\{\sum_{m=1}^{M}\left[\frac{\left(Ex_{EnSS\delta}^{DCH} - Ex_{EnSS\delta}^{CH}\right)_i^m}{(1+d)^i}\right]\right\}\right\}}.$$

Equation 2.88

$$f'_{ExSSk} = \frac{\sum_{i=1}^{n_{ExSSk}}\left\{\sum_{m=1}^{M}\left[\frac{\left(Ex_{ExSSk}^{DCH}\right)_i^m}{(1+d)^i}\right]\right\}}{\sum_{i=1}^{n}\left\{\sum_{\gamma=1}^{\Gamma}\left\{\sum_{m=1}^{M}\left[\frac{Ex_i^{G\gamma,m}}{(1+d)^i}\right]\right\} + \sum_{\delta=1}^{\Delta}\left\{\sum_{m=1}^{M}\left[\frac{\left(Ex_{EnSS\delta}^{DCH} - Ex_{EnSS\delta}^{CH}\right)_i^m}{(1+d)^i}\right]\right\}\right\}}.$$

Equation 2.89

$$LCOEx'_{SYST} = \frac{\sum_{i=0}^{n}\frac{Costs_i^{SYST}}{(1+d)^i}}{\sum_{i=1}^{n}\left\{\sum_{\gamma=1}^{\Gamma}\left\{\sum_{m=1}^{M}\left[\frac{Ex_i^{G\gamma,m}}{(1+d)^i}\right]\right\} + \sum_{\delta=1}^{\Delta}\left\{\sum_{m=1}^{M}\left[\frac{\left(Ex_{EnSS\delta}^{DCH} - Ex_{EnSS\delta}^{CH}\right)_i^m}{(1+d)^i}\right]\right\}\right\}}.$$

Equation 2.90

[5] Energy Storage System (EnSS) may refer to either electrical (ESS) or thermal (HSS) devices.

Energy multi-vector microgrid:

$$LCOEx_{\mu GRID} = \sum_{j=1}^{J}\left(f''_{Gj} \cdot LCOEx'_{Gj}\right) + \sum_{k=1}^{K}\left(f''_{ExSSk} \cdot LCOS'_{ExSSk}\right) + f''^{BUY}_{GRID} \cdot LCOEx_{GRID} + LCOEx''_{SYST} - f''^{SURPLUS}_{\mu GRID} \cdot LROEx_{GRID}.$$

Equation 2.91

$$f''_{Gj} = \frac{\sum_{i=1}^{n_{Gj}}\left\{\sum_{m=1}^{M}\left[\frac{Ex_i^{Gj,m}}{(1+d)^i}\right]\right\}}{\sum_{i=1}^{n}\left\{\sum_{m=1}^{M}\left\{\sum_{\gamma=1}^{\Gamma}\left[\frac{Ex_i^{G\gamma,m}}{(1+d)^i}\right] + \sum_{\delta=1}^{\Delta}\left[\frac{\left(Ex_{ExSS\delta}^{DCH} - Ex_{ExSS\delta}^{CH}\right)_i^m}{(1+d)^i}\right] + \frac{\left(Ex_{GRID}^{BUY} - Ex_{\mu GRID}^{SURPLUS}\right)_i^m}{(1+d)^i}\right\}\right\}}.$$

Equation 2.92

$$f''_{ExSSk} = \frac{\sum_{i=1}^{n_{ExSSk}}\left\{\sum_{m=1}^{M}\left[\frac{(Ex_{ExSSk}^{DCH})_i^m}{(1+d)^i}\right]\right\}}{\sum_{i=1}^{n}\left\{\sum_{m=1}^{M}\left\{\sum_{\gamma=1}^{\Gamma}\left[\frac{Ex_i^{G\gamma,m}}{(1+d)^i}\right] + \sum_{\delta=1}^{\Delta}\left[\frac{\left(Ex_{ExSS\delta}^{DCH} - Ex_{ExSS\delta}^{CH}\right)_i^m}{(1+d)^i}\right] + \frac{\left(Ex_{GRID}^{BUY} - Ex_{\mu GRID}^{SURPLUS}\right)_i^m}{(1+d)^i}\right\}\right\}}.$$

Equation 2.93

$$f''^{BUY}_{GRID} = \frac{\sum_{i=1}^{n}\left\{\sum_{m=1}^{M}\left[\frac{(Ex_{GRID}^{BUY})_i^m}{(1+d)^i}\right]\right\}}{\sum_{i=1}^{n}\left\{\sum_{m=1}^{M}\left\{\sum_{\gamma=1}^{\Gamma}\left[\frac{Ex_i^{G\gamma,m}}{(1+d)^i}\right] + \sum_{\delta=1}^{\Delta}\left[\frac{\left(Ex_{ExSS\delta}^{DCH} - Ex_{ExSS\delta}^{CH}\right)_i^m}{(1+d)^i}\right] + \frac{\left(Ex_{GRID}^{BUY} - Ex_{\mu GRID}^{SURPLUS}\right)_i^m}{(1+d)^i}\right\}\right\}}.$$

Equation 2.94

$$f''^{SURPLUS}_{GRID} = \frac{\sum_{i=1}^{n}\left\{\sum_{m=1}^{M}\left[\frac{\left(Ex_{\mu GRID}^{SURPLUS}\right)_i^m}{(1+d)^i}\right]\right\}}{\sum_{i=1}^{n}\left\{\sum_{m=1}^{M}\left\{\sum_{\gamma=1}^{\Gamma}\left[\frac{Ex_i^{G\gamma,m}}{(1+d)^i}\right] + \sum_{\delta=1}^{\Delta}\left[\frac{\left(Ex_{ExSS\delta}^{DCH} - Ex_{ExSS\delta}^{CH}\right)_i^m}{(1+d)^i}\right] + \frac{\left(Ex_{GRID}^{BUY} - Ex_{\mu GRID}^{SURPLUS}\right)_i^m}{(1+d)^i}\right\}\right\}}.$$

Equation 2.95

$$LCOEx''_{SYST} = \frac{\sum_{i=0}^{n} \frac{Costs_i^{SYST}}{(1+d)^i}}{\sum_{i=1}^{n}\left\{\sum_{m=1}^{M}\left\{\sum_{\gamma=1}^{\Gamma}\left[\frac{Ex_i^{G\gamma,m}}{(1+d)^i}\right] + \sum_{\delta=1}^{\Delta}\left[\frac{\left(Ex_{ExSS\delta}^{DCH} - Ex_{ExSS\delta}^{CH}\right)_i^m}{(1+d)^i}\right] + \frac{\left(Ex_{GRID}^{BUY} - Ex_{\mu GRID}^{SURPLU}\right)_i^m}{(1+d)^i}\right\}\right\}}.$$

Equation 2.96

$$LROEx_{GRID} = \frac{\sum_{i=1}^{n} \frac{Revenues_i^{GRID}}{(1+d)^i}}{\sum_{i=1}^{n}\left\{\sum_{m=1}^{M}\left[\frac{\left(Ex_{\mu GRID}^{SURPLUS}\right)_i^m}{(1+d)^i}\right]\right\}}.$$

Equation 2.97

It must be observed that the *LCOEx* of a complex energy system is not directly the sum of the *LCOEx* of its constituent generators, but it is a weighted mean of them. Moreover, the supply temperatures of the thermal energy affect the exergy associated to each single subsystem. The higher is the installed rated power of each technology and its equivalent operating hours, the higher is its weight in the global *LCOEx*. Furthermore, considering a complex system where more than one generator is used to satisfy the same demand, control logics may affect both the individual *LCOEx* of each technology and its weighting factor, in a nonlinear manner that must be analyzed case by case. For instance, the *LCOEx* of a CHP unit can change depending on the operation strategy (e.g., electrical or thermal priority).

The *LCOEx* can be a useful indicator to compare different energy system configurations taking into account not only pure electric generators but also thermal, cooling devices and CHP units. Moreover, it is possible to define a reference scenario characterized by a certain *LCOEx* ($LCOEx^{REF}$) which can be used as a reference value for benchmarking.

2.8. Summary and chapter conclusions

In this chapter the fundamentals of the Levelized Cost of Energy (and its variants for electricity, heat, cooling energy, stored energy and exergy) have been revised and analyzed in deep. A general systematic analysis approach has been presented and, then,

the definitions for a single generator, a generator with energy storage, a polygeneration system and a microgrid have been demonstrated. Depending on the characteristics of the energy community, and the focus of the analysis, the *LCOE*, *LCOH*, *LCOC*, *LCOS* or *LCOEx* must be applied. Finally, it must be highlighted that the proposed *LCOEx* results one of the most appropriate indicators for the analysis of multi-vector energy systems, as it allows the combination of the energy supply of different types and sources, keeping their physical meaning.

2.9. References

1. Kirschen DS, Strbac G (2019) Fundamentals of Power System Economics, Segunda Edición. John Wiley & Sons, West Sussex, UK

2. Ueckerdt F, Hirth L, Luderer G, Edenhofer O (2013) System LCOE: What are the costs of variable renewables? Energy 63:61–75. https://doi.org/10.1016/j.energy.2013.10.072

3. Cory K, Schwabe P (2009) Wind Levelized Cost of Energy: A Comparison of Technical and Financing Input Variables. National Renewable Energy Laboratory, Golden, CO

4. Cretì A, Fontini F (2019) Economics of Electricity. Markets, Competition and Rules, Primera Edición. Cambridge University Press, Cambridge, UK

5. Foster J, Wagner L, Bratanova A (2014) LCOE models: A comparison of the theoretical frameworks and key assumptions

6. Joskow PL (2011) Comparing the Costs of Intermittent and Dispatchable Electricity Generating Technologies. American Economic Review 101:238–241. https://doi.org/10.1257/aer.101.3.238

7. Tran TTD, Smith AD (2018) Incorporating performance-based global sensitivity and uncertainty analysis into LCOE calculations for emerging renewable energy technologies. Applied Energy 216:157–171. https://doi.org/10.1016/j.apenergy.2018.02.024

8. LCOE background. http://rincon.lbl.gov/lcoe_v2/background.html. Accessed 12 Feb 2021

9. Nian V, Sun Q, Ma Z, Li H (2016) A Comparative Cost Assessment of Energy Production from Central Heating Plant or Combined Heat and Power Plant. Energy Procedia 104:556–561. https://doi.org/10.1016/j.egypro.2016.12.094

10. Stanytsina V, Artemchuk V, Bogoslavska O, et al (2021) The influence of environmental tax rates on the Levelized cost of heat on the example of organic and

biofuels boilers in Ukraine. E3S Web Conf 280:09012. https://doi.org/10.1051/e3sconf/202128009012

11. Holttinen H, Meibom P, Orths A, et al (2011) Impacts of large amounts of wind power on design and operation of power systems, results of IEA collaboration. Wind Energy 14:179–192. https://doi.org/10.1002/we.410

12. Sijm JPM, Nederland EC (2014) Cost and revenue related impacts of integrating electricity from variable renewable energy into the power system - A review of recent literature

13. Bator FM (1958) The Anatomy of Market Failure. The Quarterly Journal of Economics 72:351–379. https://doi.org/10.2307/1882231

14. European Environment Agency (2011) Revealing the costs of air pollution from industrial facilities in Europe. European Environment Agency, Luxembourg, BEL

15. Moslehi S, Reddy TA (2019) An LCA methodology to assess location-specific environmental externalities of integrated energy systems. Sustainable Cities and Society 46:101425. https://doi.org/10.1016/j.scs.2019.101425

16. Gies E (2017) The real cost of energy. Nature 551:S145–S147. https://doi.org/10.1038/d41586-017-07510-3

17. Turconi R, Boldrin A, Astrup T (2013) Life cycle assessment (LCA) of electricity generation technologies: Overview, comparability and limitations. Renewable and Sustainable Energy Reviews 28:555–565

18. Yang X, Li H, Wallin F, Wang Z (2017) Impacts of Emission Reduction Target and External Costs on Provincial Natural Gas Distribution in China. Energy Procedia 105:3326–3331. https://doi.org/10.1016/j.egypro.2017.03.760

19. Rabl A, Spadaro JV (2016) External Costs of Energy: How Much Is Clean Energy Worth? Journal of Solar Energy Engineering 138:. https://doi.org/10.1115/1.4033596

20. Sovacool BK, Enevoldsen P, Koch C, Barthelmie RJ (2017) Cost performance and risk in the construction of offshore and onshore wind farms. Wind Energ 20:891–908. https://doi.org/10.1002/we.2069

21. Mattmann M, Logar I, Brouwer R (2016) Hydropower externalities: A meta-analysis. Energy Economics 57:66–77. https://doi.org/10.1016/j.eneco.2016.04.016

22. Bracco S, Delfino F, Laiolo P, Morini A (2018) Planning and Open-Air Demonstrating Smart City Sustainable Districts. Sustainability 10:4636. https://doi.org/10.3390/su10124636

23. de Simón-Martín M, Bracco S, Rossi M, et al (2019) A flexible test-bed pilot facility for the analysis and simulation of Smart Microgrids. In: 2019 IEEE International

Conference on Environment and Electrical Engineering and 2019 IEEE Industrial and Commercial Power Systems Europe (EEEIC / I CPS Europe). pp 1–6

24. Transparent Cost Database | Transparent Cost Database. https://openei.org/apps/TCDB/. Accessed 22 Feb 2021

25. Neff B (2019) Estimated Cost of New Utility-Scale Generation in California: 2018 Update. California Energy Commission, California, CA

26. Department of Energy & Climate Change (2013) Electricity Generation Costs 2013. Department of Energy & Climate Change, United Kingdom

27. Bureau of Resources and Energy Economics (2012) Australian Energy Technology Assessment. Bureau of Resources and Energy Economics, Australia

28. LCOE Valuation – The Prudent Way of Looking at Energy Investments. https://www.censere.com/index.php/en/articles/163-lcoe-valuation-the-prudent-way-of-looking-at-energy-investments. Accessed 12 Feb 2021

29. IRENA (2020) Global Renewables Outlook. Energy Transformation 2050. IRENA, Abu Dhabi

30. IRENA (2019) Renewable power generation costs in 2018. 1:160

31. IRENA (2021) Renewable Power Generation Costs in 2020. International Renewable Energy Agency (IRENA), Abu Dhabi

32. de Simón-Martín M, de la Puente-Gil Á, Borge-Diez D, et al (2019) Wind energy planning for a sustainable transition to a decarbonized generation scenario based on the opportunity cost of the wind energy: Spanish Iberian Peninsula as case study. Energy Procedia 157:1144–1163. https://doi.org/10.1016/j.egypro.2018.11.282

33. Pagnini L, Piccardo G, Repetto MP (2018) Full scale behavior of a small size vertical axis wind turbine. Renewable Energy 127:41–55. https://doi.org/10.1016/j.renene.2018.04.032

34. Bracco S, Delfino F, Ferro G, et al (2018) Energy planning of sustainable districts: Towards the exploitation of small size intermittent renewables in urban areas. Applied Energy 228:2288–2297. https://doi.org/10.1016/j.apenergy.2018.07.074

35. GSE. https://www.gse.it/. Accessed 14 Oct 2021

36. Munoz LAH, Huijben JCCM, Verhees B, Verbong GPJ (2014) The power of grid parity: A discursive approach. Technological Forecasting and Social Change 87:179–190. https://doi.org/10.1016/j.techfore.2013.12.012

37. Colmenar-Santos A, De Palacio C, Enríquez-García LA, López-Rey Á (2015) A Methodology for Assessing Islanding of Microgrids: Between Utility Dependence and Off-Grid Systems. Energies 8:4436–4454. https://doi.org/10.3390/en8054436

38. Lotfi H, Khodaei A (2016) Levelized cost of energy calculations for microgrids. In: 2016 IEEE Power and Energy Society General Meeting (PESGM). pp 1–5

39. Bracco S, Delfino F, Laiolo P, et al (2019) Evaluating LCOE in sustainable microgrids for smart city applications. pp 1–6

40. Lazard (2018) Lazard's Levelized Cost of Storage Analysis - Version 4.0. Lazard

41. Gabbrielli R, Castrataro P, Del Medico F, et al (2014) Levelized Cost of Heat for Linear Fresnel Concentrated Solar Systems. Energy Procedia 49:1340–1349. https://doi.org/10.1016/j.egypro.2014.03.143

42. Li H, Song J, Sun Q, et al (2019) A dynamic price model based on levelized cost for district heating. Energ Ecol Environ 4:15–25. https://doi.org/10.1007/s40974-019-00109-6

43. Batanova A, Robinson J, Wagner L (2015) Modification of the LCOE model to estimate a cost of heat and power generation for Russia. Munich Personal RePEc Archive (MPRA) 1:1–27

44. Mott MacDonald (2010) UK Electricity Generation Costs Update. Mott MacDonald, Brighton, UK

45. Moran MJ, Shapiro HN (2004) Fundamentals of Engineering Thermodynamics, Fourth Edition. John Wiley & Sons, Hoboken (NJ), USA

46. Rossi N Manuale del Termotecnico, Third Edition. Editor Ulrico Hoepli, Milan

47. Çengel YA, Boles MA (2008) Thermodynamics: an Engineering Approach, Sixth Edition. McGraw-Hill

48. Jansen S, Woudstra N (2010) Understanding the exergy of cold: Theory and practical examples. IJEX 7:693–713. https://doi.org/10.1504/IJEX.2010.035516

Levelized Cost of Energy in Sustainable Energy Communities

A systematic approach for multi-vector energy systems

CHAPTER 3 – Application to real case studies

3.1 Introduction

This chapter applies the theoretical framework shown in chapter 2 through several examples. More specifically, the calculation of the *LCOEn* and its variants is discussed through three representative case studies. The first case study focuses on the Smart Polygeneration Microgrid (SPM), a low voltage microgrid in the Savona Campus of the University of Genoa (Italy) which includes both thermal and electrical generation plants and loads. The second case study analyzes the Smart Energy Building (SEB), also placed at the Savona Campus, which represents a particular case of a smart building, analyzed as a nanogrid with thermal and electrical appliances. Finally, the third case study covers the ERESMAGrid, an electrical microgrid at the Campus of Vegazana of the University of León (Spain) which includes several renewable energy generators and an electrochemical storage system. In the aforesaid three cases, a probabilistic methodology is applied, considering the variation of the main input parameters and their impact on the calculation of *LCOEn* indicators.

3.2 Methodology

3.2.1 Probabilistic Assessment

Let be *R* a metric that quantifies the *LCOEn* (any of its variants *LCOE*, *LCOH*, *LCOC*, etc.). In chapter 2 it has been expressed by a functional relationship $R=g(\boldsymbol{X})$, being $\boldsymbol{X}=\{x_1, x_2,\ldots,x_n\}^T$ a vector listing the input parameters governing the energy production and the costs. Unfortunately, the estimate of these quantities is uncertain due to inherent randomness, lack of measurements, simplification on modeling and errors in estimates [1]. These errors propagate in the evaluation of the metric, either softened or intensified, revealing that conventional evaluations, based on nominal values, can lead to overestimates or underestimates, compromising the validity of the results.

When a large amount of sample data for $\boldsymbol{X}$ is available, it is possible to define the probability density functions (pdfs) of the uncertain quantities. The probability distribution of R, F_R, is given by:

$$F_R(r) = P(R \leq r) = P[R = g(x_1, x_2, \dots, x_n) \leq r]$$
$$= \int_{D_{\boldsymbol{X}(r)}} f(\ x_1, x_2, \dots, x_n) dx_1 dx_2 \dots dx_n,$$

Equation 3.1

where $f(x_1, x_2, \dots, x_n)$ is the joint probability density function (pdf) of $x_1, x_2, \dots, x_n$ and $D_{\boldsymbol{X}(r)}$ is the domain of $x_1, x_2, \dots, x_n$ where $D_{\boldsymbol{X}(r)} = \{(x_1, x_2, \dots, x_n) : g(x_1, x_2, \dots, x_n) \leq r\}$. The probability density function of *R* is obtained by the derivative of F_R.

Equation 3.1 provides, at least in principle, the full probabilistic description of the target function. However, it poses criticalities in engineering applications as the solution is very burdensome in its general formulation. Moreover, it requires the knowledge of the joint probability density function of the uncertain involved quantities. Unfortunately, information on the statistical properties of the input parameters in this case, i.e., when evaluating the *LCOEn*, is usually very poor, so that the accuracy of a full probabilistic approach becomes questionable.

A number of procedures exists which allow to propagate the uncertainties on the objective function. The study can be carried out either by advanced procedures, involving refined mathematical models (e.g., models such as those presented in [2]) or by classic methods suitable for technical applications (e.g., the one shown in [3]). The present section recalls the mean value Taylor Series Expansion (TSE) method and Monte Carlo (MC) simulations.

TSE is an approximate procedure in which the statistical information on the objective function is obtained in an approximate way as a function of the information available on the input parameters. On the other hand, MC simulation represents the most general and conceptually simple method for estimating statistical properties of the objective function and can deliver the description of its probability law. It involves the generation of representative samples of the random input parameters with a given distribution, the numerical solution of the problem for each realization and in the last end, the estimation of the statistical properties of the samples of the output process. MC simulation method

can be applied to linear and non-linear problems, and its precision is not affected by the entity of uncertainties. However, as it is completely numerical, the procedure does not provide an interpretative model. Especially, the statistical information on the random parameters on which the objective function depends is usually very poor. Therefore, the user has to postulate the probability distribution of the involved quantities.

The function R can be expressed by TSE around the mean value of $\boldsymbol{X}$, i.e., $E[\boldsymbol{X}] = \{E[x_1], E[x_2], \dots, E[x_n]\}$:

$$R(\boldsymbol{X}) = R|_{E[\boldsymbol{X}]} + \sum_{i=1}^{n} \left[(x_i - E[x_i]) \frac{\partial R}{\partial x_i}\Big|_{E[\boldsymbol{X}]} \right] + \frac{1}{2} \sum_{i=1}^{n} \left[(x_i - E[Xx_i])^2 \frac{\partial^2 R}{\partial X x_i^2}\Big|_{E[\boldsymbol{X}]} \right] + \cdots,$$

Equation 3.2

where $E[\bullet]$ is the mean value operator and $\bullet|_{E[\boldsymbol{X}]}$ means the quantity calculated considering the mean values of the parameters. Applying statistical operators to Equation 3.2, the statistical moments of R can be obtained, according to the information available on the statistical moments of $\boldsymbol{X}$. Retaining up to the first order terms (i.e., first-order TSE), it derives:

$$E[R] = R|_{E[\boldsymbol{X}]}, \quad \sigma^2[R] = \nabla^T R|_{E[\boldsymbol{X}]} \boldsymbol{C_X} \nabla R|_{E[\boldsymbol{X}]},$$

Equation 3.3

where $\nabla R = \left\{ \frac{\partial R}{\partial x_1}, \frac{\partial R}{\partial x_2}, \dots, \frac{\partial R}{\partial x_n} \right\}^T$ stands for the gradient of R and $\boldsymbol{C_X}$ is the covariance matrix of $\boldsymbol{X}$. When the covariance among different random parameters can be neglected, $\boldsymbol{C_X}$ can be taken as a diagonal matrix, and the second statistical moment of R, shown in Equation 3.3, simplifies to:

$$\sigma_R^2 \simeq \sum_{i=1}^{n} \frac{\partial R}{\partial X_i}\Big|_{E[\boldsymbol{X}]}^2 \sigma_{x_i}^2,$$

Equation 3.4

where σ_{Xi}, σ_R are the standard deviation of X_i and R, respectively.

First order TSE implies a linear approximation around the expansion point. When the parameters are scattered, the more $R(\boldsymbol{X})$ deviates from the linear approximation in the neighborhood of the expansion point, the more expressions in Equation 3.3.4 loses accuracy. The use of second order terms in the TSE allows gaining accuracy in $E[R]$, while it seems less remarkable in $\mathrm{V}[R]$ [4]. Applying second order TSE, the mean value derives:

$$E[R] = R|_{E[\boldsymbol{X}]} + \frac{1}{2}\sum_{i=1}^{n}\left(\left.\frac{\partial^2 R}{\partial x_i^2}\right|_{E[\boldsymbol{X}]} \cdot \sigma^2[x_i]\right).$$

Equation 3.5

Equation 3.3, 3.4 and 3.5 supply mean and standard deviation of the objective function as a function of the mean and the standard deviation of the input parameters. From the one hand, it can be used to propagate uncertainties when $R(\boldsymbol{X})$ is described by an analytical model through symbolic calculation tools. Facing with few parameters, TSE can be developed by closed form solutions, giving a direct functional relationship linking R to each uncertain quantity. On the other hand, it supplies an approximate expression that allows appreciating the contribution of each parameter and its scattering.

Equation 3.3 shows that, according to the first order approximation, the mean value of the objective function coincides with the function evaluated for the mean values of the parameters. **Errore. L'origine riferimento non è stata trovata.** shows that the goodness of the approximation decreases as long as the relationship between R and X_i is non-linear.

Equation 3.4 allows quantifying the scattering of the objective function. However, the standard deviation of a random variable does not clearly indicate its degree of dispersion, that is most effectively provided by taking the ratio of the standard deviation and the mean value. It derives:

$$\delta_R^2 \simeq \sum_{i=1}^{n} \delta_{Ri}^2$$

Equation 3.6

$$\delta_{Ri} = \left|c_{x_i}^R\right| \cdot \delta_{x_i}$$

Equation 3.7

$$c_{x_i}^R = \frac{\partial R}{\partial x_i}\Big|_{E[\boldsymbol{X}]} \cdot \frac{E[x_i]}{E[R]}$$

Equation 3.8

where $\delta_{x_i} = \sigma_{x_i}/\mu_{x_i}$ is the coefficient of variation of the *i*-th input parameter x_i, $\delta_R = \sigma_R/\mu_R$ is the coefficient of variation of R. It is expressed as the square root of the sum of contributions $\delta_{R_i} = \sigma_{R_i}/\mu_{R_i}$ related to each parameter x_i. Term c_{Xi} is a propagation coefficient [5]. Therefore, Equation 3. provides the scattering in the target function as the sum of contributions related to the scattering of each input parameter. Each contribution is given by the product of two quantities, respectively, the coefficient of variation of the input parameter, quantifying its scattering, and the propagation coefficient, that quantifies the functional law that relates the objective function to the variation of the parameter itself.

Different scenarios can arise. When $c_{x_i} > 1$, uncertainties in x_i are amplified over the objective function. Therefore, even small errors in the parameter propagate over R giving rise to large scatter. In this case, an accurate evaluation of x_i is recommended. When $c_{x_i} < 1$, uncertainties in x_i are softened over the objective function. However, they can propagate significantly when uncertainties on x_i are very large.

3.2.2 Parameter Modeling

LCOEn and its variants have been expressed by a deterministic functional relationship of a number of input parameters which are not deterministic, but show some scattering due to inherent randomness and uncertainty in their estimation. These stochastic parameters can be classified into operation parameters and economic parameters. Among the operation parameters, it can be considered as stochastic or semi-stochastic variables the *EOH*, the electricity consumption and the energy charged in the ESS. In the

economic category, it can be considered with a stochastic behaviour the *OPEX*, the discount rate, the fuel purchase price and the purchase and selling prices of electricity.

EOH synthetizes a number of factors related to the energy production. It is a random quantity affected in turns by the intermittency of the source (e.g., solar radiation or wind speed), the uncertain behaviour of the in-field plant (e.g., small wind turbines, emerging technologies such as wave energy, tidal energy or other pioneering systems), or the energy demand (e.g., dispatchable gas turbine). Among the power units considered in the following sections, small wind turbines are by far the technology with the greatest uncertainties when considering the *EOH*. By way of example, in [6] supply a general survey on a large sample of small wind turbines in Italy, showing a huge variability of power production between the different installations. For target power up to 20 kW, the average *EOH* estimated on a sample of 211 installations is 1,337 hours/year with a coefficient of variation of about 0.8. Besides the rather low level of average production, data highlight considerable heterogeneity, especially for smaller plants (many plants are practically at a standstill). Uncertainties in predictions of the actual behavior of micro wind turbines are even higher. In [7] a comparison between actual energy production and the forecast based on manufacturer supplied power curves for 26 wind turbines installed on buildings across the UK is shown. Besides highlighting large discrepancies between the prediction and the actual behavior, it is found that *EOH*s range from about 0 to 1,450 hours/year and the overall average is about 364 hours/year. Similarly, the energy output of 21 small wind turbines examined in [8] was approximately the 29% of the energy that manufacturers predicted they would. As a consequence of frequent malfunctions or intense vibratory effects, that reduce the performance and fatigue life [9–11], small wind turbines require frequent maintenance interventions which are difficult to be planned and are often higher than expected. Given these data, it is clear that the maintenance costs (i.e., *OPEX*) are very uncertain too.

Electricity consumption is related to the user behavior and varies in time. Forecasting methods still pose important limitations [12, 13]. They either imply a high computational burden, or provide very uncertain estimates [14]. In [15] some data of the electrical demand profiles of a university campus, a school and a block of buildings are reported.

In the residential context, the electrical load is higher in the early morning and in the late evening, and it is usually lower in summer time than in winter. In the university campus and in the school, the electrical load is higher in the central hours of the day, when school-related activities are in progress and in summer time (during the lessons period), due to the energy demand for cooling. Analyses of specific case studies may derive statistical information from the data sample when available, considering annual averages or average values of representative days or hourly average values. However, yearly variations are usually limited for this sort of facilities [16].

The operation of the ESS depends strongly on the application and it is also linked to the user load profile. In the case of battery banks, the most often operation mode is peak shaving, i.e., the reduction of the peak hours power load by increasing the power demand in the valley hours. The ESS are usually charged with surplus energy from RES generators, such as solar PV fields or WTG units, or, in the case of scarcity of the resource, by purchasing electricity from the external power grid during the lowest cost hours. Then, both the uncertainty of the sources and of the power load affect significantly the energy charged and discharged in the ESS. The Energy Management Systems (EMS) and the Battery Management Systems (BMS) of these devices play a relevant role both in the operation and maintenance costs. Moreover, it must be considered that, depending on the working conditions, the equivalent charging-discharging cycles, i.e., the useful life of the device, may be affected and thus, have a great impact on both the *EOH* and the *OPEX*.

Given the variability of possible scenarios, and the lack of knowledge about the distributions of the considered quantities, these quantities are commonly modelled by normal Gaussian distributions in some applications, lognormal or uniform distributions [17, 18].

Electricity purchasing and selling prices, fuel purchasing price and discount rate are parameters related to the trend of the markets. A variety of methods for the electricity price estimations is discussed in [19–21], highlighting its complex nature, which makes this quantity very volatile. The fuel purchase price also shows a high volatility and it is

observed that it depends strongly on the seasonal variation in the supply, the thermal demand trend and on the weather severity [22].

Finally, the discount rate is inherent random as it is somehow related to risk assessment. Sensitivity analyses are usually carried out considering different values ranging from a base scenario and then assumed according broad intervals [23, 24]. When the maximum and minimum values are considered quite certain, the discount rate is also simulated according to the minimum and best-case scenarios, using uniform [17] or triangular [25] distributions.

In the examples described in the present chapter, the sensitivity of *LCOEn* metrics is investigated by MC simulations of the input parameters. The analyses are carried out postulating normal distributions for the stochastic operation parameters, while quantities related to the trend of the markets are represented by triangular distributions. The parameters of the distributions are assumed according to the information available on the specific case study, either evaluated from the recorded data, or postulated according to reasonable values. In case of normal distribution, the mean (μ) and standard deviation (σ) of the random variables are provided, whereas for triangular distribution, the lower limit (A), mode (B) and upper limit (C) are supplied. For the aforesaid parameters, deterministic analyses are carried out assuming values equal to the mean of their distribution.

The presentation of the results is organized as follows. The first step of the analysis applies MC simulations to the evaluation of *LCOE*, *LCOS* and *LCOEx* of the single technologies belonging to the different case studies. Firstly, these indicators are assessed by evaluating their pdf when all input parameters are uncertain. Then, for each indicator, a "tornado diagram" is built considering one input parameter uncertain at a time while the other ones assume deterministic values. This diagram allows to evaluate the dependency of the scattering of the considered indicator on the uncertainty of each input parameter. Tornado diagrams show the confidence interval of each indicator between the 5^{th} and the 95^{th} percentiles. A vertical baseline shows the value of the indicator calculated assuming deterministic values for the input parameters.

Furthermore, for each technology the results are synthetized by a table showing: the mean value (μ_{Xi}) and the coefficient of variation (δ_{Xi}) of the considered input parameter x_i, the mean value (μ_{Ri}) and coefficient of variation (δ_{Ri}) of the indicator R, and the propagation coefficient $c_{Xi}^{R} = \delta_{Ri} / \delta_{Xi}$ of each input parameter to the indicator uncertainty (see Equation 3.7).

The second step of the analysis investigates the *LCOEx* of each facility according to the formulation addressed in chapter 2. The analysis considers a time frame of 20 years. All technologies having a useful life lower than the aforesaid time frame are replaced before the 20th year, taking into account a new investment modulated by the *CAPEX* reduction [%/year] factor. Moreover, the residual value of each technology is considered in terms of negative discounted *CAPEX* (using a linear relationship with $CAPEX_0$).

3.3 First case study: Smart Polygeneration Microgrid (SPM)

This first case study is relative to the Smart Polygeneration Microgrid (SPM) which is a low voltage microgrid installed in 2014 at the Savona Campus of the University of Genoa, in the North of Italy [26, 27], within the Energia 2020 project [28]. The microgrid, funded by the Italian Ministry of Education, University and Research, has been conceived as an R&D facility to provide electrical and thermal energy to the buildings of the campus in a renewable and sustainable way. Although the main characteristics of the real facility have been taken into account, some simplifications have been considered in the calculation of the indicators.

3.3.1 Description of the SPM

The SPM is characterized by the presence of renewable energy power plants, cogeneration and trigeneration plants, as well as storage systems and electric vehicle charging infrastructures. The power plants installed in the SPM are:

- Two solar photovoltaic fields (PV1 and PV2), having a total peak power of 95 kW_p,

with respectively 336 and 60 polycrystalline silicon modules installed on the flat roof of a building [29, 30].

- Two cogeneration (CHP) microturbines (Capstone C65 model) fed by natural gas and used to provide both electricity and warm water (this last used for space heating purposes during the winter season and for space cooling in summer when coupled with absorption chillers).
- Two boilers fed by natural gas with a total thermal rated power of 900 kW_{th}.
- Two absorption chillers (water / lithium bromide technology) with a total rated cooling power of 220 kW_{th}.
- One electrical storage system (ESS) composed of six ST523 SoNick batteries with a total nominal capacity of 141 kWh [31].

In the SPM there are also two 22 kW_{AC} AC charging points for electric vehicles and one 15 kW_{DC} DC vehicle-to-grid (V2G) station which is used to exploit electric vehicles as storage systems.

Figure 3.1. PV power plants of the SPM.

Figure 3.2. Microturbines (left) and one boiler (right) of the SPM [32].

Figure 3.3. Absorption chillers of the SPM [32].

Figure 3.4. Electrical storage system of the SPM [32].

In Figure 3.5 the simplified electrical diagram of the whole campus is reported with the aim of showing the scheme of the SPM in detail. The campus has a single point of common coupling (PCC) to the medium voltage AC distribution grid; the contracted power supply is of 451 kW_{AC}. Two MV/LV transformers, having a rated apparent power respectively of 630 and 400 kVA_{AC}, are used to feed the majority of buildings, whereas the SPM and some laboratories are connected to a third MV/LV transformer (800 kVA_{AC} rated power). The only building directly connected to the SPM is the Smart Energy Building (SEB) described in section 3.4. Both generation units and loads are real-time monitored through the electric and thermal SCADA systems (respectively SIMATIC WinCC and DESIGO) which connect smart meters and local automation devices with the EMS of the whole SPM.

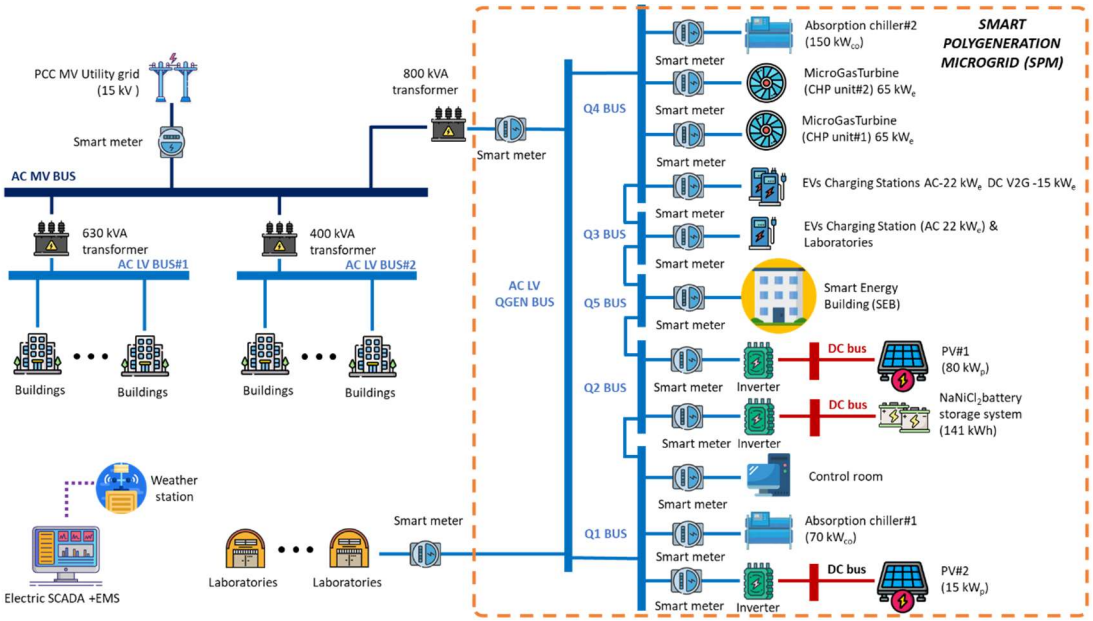

Figure 3.5. Simplified electrical scheme of the Savona Campus.

From the thermal point of view, as aforesaid the SPM is used to supply both heat and cooling energy to the buildings of the campus. As visible in Figure 3.6, there is a thermal network composed of several underground pipelines which convey warm water produced by the boilers and the microturbines to heat the buildings typically from the

end of October till the mid of April. On the other hand, from June to September the boilers are off and the space cooling is guaranteed by compression chillers in the majority of buildings, while the library and one of the largest building are conditioned by the two absorption chillers thermally driven by the microturbines.

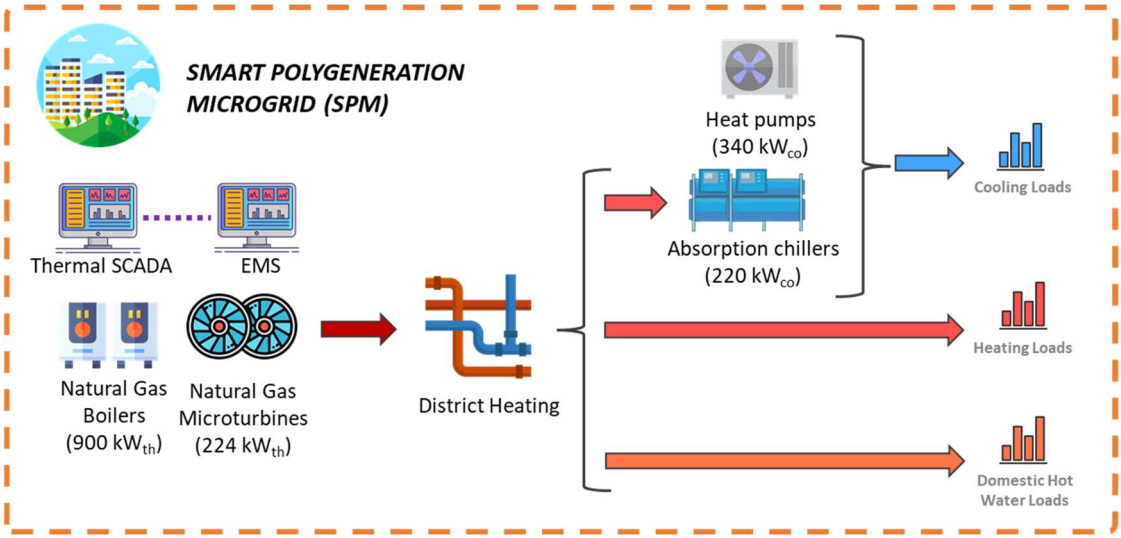

Figure 3.6. Thermal and cooling energy production in the SPM.

The optimal scheduling of dispatchable power plants, namely the microturbines, the boilers and the storage system, is determined day-by-day by the EMS, whose main aim is that of minimizing operating costs and/or carbon dioxide emissions. Such costs mainly derive from the purchased natural gas (used to feed microturbines and boilers) and the electricity withdrawn from the national grid. The EMS is based on a Mixed Integer Linear Programming (MILP) mathematical model which needs as input economic parameters (natural gas and electricity prices, etc.) and technical performance data of power plants (at nominal and partial loads operating conditions). The EMS also includes forecasting tools to estimate the electrical and thermal load profiles as well as the power production from the solar source.

3.3.2 Adopted hypotheses and boundary conditions

In Table 3.1 the main input parameters used to calculate the *LCOEn* (and its variants) of each technology and of the whole SPM are reported. As highlighted in the table, some parameters are kept constant, while others are assumed to follow a normal or triangular distribution. From the electrical point of view, the SPM has been modelled as a single bus system, thus neglecting power losses; a similar approach has been adopted for the thermal part since the thermal network and its losses have not been considered. The equivalent operating hours (*EOH*) of the dispatchable sources as well as the estimation of the power output of PV fields and the energy charged to the storage system (E^{ch}) have been evaluated through the analysis of historical operating data collected from 2014 till 2021. For all the technologies, the capital expenditures at year 0 ($CAPEX_0$) indicates the purchase and installation cost whereas the assumption on the *CAPEX* reduction has been considered to estimate the replacement cost at the end of the useful life. Indeed, the time horizon of the analysis has been assumed equal to 20 years, but some devices (such as the microturbines, the absorption chillers and the storage batteries) are characterized by a lower useful life, and so they need to be substituted with new ones before the end of the 20th year. The term *OPEX* mainly indicates maintenance costs while fuel costs of cogeneration units and boiler is computed separately, as described in chapter 2. For both *EOH* and *OPEX* values, normal distributions have been assumed while triangular distributions have been preferred to represent the scattering of electricity and fuel prices. Some further considerations can be drawn from the analysis of the information reported in Table 3.1. The Microgrid System indicates the hardware and software of the SCADA and the EMS through which it is possible to monitor and manage the SPM. For the boilers and the CHP units the supplied temperature refers to the warm water outlet, while for heat pumps and absorption chillers it indicates the outlet temperature of the chilled water. Then, nominal conversion efficiency of technologies is also reported in Table 3.1 together with the electrical and thermal rated power or energy values. In order to calculate the *LCOEx*, it has been necessary to assume reference indoor temperatures for the buildings equal to 18°C in winter and 26°C in summer.

Table 3.1. Input parameter values for the analysis of the SPM case study.

MICROGRID SYSTEM			
Parameter	**Deterministic value**	**Distribution**	**Distr. parameters**
Useful life [years]	20	-	-
CAPEX$_0$ [€]	196,800	-	-
OPEX [€/year]	1,700	Normal	μ=1,700, σ=300
EOH [h/year]	8,760	-	-
CAPEX reduction [%/year]	2	-	-
PV1 (80 kW$_{AC}$ / 80 kW$_p$)			
Parameter	**Deterministic value**	**Distribution**	**Distr. parameters**
Useful life [years]	20	-	-
CAPEX$_0$ [€]	120,000	-	-
OPEX [€/year]	1,280	Normal	μ=1,280, σ=280
EOH [h/year]	1,200	Normal	μ=1,200, σ=68.4
CAPEX reduction [%/year]	2	-	-
PV2 (15 kW$_{AC}$ / 15 kW$_p$)			
Parameter	**Deterministic value**	**Distribution**	**Distr. parameters**
Useful life [years]	20	-	-
CAPEX$_0$ [€]	22,500	-	-
OPEX [€/year]	240	Normal	μ=240, σ=52.5
EOH [h/year]	1,200	Normal	μ=1,200, σ=68.4
CAPEX reduction [%/year]	2	-	-
ESS (141 kWh)			
Parameter	**Deterministic value**	**Distribution**	**Distr. parameters**
Useful life [years]	8	-	-
CAPEX$_0$ [€]	211,500	-	-
OPEX [€/year]	3,500	Normal	μ=3,500, σ=705
E^{ch} [kWh/year]	77,550	Normal	μ=77,500, σ=10,000
Min SoC [%]	10	-	-
Max SoC [%]	100	-	-
Round trip efficiency [%]	74	-	-
Capacity reduction [%/year]	0	-	-
CAPEX reduction [%/year]	2	-	-
LOAD (451 kW$_{AC}$)			
Parameter	**Deterministic value**	**Distribution**	**Distr. parameters**
Electricity consumption [kWh/year]	1,100,000	Normal	μ=1,100,000, σ=100,000
Demand variation [%/year]	0	-	-
Electricity purchase price [€/MWh]	170	Triangular	A=100, B=160, C=250
Electricity selling price [€/MWh]	46.7	Triangular	A=20, B=40, C=80
Natural gas price [€/Sm^3]	0.42	Triangular	A=0.25, B=0.4, C=0.6
Prices variation [%/year]	0	-	-
Discount rate [%]	5	Triangular	A=2, B=5, C=8
Boilers (900 kW$_{th}$)			
Parameter	**Deterministic value**	**Distribution**	**Distr. parameters**
Useful life [years]	20	-	-
CAPEX$_0$ [€]	79,200	-	-
OPEX [€/year]	13,500	Normal	μ=13,500, σ=6,300
EOH [h/year]	900	Normal	μ=900, σ=100
Global efficiency [%]	65	-	-
Supply temperature [°C]	60	-	-
CAPEX reduction [%/year]	2	-	-
Heat pumps (340 kW$_{co}$)			
Parameter	**Deterministic value**	**Distribution**	**Distr. parameters**
Useful life [years]	20	-	-
CAPEX$_0$ [€]	294,780	-	-
OPEX [€/year]	5,100	Normal	μ=5,100, σ=1,700
EOH [h/year]	600	Normal	μ=600, σ=100
EER [-]	2.3	-	-
Supply temperature [°C]	6	-	-
CAPEX reduction [%/year]	2	-	-
Absorption chillers (220 kW$_{co}$)			
Parameter	**Deterministic value**	**Distribution**	**Distr. parameters**
Useful life [years]	10	-	-
CAPEX$_0$ [€]	330,00	-	-

OPEX [€/year]	4,400	Normal	μ=4,400, σ=1,100
EOH [h/year]	1,000	Normal	μ=1,000, σ=80
Global efficiency [-]	0.87	-	-
Supply temperature [°C]	7	-	-
CAPEX reduction [%/year]	2	-	-
CHP units (130 kW_{el}, 224 kW_{th})			
Parameter	**Deterministic value**	**Distribution**	**Distr. parameters**
Useful life [years]	10	-	-
$CAPEX_0$ [€]	215,930	-	-
OPEX [€/year]	10,000	Normal	μ=10,000, σ=650
EOH [h/year]	2,500	Normal	μ=2,500, σ=200
Thermal/electrical production ratio [-]	1.72	-	-
Supply temperature [°C]	60	-	-
CAPEX reduction [%/year]	2	-	-

3.3.3 Results and discussion for the SPM

In the following the main results for the SPM case are presented.

***LCOE* distribution of the PV1 and PV2 power plants**

Figure 3.7 (left) shows the *LCOE* pdf for the PV1 power plant, while Figure 3.7 (right) reports the corresponding tornado diagram. Moreover, Table 3.2 presents the mean value and the coefficient of variation for each input parameter, as well as the corresponding mean value, coefficient of variation and propagation coefficient of the *LCOE for this generation power plant*.

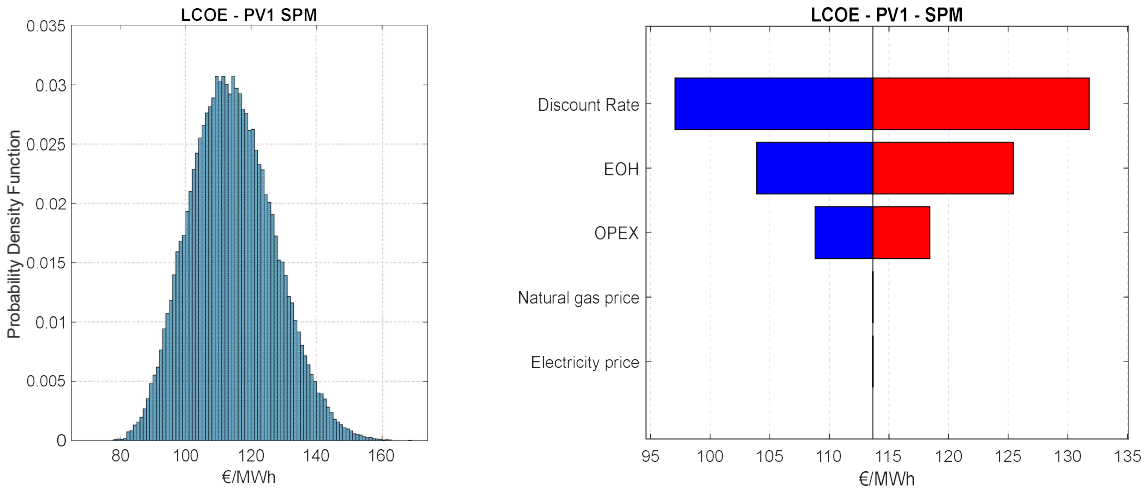

Figure 3.7. Probability density function (left) and tornado diagram (right) for the LCOE of the PV1 plant of the SPM according to the Monte Carlo analysis.

The distribution of the *LCOE* for this generator is normal-like, with a mean value of € 114/MWh and a standard deviation of € 12.73/MWh. These values are in the current range for this technology (see chapter 2). The mean *LCOE* is quite competitive overtaking the grid parity by far. Looking at the tornado diagram and at Table 3.2, it can be observed that the high dispersion of the *LCOE* is mainly due to the discount rate, which is the most uncertain quantity among the considered input parameters (having the highest δ value). On the other hand, the parameter *EOH* has a significant impact on the *LCOE* uncertainty due to its high propagation coefficient despite being characterized by a very small intrinsic uncertainty. Although the *OPEX* uncertainties are quite large, their impact on the *LCOE* is mitigated.

Table 3.2. Variation and propagation coefficients for the PV1 plant of the SPM.

Stochastic input parameter	μ	δ **[-]**	μ_{LCOE} **[€/MWh]**	δ_{LCOE} **[-]**	C_{LCOE} **[-]**
EOH [h/year]	1,200	0.06	114.01	0.06	1.01
OPEX [€/kW year]	16	0.22	113.64	0.03	0.11
Discount rate [%]	5	0.25	113.90	0.09	0.37

The same results can be found for the PV2 plant since it has the same characteristics of the PV1 plant, in terms of panel type and installation (azimuth and tilt angles), maintenance interventions, etc. Moreover, they have the same investment costs per installed power due to their concurrent installation.

LCOS distribution of the Energy Storage System

Figure 3.8 (left) shows the *LCOS* pdf for the ESS, while Figure 3.8 (right) shows the associated tornado diagram. Table 3.3 shows the synthesis of results.

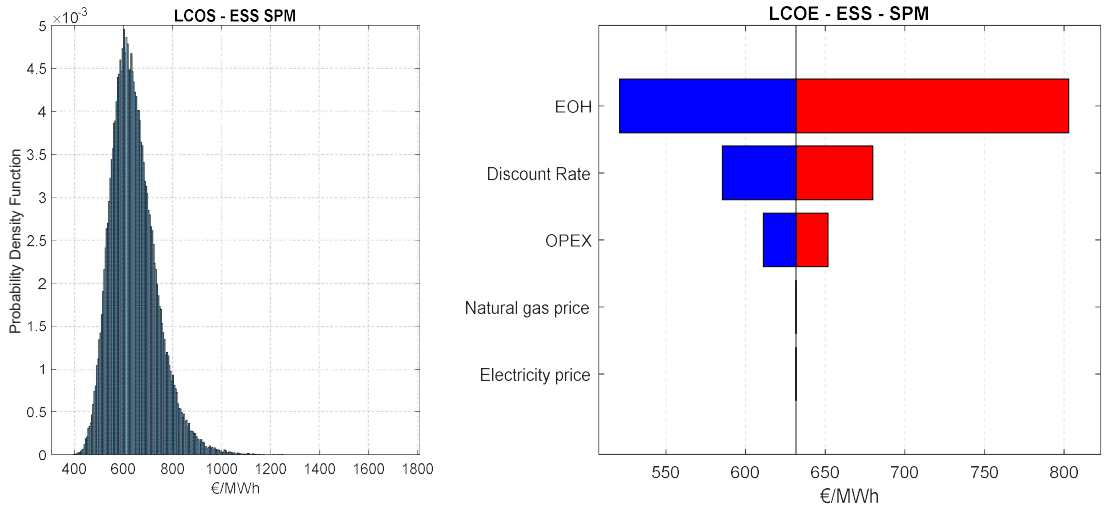

Figure 3.8. Probability density function (left) and tornado diagram (right) for the LCOS of the ESS of the SPM according to the Monte Carlo analysis.

The distribution of the *LCOS* is normal-like, with a mean value of € 642/MWh and a standard deviation of € 93/MWh, which represent typical current values (see chapter 2). As it can be noted, the *LCOS* is quite far from the grid parity. Looking at the tornado diagram and at Table 3.3 it can be observed that in this case the *EOH* (expressing the number of charging and discharging cycles) is quite scattered and its uncertainty deeply propagates over the results. As expected, the scheduling of the ESS heavily impacts on its *LCOS. OPEX* and discount rate uncertainties play a minor role on the *LCOS* due to a quite low propagation coefficient.

Table 3.3. Variation and propagation coefficients for the ESS of the SPM.

Stochastic input parameter	μ	δ [-]	μ_{LCOS} [€/MWh]	δ_{LCOS} [-]	C_{LCOS} [-]
EOH [h/year]	77,550	0.13	642.76	0.14	1.05
OPEX [€/kW year]	24.82	0.20	631.53	0.02	0.10
Discount rate [%]	5	0.25	631.89	0.04	0.18

LCOEx distribution of Boilers

Figure 3.9 (left) shows the *LCOEx* pdf for the boilers, while Figure 3.9 (right) shows two tornado diagrams respectively for *LCOH* and *LCOEx*. Table 3.4 presents the mean value and the coefficient of variation for each input parameter, together with the

corresponding mean, coefficient of variation and propagation coefficient of the *LCOEx*.

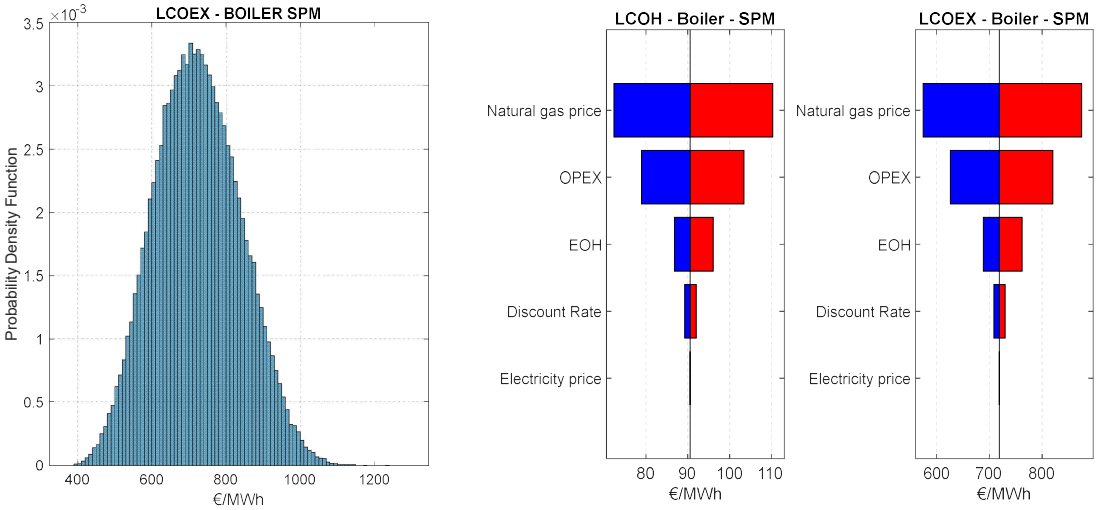

Figure 3.9. Probability density function (left) and tornado diagrams (right) for the LCOH and LCOEx of boilers of the SPM according to the Monte Carlo analysis.

The tornado diagrams in Figure 3.9 show that the values of *LCOEx* are significantly higher than the *LCOH* ones. The *LCOH* is actually comparable with the *LCOE* values which have been calculated for the PV plants in spite of referring to different kinds of energy. The *LCOEx* indicator takes into account the different technical value between heat and electricity, introducing as a common denominator the equivalent mechanical work or exergy. In this way, the *LCOE* values of PV plants can be compared with the present *LCOEx.* The distribution of the *LCOEx* for the boilers is normal-like, with a mean value of € 723/MWh and a standard deviation of € 116/MWh.

Although the natural gas has been characterized by a modest scattering, it affects mostly the results due to its high propagation coefficient. Therefore, this parameter is the one which has to be estimated with the highest accuracy.

Table 3.4. Variation and propagation coefficients for the boilers of the SPM.

Stochastic input parameter	μ	δ [-]	μ_{LCOEx} [€/MWh]	δ_{LCOEx} [-]	C_{LCOEx} [-]
EOH [h/year]	900	0.11	721.06	0.03	0.28
OPEX [€/kW year]	15	0.47	721.32	0.08	0.17
Discount rate [%]	5	0.25	718.79	0.01	0.04
Natural gas price [€/m³]	0.42	0.17	718.63	0.13	0.73

LCOEx distribution of the CCHP units

Figure 3.10 shows the *LCOEx* pdf for the trigeneration plant (composed of microturbines and absorption chillers) considering all the parameters uncertainty. When dealing with polygeneration units, it is significant to address all the energy outcomes in order to correctly assess the considered technology. The three tornado diagrams depicted in grey in Figure 3.11 evaluate only one energy outcome at a time, neglecting the intrinsic benefits of cogeneration and trigeneration systems. As it can be clearly seen, typical *LCOE, LCOC, LCOH* overestimate the results in comparison to the *LCOEx*, since each of them computes all the costs of the CCHP plant but only one useful effect, namely the production of electrical, cooling or thermal energy. The distribution of the *LCOEx* for the CCHP plant is normal-like, with a mean value of € 352/MWh and a standard deviation of € 38/MWh.

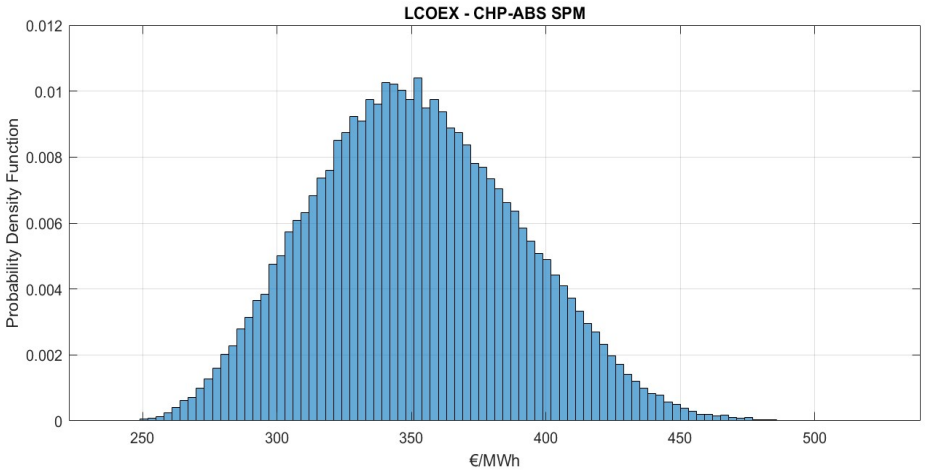

Figure 3.10. Probability density function for the LCOEx of the CCHP plant of the SPM according to the Monte Carlo analysis.

Figure 3.11 and Table 3.5 show that the natural gas price (large scattering) and *EOH* (large propagation coefficient) are the parameters which affect the most the scattering of the results.

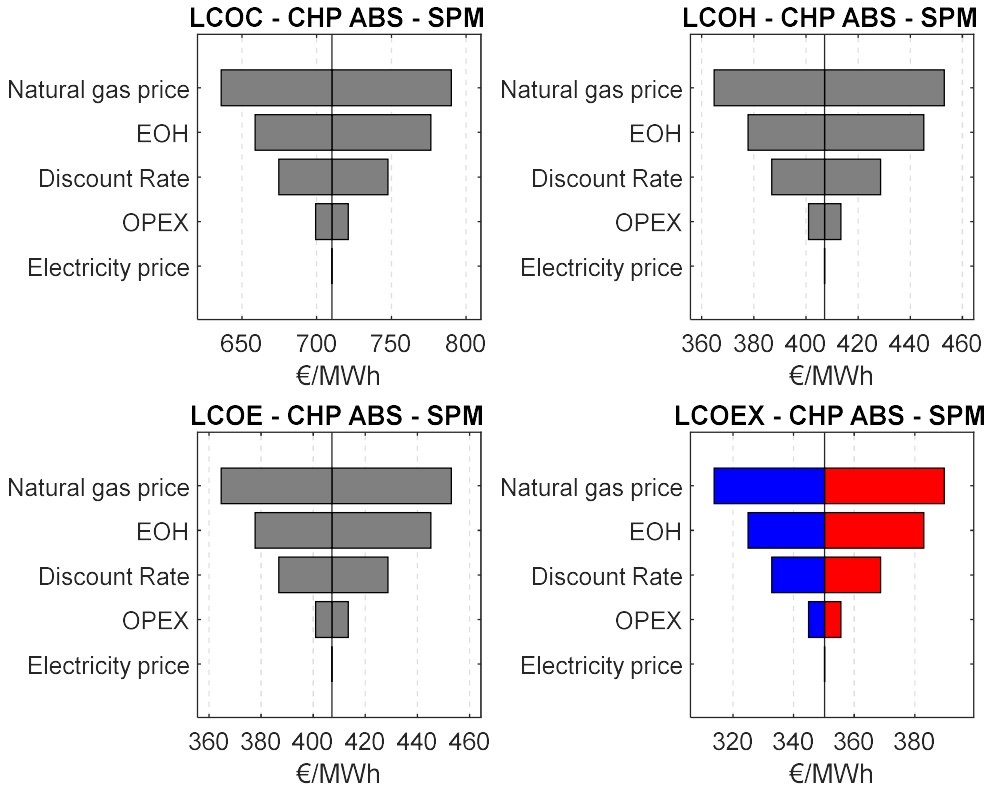

Figure 3.11. Tornado diagrams for the LCOC, LCOH, LCOE and LCOEx of the CCHP plant of the SPM according to the Monte Carlo analysis.

Table 3.5. Variation and propagation coefficients for the CCHP plant of the SPM.

Stochastic input parameter	μ		δ [-]		μ_{LCOEx} [€/MWh]	δ_{LCOEx} [-]	C_{LCOEx} [-]
	CHP	*ABS*	*CHP*	*ABS*			
EOH [h/year]	2,500		0.08		351.61	0.05	0.63
OPEX CHP [€/kW year]	76.92	20	0.07	0.25	350.26	0.01	0.14
Discount rate [%]	5		0.25		350.40	0.03	0.13
Natural gas price [€/m³]	0.42		0.17		350.25	0.06	0.38

LCOEx distribution of the heat pumps

Figure 3.12 (left) shows the *LCOEx* pdf for the heat pumps (operating in cooling mode) when all the parameters are uncertain, while Figure 3.12 (right) shows two tornado

diagrams respectively for *LCOC* and *LCOEx* where the uncertain parameters are considered one by one. Moreover, Table 3.6 reports a synthesis of the results.

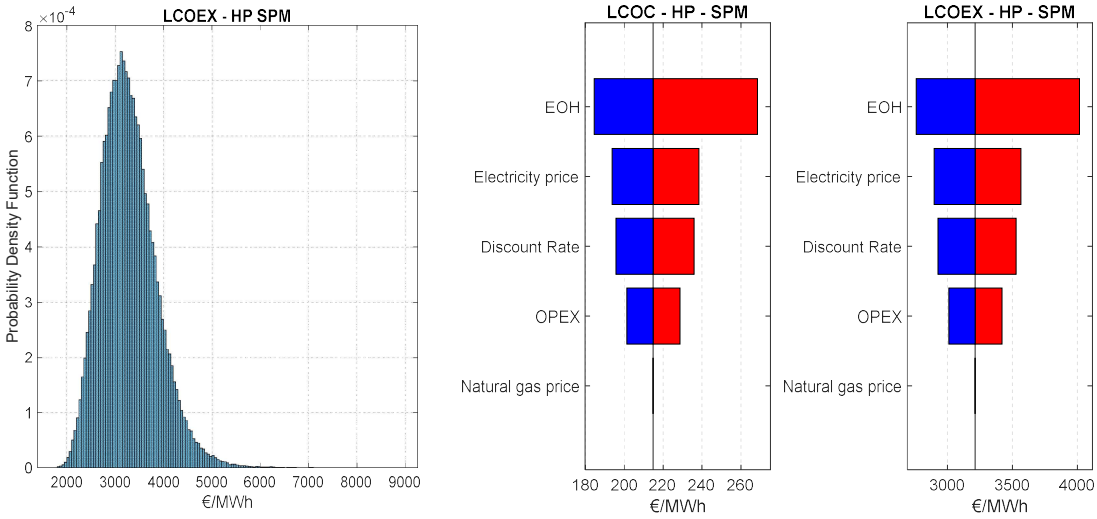

Figure 3.12. Probability density function (left) and tornado diagrams (right) for the LCOC and LCOEx of the HPs of the SPM according to the Monte Carlo analysis.

From the analysis of the two tornado diagrams reported in Figure 3.12, it can be seen how the values of *LCOEx* are significantly higher than the *LCOC.* The *LCOEx* is a more suitable indicator since it takes into account the different technical value between cooling energy and electricity, introducing as a common denominator the equivalent mechanical work or exergy. The distribution of the *LCOEx* for this plant is almost normal-like, with a mean value of € 3,283/MWh and a standard deviation of € 574/MWh.

Table 3.6 highlights that, compared to the CCHP plant and boilers, where the price of primary energy source (i.e. natural gas) had a higher propagation coefficient than *EOH*, the price of the HP primary energy source (i.e. electricity) has a propagation coefficient lower than *EOH*. Therefore, *EOH* has the highest impact on the results.

Table 3.6. Variation and propagation coefficients for the HPs of the SPM.

Stochastic input parameter	μ	δ [-]	μ_{LCOEx} [€/MWh]	δ_{LCOEx} [-]	C_{LCOEx} [-]
EOH [h/year]	600	0.17	3,277.30	0.12	0.74
OPEX [€/kW year]	15	0.33	3,214.80	0.04	0.12
Discount rate [%]	5	0.25	3,218.30	0.06	0.23
Electricity price [€/MWh]	170	0.18	3,213.80	0.06	0.34

LCOEx distribution of the whole microgrid

Finally, the overall SPM is considered addressing all the technologies together, in order to satisfy the electrical, heating and cooling demand. Figure 3.13 reports the LCOEx pdf of the SPM, that following the distribution of the price parameters is triangular-like. The values are significantly higher than the price of the electricity, but it must be considered that the SPM is a polygeneration microgrid (with multiple energy outcomes) and an R&D testing facility where the cost of integration and supervision of the whole system are considerably higher. Moreover, the inclusion of internalities (in terms of positive image and benefits for the research groups of the campus) and positive externalities (e.g. environmental and social benefits) would reduce the raw value of LCOEx calculated here.

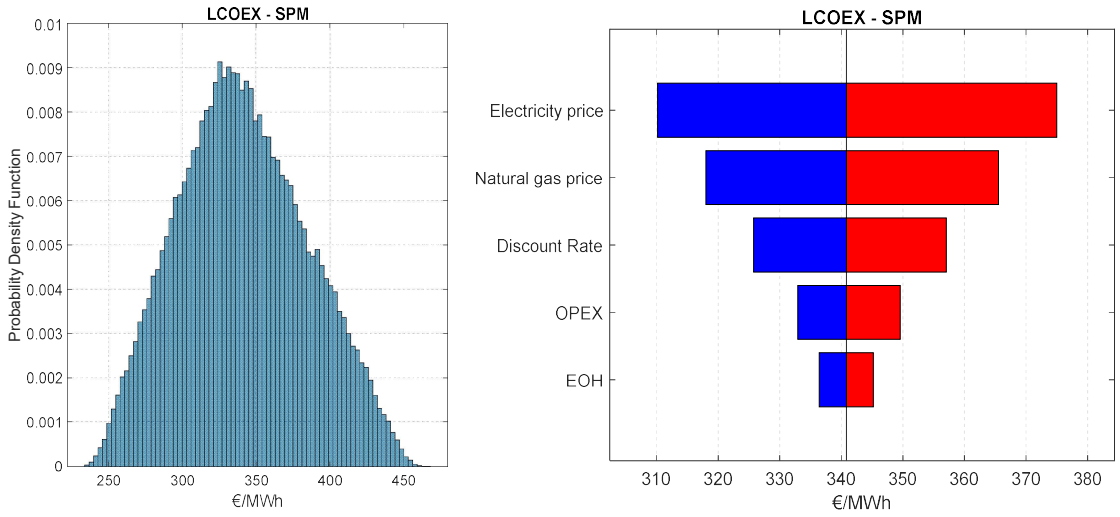

Figure 3.13. Probability density function (left) and tornado diagram (right) for the LCOEx of the whole SPM according to the Monte Carlo analysis.

As the tornado diagram suggests, the electricity price still has the main impact on the *LCOEx*; this can be explained by considering that the majority of the electricity absorbed from the load of the SPM comes from the external grid, directly affecting the heat pumps *LCOEx*. Moreover, the natural gas price is also extremely significant, affecting the CCHP units and boilers. Discount rate, *OPEX* and *EOH* have a relative lower impact on the final results. It should be noted that the *EOH* of dispatchable technologies (boilers, CCHP

plant, heat pumps, storage system) are influenced by the predetermined operation strategy of the microgrid and therefore their variation is somehow limited. As a consequence, its role on the *LCOEx* scattering is somehow limited.

3.4 Second case study: Smart Energy Building (SEB)

The second case study is relative to the Smart Energy Building (SEB) which is an energy prosumer installed in 2017 at the Savona Campus of the University of Genoa, within the Energia 2020 project [28]. The building, funded by the Italian Ministry for the Environment and the Protection of Land and Sea, has been designed as an R&D facility to test the interaction between energy efficient buildings and microgrids. Indeed, as shown in Figure 3.5, the SEB is the only building of the campus directly connected to the SPM. As done for the SPM, even if the main characteristics of the building have been taken into account, some simplifications have been considered in the calculation of the indicators.

3.4.1 Description of the SEB

The SEB, whose some representative pictures are reported in Figure 3.14, is characterized by high performance thermal insulation materials for building applications and presents:

- A solar photovoltaic field having a total peak power of 21 kW_p, with respectively 85 polycrystalline silicon panels installed on the flat roof of the building.
- A geothermal heat pump (46 kW_{th} rated thermal power, 44.3 kW_{th} rated cooling power) coupled with eight borehole heat exchangers.
- An air source heat pump (11.5 kW_{th} nominal thermal power).
- A controlled mechanical ventilation plant.
- Two vacuum solar collectors.
- Low consumption LED lamps.
- A rainwater collector system.

The heating system is supplied by the geothermal heat pump, whereas the domestic hot water is jointly produced by the geothermal heat pump, the solar collectors and the air source heat pump. The summer cooling is guaranteed by the geothermal heat pump.

Figure 3.14. Some pictures of the SEB.

The electrical scheme of the SEB is reported in Fig. 3.15, where it is possible to see the connection of the SEB to the SPM. Inside the building there are also some charging stations for electric vehicles: in particular, two AC charging points and a DC station able to apply vehicle-to-building (V2B) technology. By this way, electric vehicles can be used as storage systems which can also provide energy to the building when they are discharged.

The SEB is daily managed by a Building Management System (BMS) that interacts with the EMS of the SPM [32]. Generation units and loads of the building are real-time monitored and managed to reduce primary energy consumptions and so the carbon footprint of the SEB. The BMS applies operating strategies to optimally control the comfort level inside each room of the building. Moreover, research activities are developed to test demand response applications and the possibility of operating the SEB together with other devices of the SPM in island mode.

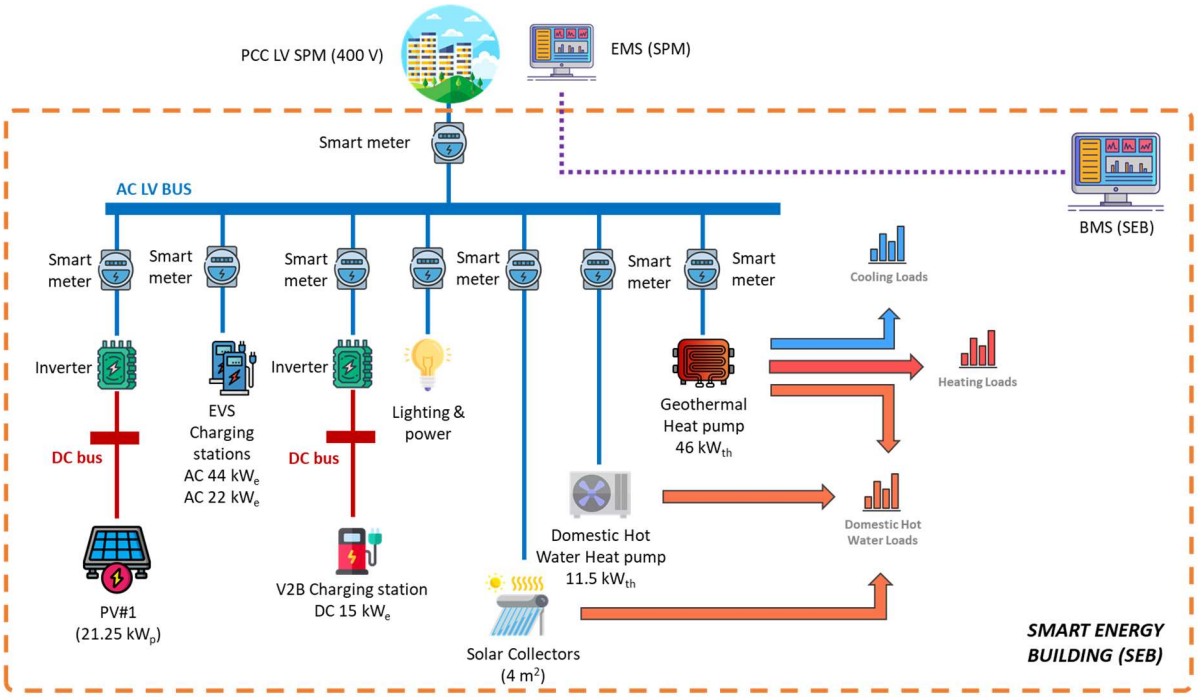

Figure 3.15. Electrical scheme of the SEB.

3.4.2 Adopted hypotheses and boundary conditions

Table 3.7 shows the main input parameters used to calculate the *LCOEn* (and its variants) of each technology and of the whole SEB. Similarly to what done for the SPM, some parameters are kept constant, while others are assumed to follow a normal or triangular distribution. The SEB has been modelled as a single bus system, thus neglecting electrical and thermal power losses. The *EOH* of the heat pumps and the forecast of the power produced by the solar PV field have been evaluated through the analysis of historical operating data collected from 2017 till 2021. Like for the SPM, all the technologies are characterized by the capital expenditures at year 0 ($CAPEX_0$) and the *CAPEX* annual reduction percentage, the latter used to calculate replacement costs. Also in this case, the time horizon of the analysis has been assumed equal to 20 years. Normal distributions have been assumed for both *EOH* and *OPEX* values, while triangular distributions have been preferred to represent the scattering of the electricity price and the discount rate. In Table 3.7 the Nanogrid System refers to the hardware and software (BMS) used to monitor and manage the SEB. Table 3.7 also reports the assumed value of supply temperature for solar collectors and heat pumps. The *LCOEx* has been

calculated considering reference indoor temperatures for the building equal to 18°C in winter and 26°C during summer.

Table 3.7. Input parameter values for the analysis of the SEB case study.

NANOGRID SYSTEM			
Parameter	**Deterministic value**	**Distribution**	**Distr. parameters**
Useful life [years]	20	-	-
$CAPEX_0$ [€]	119,000	-	-
OPEX [€/year]	1,500	Normal	μ=1,500, σ=200
EOH [h/year]	8,760	-	-
CAPEX reduction [%/year]	2	-	-
PV (21 kW_{AC} / 21.25 kW_p)			
Parameter	**Deterministic value**	**Distribution**	**Distr. parameters**
Useful life [years]	20	-	-
$CAPEX_0$ [€]	34,000	-	-
OPEX [€/year]	264.7	Normal	μ=264.7, σ=74.3
EOH [h/year]	1100	Normal	μ=1,100, σ=62.7
CAPEX reduction [%/year]	2	-	-
LOAD			
Parameter	**Deterministic value**	**Distribution**	**Distr. parameters**
Electricity consumption [kWh/year]	100,000	Normal	μ=100,000, σ=10,000
Demand variation [%/year]	0	-	-
Electricity purchase price [€/MWh]	170	Triangular	A=100, B=160, C=250
Prices variation [%/year]	0	-	-
Discount rate [%]	5	Triangular	A=2, B=5, C=8
Solar collectors (4 m^2)			
Parameter	**Deterministic value**	**Distribution**	**Distr. parameters**
Useful life [years]	25	-	-
$CAPEX_0$ [€]	4,059	-	-
OPEX [€/year]	200	-	-
Average thermal production [kWh/(m^2 year)]	749	Normal	μ=749, σ=100
Supply temperature [°C]	50	-	-
CAPEX reduction [%/year]	2	-	-
Domestic hot water heat pump (11.5 kW_{th})			
Parameter	**Deterministic value**	**Distribution**	**Distr. parameters**
Useful life [years]	20	-	-
$CAPEX_0$ [€]	12,535	-	-
OPEX [€/year]	172.50	Normal	μ=172.5, σ=57.5
EOH [h/year]	400	Normal	μ=400, σ=70
COP [-]	2.6	-	-
Supply temperature [°C]	55	-	-
CAPEX reduction [%/year]	2	-	-
Geothermal heat pump (46 kW_{th}, 44.3 kW_{co})			
Parameter	**Deterministic value**	**Distribution**	**Distr. parameters**
Useful life [years]	20	-	-
$CAPEX_0$ [€]	71,169	-	-
OPEX [€/year]	690	Normal	μ=690, σ=276
EOH in heating mode [h/year]	489	Normal	μ=489, σ=100
EOH in cooling mode [h/year]	368	Normal	μ=368, σ=80
COP [-]	2.8	-	-
EER [-]	2.6	-	-
Supply temperature in heating mode [°C]	45	-	-

Supply temperature in cooling mode [°C]	7	-	-
CAPEX reduction [%/year]	2	-	-

3.4.3 Results and discussion for the SEB

The main results for the SEB case are here presented.

***LCOE* distribution of the PV plant**

The PV plant of the SEB presents higher average values for the *LCOE* (Figure 3.16) compared to the PV plants of the SPM, due to higher investment and maintenance costs (derived from its lower size) and a non-optimal installation in terms of tilt angle. However, the qualitative framework of the outcome variability (Table 3.8) is almost the same (Table 3.2).

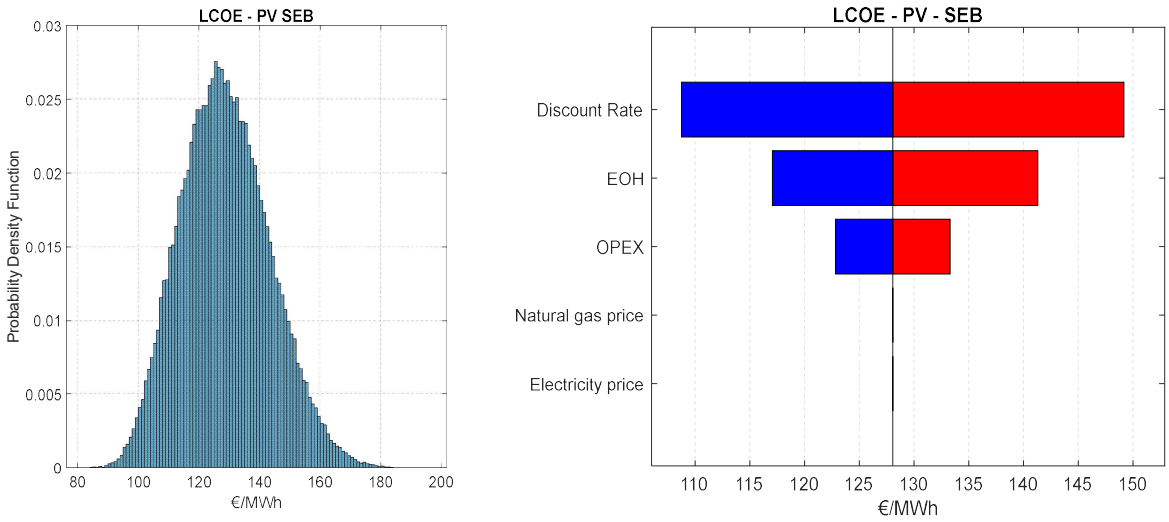

Figure 3.16. Probability density function (left) and tornado diagram (right) for the LCOE of the PV plant of the SEB according to the Monte Carlo analysis.

Table 3.8. Variation and propagation coefficients for the PV plant of the SEB.

Stochastic input parameter	μ	δ [-]	μ_{LCOE} [€/MWh]	δ_{LCOE} [-]	C_{LCOE} [-]
EOH [h/year]	1,100	0.06	128.45	0.06	1.01
OPEX [€/(kW year)]	13	0.28	128.05	0.02	0.09
Discount rate [%]	5	0.25	128.35	0.09	0.38

LCOEx distribution of the solar collectors

Figure 3.17 (left) shows the *LCOEx* pdf for the solar collectors, while Figure 3.17 (right) shows two tornado diagrams respectively for the *LCOH* and the *LCOEx*. Table 3.9 reports the mean value and the coefficient of variation for each input parameter, together with the corresponding mean value, coefficient of variation and propagation coefficient of the *LCOEx*. The *EOH* (influencing the annual thermal production) is the parameter which has the highest impact on the results. As already mentioned for other thermal generation technologies, solar collectors present values of *LCOEx* significantly higher than *LCOH* ones, since *LCOEx* also considers the supply temperature as reported in chapter 2.

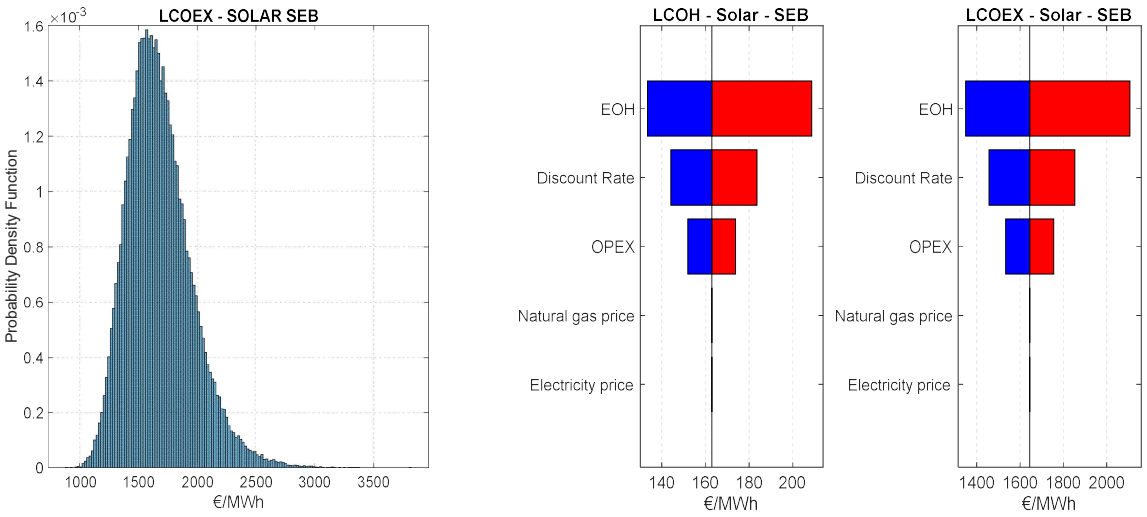

Figure 3.17. Probability density function (left) and tornado diagram (right) for the LCOH and LCOEx of the solar collectors of the SEB according to the Monte Carlo analysis.

Table 3.9. Variation and propagation coefficients for the solar collectors of the SEB.

Stochastic input parameter	μ	δ [-]	μ_{LCOEx} [€/MWh]	δ_{LCOEx} [-]	C_{LCOEx} [-]
Thermal production [kWh/year]	749	0.13	1,675.80	0.14	1.06
OPEX [€/(kW year)]	50	0.10	1,644.80	0.04	0.41
Discount rate [%]	5	0.25	1,648.40	0.07	0.29

LCOEx distribution of the domestic hot water heat pump

Figure 3.18 (left) shows the *LCOEx* pdf for the heat pump used to produce domestic hot water, assuming all the parameters' uncertainty. The tornado diagrams in Figure 3.18 (right) show the *LCOH* and the *LCOEx* scattering where the uncertain parameters are considered one by one. Table 3.10 reports a synthesis of the results. The main difference with respect to the heat pumps of the SPM is the lower value of *LCOEx*. This can be referred to the higher average efficiency. *EOH* still remains the input parameter having the greater influence on both *LCOH* and *LCOEx*.

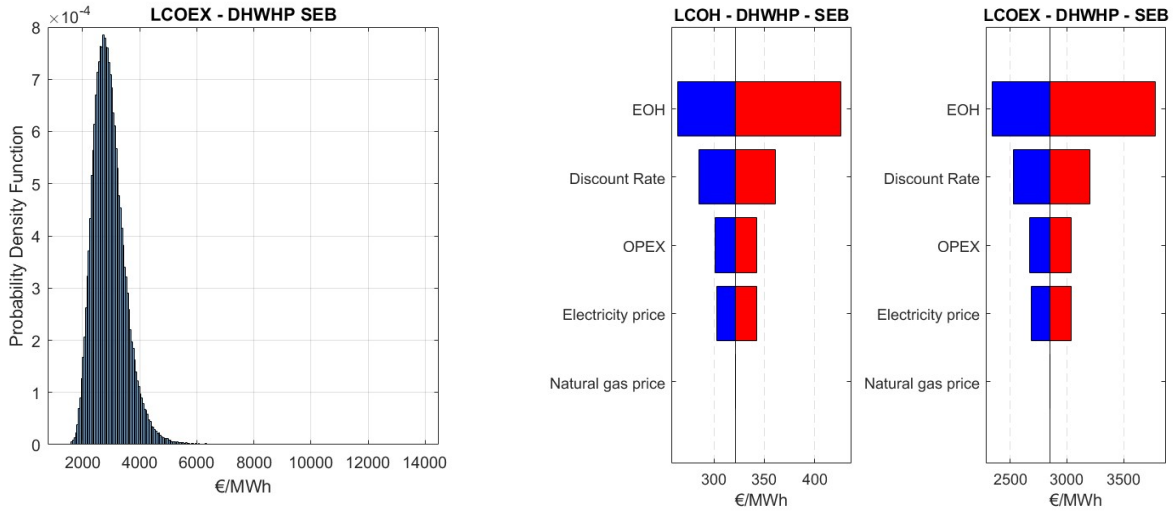

Figure 3.18. Probability density function (left) and tornado diagrams (right) for the LCOH and LCOEx of the domestic hot water heat pump of the SEB according to the Monte Carlo analysis.

Table 3.10. Variation and propagation coefficients for the domestic hot water heat pump of the SEB.

Stochastic input parameter	μ	δ [-]	μ_{LCOEx} [€/MWh]	δ_{LCOEx} [-]	C_{LCOEx} [-]
EOH [h/year]	400	0.18	2,932.0	0.16	0.90
OPEX [€/(kW year)]	15	0.33	2,852.4	0.04	0.12
Discount rate [%]	5	0.25	2,856.8	0.07	0.29
Electricity price [€/MWh	170	0.18	2,851.7	0.04	0.20

LCOEx distribution of the geothermal heat pump

The *LCOC*, *LCOH* and *LCOEx* tornado diagrams for the geothermal heat pump are reported in Figure 3.19, while Figure 3.20 shows the *LCOEx* pdf. The plant presents values of *LCOC* and *LCOH* higher than those of both the heat pumps of the SPM (which only produce cooling energy) and the domestic hot water heat pump of the SEB (which only produces thermal energy) due to a higher investment cost (per unit of power). Nevertheless, *LCOEx* average values tend to be lower benefitting from the production of two useful effects (thermal and cooling energy). As it can be deduced from Table 3.11, the number of *EOH* in heating and cooling mode contributes most to the variability of the outcome having moderate scattering and a large propagation coefficient.

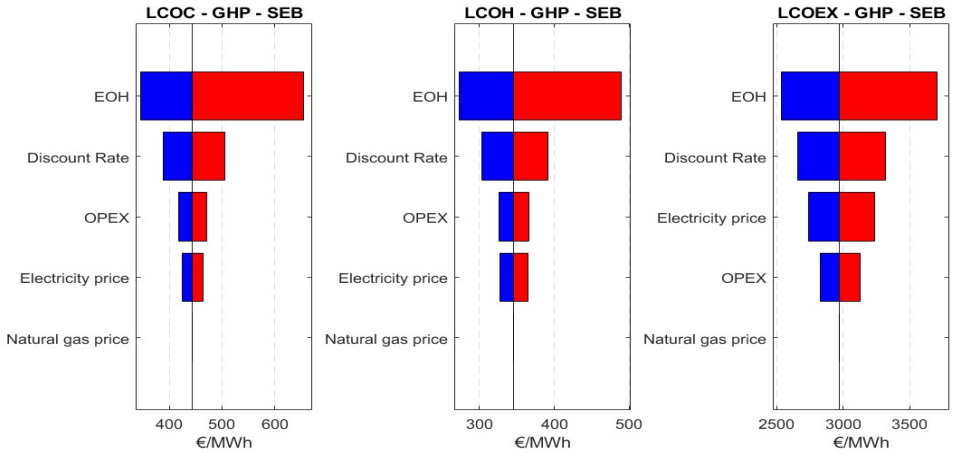

Figure 3.19. Tornado diagrams for the LCOC, LCOH and LCOEx of the geothermal heat pump of the SEB according to the Monte Carlo analysis.

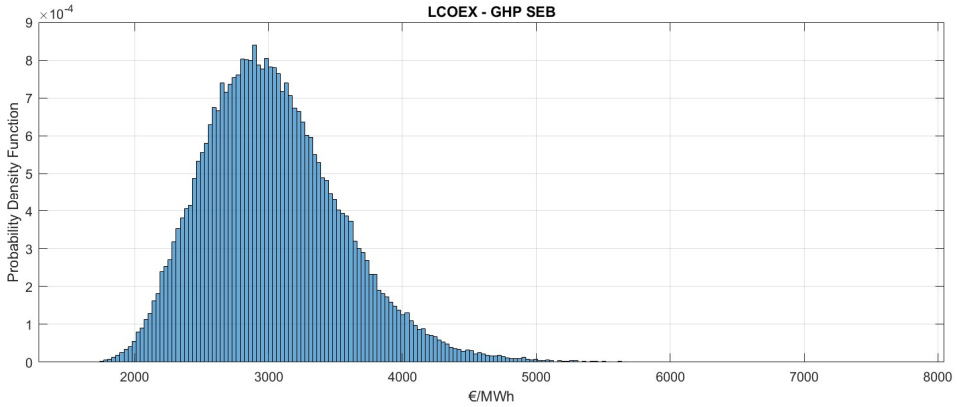

Figure 3.20. Probability density function for the LCOEx of the geothermal heat pump of the SEB according to the Monte Carlo analysis.

Table 3.11. Variation and propagation coefficients for the geothermal heat pump of the SEB.

Stochastic input parameter	μ	δ [-]	μ_{LCOEx} [€/MWh]	δ_{LCOEx} [-]	C_{LCOEx} [-]
EOH Heating [h/year]	489	0.20	3,028.00	0.12	0.60
EOH Cooling [h/year]	368	0.22			0.56
OPEX [€/(kW year)]	15	0.40	2,975.40	0.03	0.08
Discount rate [%]	5	0.25	2,978.50	0.07	0.27
Electricity price[€/MWh]	170	0.18	2,973.50	0.05	0.28

LCOEx distribution of the SMART ENERGY BUILDING

Figure 3.21 shows the LCOEx pdf of the whole SEB. The LCOEx average value is lower than the SPM one, since the SEB is characterized by more efficient and newer power plants. It is possible to highlight that the discount rate is the uncertain parameter which affects the most the results. LCOEx assumes a triangular-like pdf following the discount rate one. The inclusion of internalities and positive externalities could reduce the value of LCOEx.

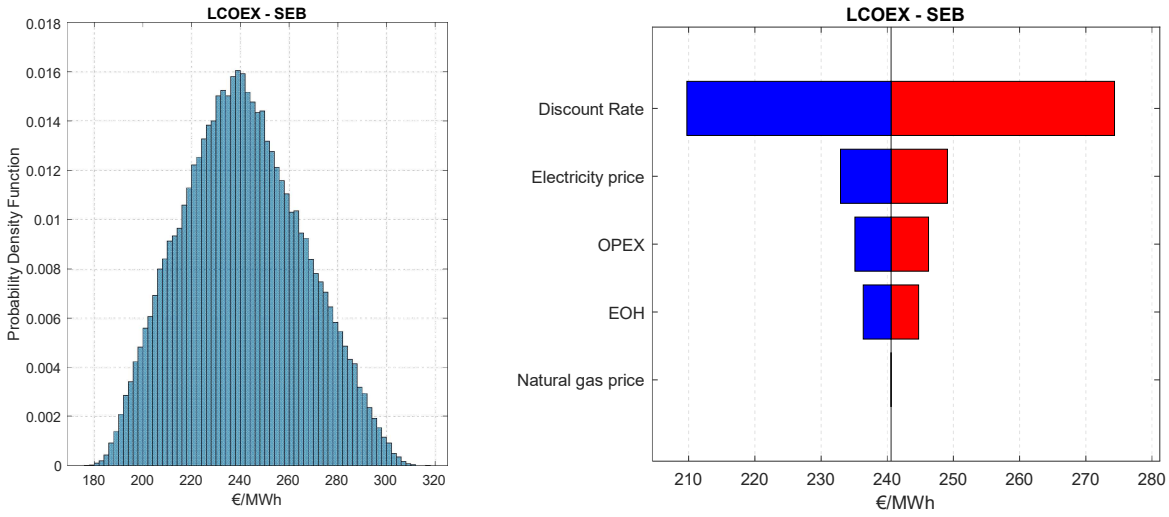

Figure 3.21. Probability density function (left) and tornado diagram (right) for the LCOEx of the SEB according to the Monte Carlo analysis.

3.5 Third case study: ERESMAGrid

This case study is based on a microgrid which includes only electrical appliances. Moreover, it accounts only with renewable energy generators and works connected to

the external power grid. However, the microgrid is not allowed to inject surplus energy to the external grid. Then, it accounts with a battery bank and two controllable loads in order to minimize the curtailment of the production from the renewable energy sources. Although the main characteristics of the real facility have been considered, some simplifications have been assumed in the calculation of the indicators.

3.5.1 Description of the ERESMAGrid

The ERESMA Grid is a test bed pilot microgrid which is placed at the University Campus of Vegazana of the University of León, in León (Spain). More specifically, it is integrated in the Laboratory of Power Systems and Smart Grids, placed in the building of the School of Mining Engineering. The ERESMAGrid is a microgrid designed both for research and teaching purposes. It accounts with three main generation sources, which are two solar PV plants and a micro wind-turbine (μWTG). A detailed scheme can be seen in Figure 3.22. while a more detailed description can be obtained from [33–36].

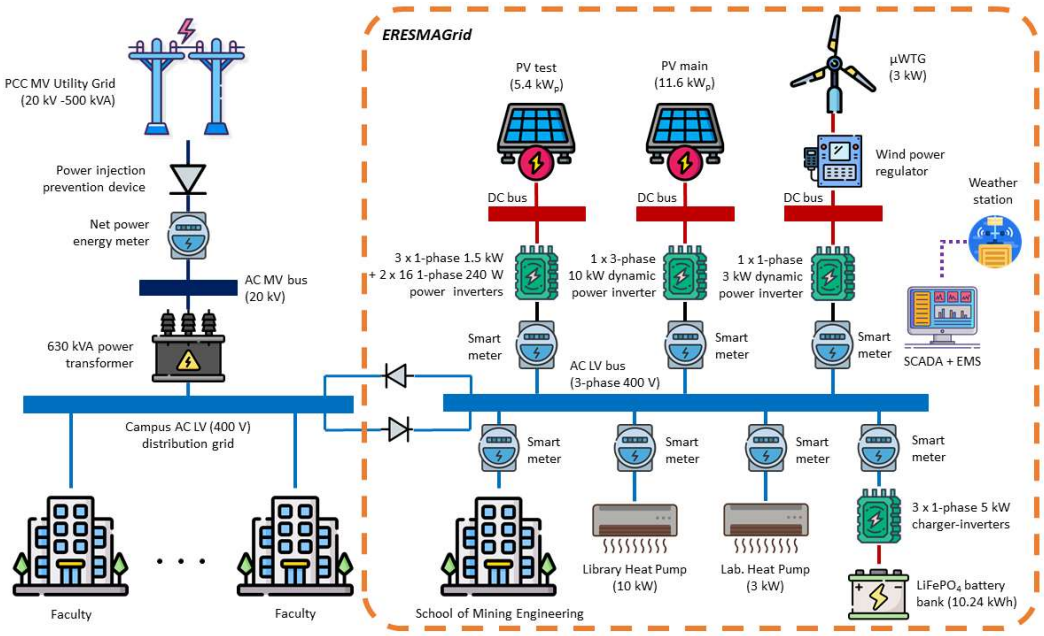

Figure 3.22. Electrical scheme of the ERESMAGrid.

The main PV field is set in the upper rooftop of the building and is composed of two strings of 22 mono-silicon PV panels each, which sum 11.6 kW_p of total installed peak power (see Figure 3.23). Both strings are connected to a 3-phase solar dynamic inverter of 10 kW_{AC} of rated power, which is then connected to the AC bus of the microgrid. All the PV panels are mounted on inclined fixed racks pointing the South. The second PV field is placed on another rooftop of the building and it is mounted on modular regulating racks (see Figure 3.24). It is intended to be a test bed platform for PV technologies and is formed by three single-phase inverters of 1.5 kW_{AC} of rated power each and two multigate inverters up to concentrate 16 micro-inverters each. Each micro-inverter has a rated power of 240 W_p. Connected to each 1.5 kW_{AC} inverters there is a set of thin-film PV modules, a set of bifacial PERC modules and a set of standard mono-silicon PV modules (reference system), respectively. Moreover, several damaged PV modules of different technologies which are monitored under real outdoor conditions are connected to the micro-inverters.

Figure 3.23. Main PV plant of the ERESMAGrid.

Figure 3.24. Test platform for PV technologies of the ERESMAGrid.

In parallel with both PV plants, the microgrid accounts with a horizontal axis two-bladed µWTG installed on a metallic tower of 20 m height, 8 m higher than the rooftop of the building, and free of obstacles in the near surroundings (see Figure 3.25 left). It has 3 kW_{AC} of rated power and accounts with stall control and Maximum Power Point Tracking (MPPT) regulation, providing 240 V_{AC} through a regulator and a single-phase inverter.

Figure 3.25. µWTG (left) and weather station (right) of the ERESMAGrid.

The generators are supported by a $LiFePO_4$ battery bank, composed of 4 battery units of 200 Ah of power capacity and 12.8 V_{DC} of nominal voltage each (see Figure 3.26). The four units are grouped in series and connected to the AC bus by three single-phase charger-inverters of 5 kW_{AC} of rated power each. The ESS can be charged both by the generators of the microgrid or through the electricity purchased from the external power grid.

Moreover, the microgrid has the ability to apply flexible demand strategies through two flexible power loads: two electrical air heat pumps of 3 kW_{AC} and 10 kW_{AC}, respectively. The 3 kW_{AC} unit is used for heating/cooling the laboratory stay, while the 10 kW_{AC} unit heats/cools the library. It must be noted that, due to the existing regulations in Spain when the microgrid was set up (Royal Decree 900/2015, from 9th October), no surplus

injections to the external power grid are allowed for the system. Thus, the microgrid is equipped with an injection controller in the PCC with the external grid which prevents from any power injection. Thus, the surplus or RES generation is curtailed in the case that it cannot be stored in the battery bank or used to dispatch the flexible power loads.

Figure 3.26. $LiFePO_4$ battery bank of the ERESMAGrid.

Finally, the whole system is supervised and managed through a centralized Supervisory Control and Data Acquisition (SCADA) System, which incorporates an Energy Management System (EMS) tool (see Figure 3.27). It receives real time information regarding the local weather conditions though its own weather station placed on the rooftop (see Figure 3.25 right) and takes control of all the generators, the ESS and the dispatchable loads.

Figure 3.27. Interface of the SCADA of the ERESMAGrid.

3.5.2 Adopted hypotheses and boundary conditions

The case study has been modeled as a single bus system, where power losses can be considered negligible, and all generators and power loads are connected to the same bus. The dispatchable power loads have been discarded for simplicity. In order to evaluate the yearly distribution of the equivalent hours of each generator, the microgrid power load and the energy charged in the ESS, a timeseries of three years (2017-2019) has been examined. On the other hand, none externalities or internalities have been included in the analysis. Moreover, all *CAPEX*, *OPEX* and electricity prices have been considered before taxes and updated to year 2021. For simplicity, no yearly reduction in the generation capacity, yearly increment in the power demand or yearly prices scalations have been taken into account. Table 3.12 summarizes the values and distributions of the input parameters assumed in the following calculations. The second column reports the nominal values of parameters used in the deterministic evaluation; second and third columns provide the probabilistic model and the model parameters.

Table 3.12. Input parameter values for the analysis of the ERESMAGrid case study.

MICROGRID SYSTEM			
Parameter	**Deterministic value**	**Distribution**	**Distr. parameters**
Useful life [years]	20	-	-
$CAPEX_0$ [€]	5,170	-	-
OPEX [€/year]	50	Normal	μ=50, σ=5
EOH [h/year]	8,760	-	-
CAPEX reduction [%/year]	2	-	-
PV MAIN (10 kW_{AC} / 11.6 kW_P)			
Parameter	**Deterministic value**	**Distribution**	**Distr. parameters**
Useful life [years]	20	-	-
$CAPEX_0$ [€]	21,180	-	-
OPEX [€/year]	150	Normal	μ=150, σ=50
EOH [h/year]	1,134	Normal	μ=1,134, σ=58
CAPEX reduction [%/year]	2	-	-
PV TEST (4.5 kW_{AC} / 5.4 kW_P)			
Parameter	**Deterministic value**	**Distribution**	**Distr. parameters**
Useful life [years]	15	-	-
$CAPEX_0$ [€]	12,300	-	-
OPEX [€/year]	50	Normal	μ=50, σ=5
EOH [h/year]	1,054	Normal	μ=1,054, σ=54
CAPEX reduction [%/year]	2	-	-
µWT (3 kW_{AC})			
Parameter	**Deterministic value**	**Distribution**	**Distr. parameters**
Useful life [years]	15	-	-
$CAPEX_0$ [€]	9,500	-	-
OPEX [€/year]	421	Normal	μ=421, σ=215
EOH [h/year]	685	Normal	μ=685, σ=103

CAPEX reduction [%/year]	2	-	-
ESS (10.24 kWh)			
Parameter	**Deterministic value**	**Distribution**	**Distr. parameters**
Useful life [years]	7	-	-
CAPEX$_0$ [€]	19,800	-	-
OPEX [€/year]	210	Normal	μ=210, σ=160
E^{ch} [kWh/year]	9,012	Normal	μ=9,012, σ=325
Min SoC [%]	20	-	-
Max SoC [%]	100	-	-
Round trip efficiency [%]	81	-	-
Capacity reduction [%/year]	0	-	-
CAPEX reduction [%/year]	2	-	-
LOAD (30 kW$_{AC}$)			
Parameter	**Deterministic value**	**Distribution**	**Distr. parameters**
Electricity consumption [kWh/year]	86,449	Normal	3,959
Demand variation [%/year]	0	-	-
Electricity purchase price [€/MWh]	140	Triangular	*A*=60, *B*=110, *C*=250
Electricity selling price [€/MWh]	n/a	-	-
Prices variation [%/year]	0	-	-
Discount rate [%]	5	Triangular	*A*=2, *B*=5, *C*=8

3.5.3 Results and discussion for the ERESMAGrid

In the following, the presentation of results for ERESMAGrid is reported.

LCOE distribution of the PV Main power plant

Figure 3.28 (left) shows the *LCOE* pdf for the PV Main plant, while Figure 3.28 (right) reports the corresponding tornado diagram. Then, Table 3.13 presents the main results.

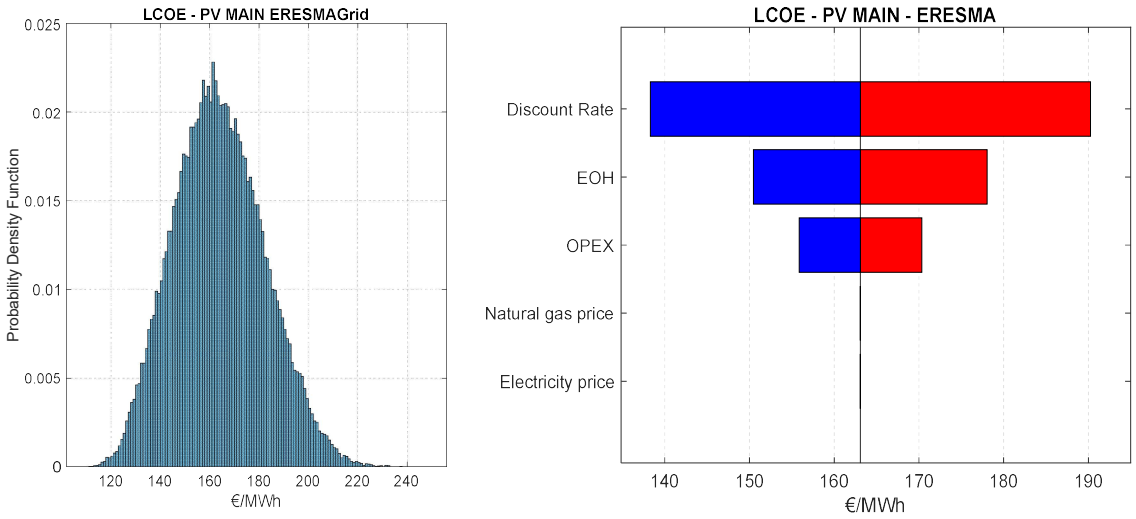

Figure 3.28. Probability density function (left) and tornado diagram (right) for the LCOE of the PV Main plant of ERESMAGrid according to the Monte Carlo analysis.

The distribution of the *LCOE* for this generator is normal-like, with a mean value of € 164/MWh and a standard deviation of € 18.24/MWh. These values are in the current range for this technology (see chapter 2), considering the small size of the facility. In this case, the probability to achieve the grid parity is less than 8.5% (value taken from the cumulative probability density function or cdf).

The distribution of the *LCOE* is almost symmetrical respect to the deterministic value (€ 163.90/MWh). The observed high dispersion is mainly due to the scattering of the discount rate itself rather than to its propagation coefficient, as can be seen in Table 3.13. On the other hand, *EOH* is the second input parameter with the highest impact on the *LCOE*, even though it shows the lowest δ. Its impact is explained due to its high coefficient of propagation. Finally, it can be observed that the scattering of the *OPEX* values causes a variation of *LCOE* of less than € 15/MWh (90% confidence interval).

Table 3.13. Variation and propagation coefficients for the PV Main plant of ERESMAGrid.

Stochastic input parameter	μ	δ [-]	μ_{LCOE} [€/MWh]	δ_{LCOE} [-]	C_{LCOE} [-]
EOH [h/year]	1134	0.05	163.53	0.05	1.01
OPEX [€/kW year]	15	0.33	163.10	0.03	0.08
Discount rate [%]	5	0.25	163.49	0.10	0.39

LCOE distribution of the PV Test plant

In Figure 3.29 (left) the *LCOE* pdf of the PV Test plant is presented, while Figure 3.29 (right) shows the corresponding tornado diagram. As expected, the behavior of the results is similar to the one of the PV Main power plant, although the range of the values is significantly larger due to the plant lower efficiency. Indeed, it is an experimental facility, with some partially damaged PV panels.

Analogously to the PV Main power plant, the distribution of the *LCOE* for this generator is normal-like, with a mean value of € 261/MWh and a standard deviation of € 24.68/MWh. In this case, it would be impossible to achieve the grid parity, as the lowest achievable *LCOE* value is around € 220/MWh (5th percentile), about € 80/MWh higher than the average price of the electricity purchased from the external power grid.

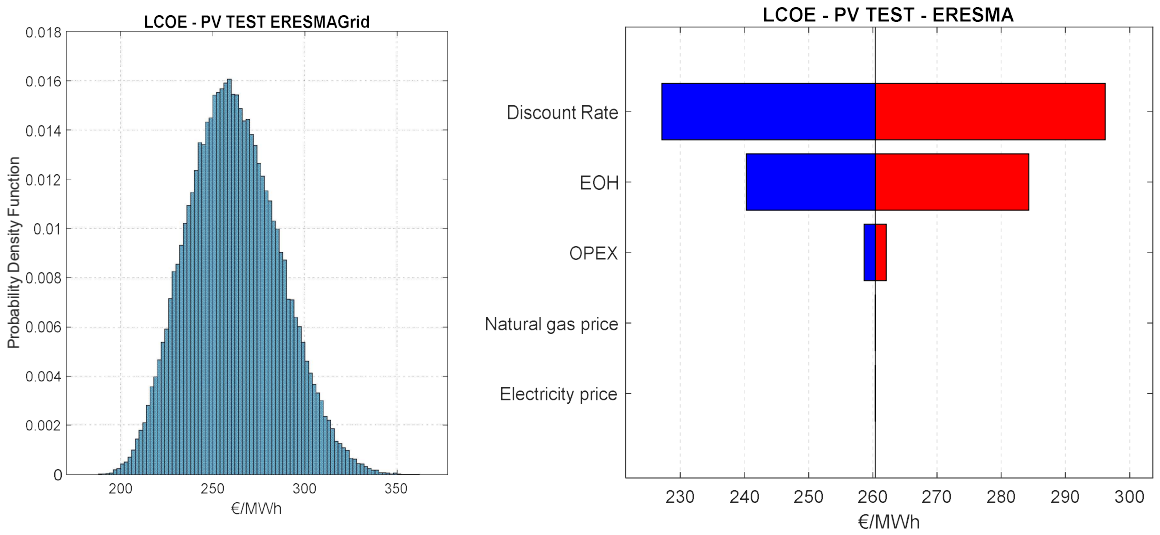

Figure 3.29. Probability density function (left) and tornado diagram (right) for the LCOE of the PV Test plant of ERESMAGrid according to the Monte Carlo analysis.

Table 3.14. Variation and propagation coefficients for the PV Test plant of ERESMAGrid.

Stochastic input parameter	μ	δ [-]	μ_{LCOE} [€/MWh]	δ_{LCOE} [-]	C_{LCOE} [-]
EOH [h/year]	1054	0.05	261.06	0.05	1.01
OPEX [€/kW year]	11	0.10	260.38	0.01	0.04
Discount rate [%]	5	0.25	260.81	0.08	0.32

In Table 3.14 shows that, similarly to the PV Main case, the input variable which produces the highest impact is, again, the discount rate, followed by the *EOH*. In this case, it is observed a lower dependence of the *LCOE* on the variation of the *OPEX*, due to its lower uncertainty. Moreover, the significant increment in the specific $CAPEX_0$ values, from € 2,180/kWp to € 2,733/kWp (25% increase) and the reduction of *EOH*, from 1,134 h/year to 1,054 h/year (7% decrease) leads to a significant increase in the average *LCOE* value, with an approximate difference of € 100/MWh (60% increase).

LCOE distribution of the micro wind turbine

Figure 3.30 (left) shows the *LCOE* pdf for the micro wind turbine, while Figure 3.30 (right)

highlights the corresponding tornado diagram. In this case, the pdf function is more Beta-like, with the most probable value at € 625/MWh and a mean value of € 673/MWh. The right tail of the pdf is significantly larger than the left tail. At any case, the *LCOE* is far from grid parity, and the minimum (5th percentile) attainable value is € 450/MWh. According to the cdf, the *LCOE* of this generator is lower than € 880/MWh with a 90% probability.

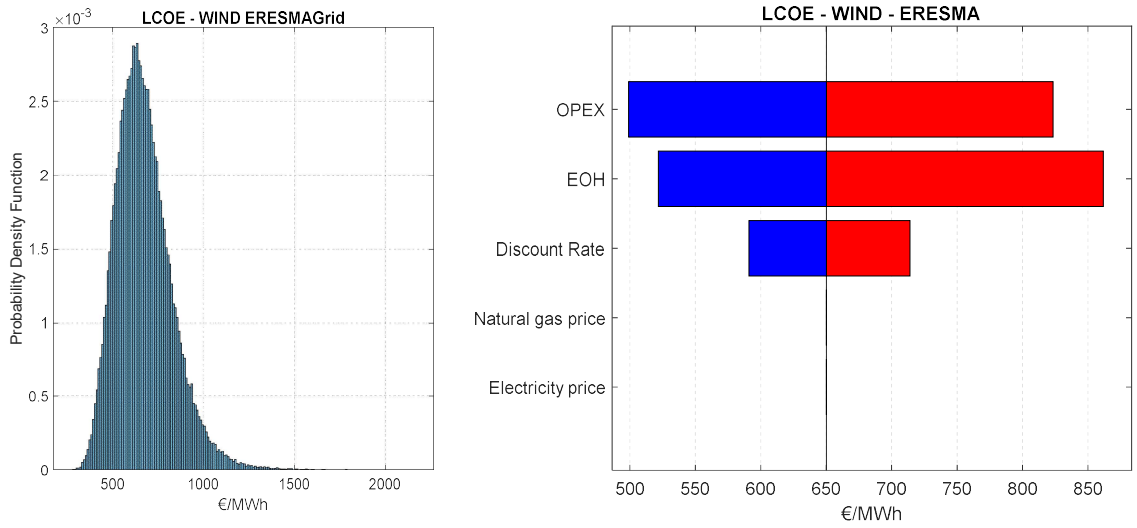

Figure 3.30. Probability density function (left) and tornado diagram (right) for the LCOE of the micro wind turbine of ERESMAGrid according to the Monte Carlo analysis.

According to the tornado diagram, differently from the PV power plants, the most significant variation of the *LCOE* is due to *OPEX* and *EOH*. Moreover, the impact of the scattering of both variables is not symmetric respect to the assumed baseline. The lowest value of *OPEX* determines a minimum (5th percentile) value of *LCOE* around € 500/MWh, while the minimum *EOH* lead to maximum (95th percentile) *LCOE* values around € 860/MWh. The very high uncertainty of both *EOH* and *OPEX* greatly affects the scattering of *LCOE*.

Table 3.15. Variation and propagation coefficients for the micro wind turbine of ERESMAGrid.

Stochastic input parameter	μ	δ [-]	μ_{LCOE} [€/MWh]	δ_{LCOE} [-]	C_{LCOE} [-]
EOH [h/year]	685	0.15	665.70	0.16	1.07
OPEX [€/kW year]	140	0.51	656.58	0.15	0.29
Discount rate [%]	5	0.25	651.00	0.06	0.23

Finally, as it can be seen in Table 3.15, both the highest δ and *c* values of *LCOE* are obtained varying the *EOH* input parameter, demonstrating the high impact of the operating conditions for this technology. Furthermore, the *EOH* are characterized by a lower scattering (δ) but present a higher propagation coefficient compared to the *OPEX*.

It must be also noted that the *LCOE* for this technology doubles the value of the solar PV Test platform and it is almost four times higher than that of the PV Main plant. This can be explained by considering the very high specific $CAPEX_0$ for this technology (not comparable to utility-scale wind turbines) and the very low *EOH* which characterize the installation site.

LCOS distribution of the ESS

Figure 3.31 (left) shows the *LCOS* pdf for the ESS ($LiFePO_4$ battery), while Figure 3.31 (right) plots the corresponding tornado diagram. In this case, the pdf function is normal-like, with a mean value of € 502/MWh and a standard deviation of € 33.40/MWh. In the best working conditions of the storage system, the *LCOS* can achieve a value of € 447/MWh (5^{th} percentile), and, with a 90% probability, the *LCOS* is lower than € 546/MWh.

The tornado diagram for the ESS shows that the input variable which has the highest impact on the *LCOS* is the discount rate, although slight differences can be observed with *EOH* and *OPEX* parameters. The comparison is not easy as the discount rate has an almost symmetric impact on the *LCOS* scattering, while *EOH* and *OPEX* present an asymmetric impact. Actually, it can be observed that they determine an increase of *LCOS* in the worst operating conditions higher than its decrease in the most favorable working

conditions. Regarding this aspect, it must be considered that *EOH*, i.e., the energy discharged by the ESS, depend on the energy charged, which is a sort of "semi-stochastic variable" since it also depends on the energy balance of the whole microgrid. The lowest values of the discount rate may conduct to a minimum value of *LCOS* around € 464/MWh, while the maximum *OPEX* can increase *LCOS* up to € 534/MWh. It is observed that the very high uncertainty of both *EOH* and *OPEX* highly affects the scattering of the *LCOS*.

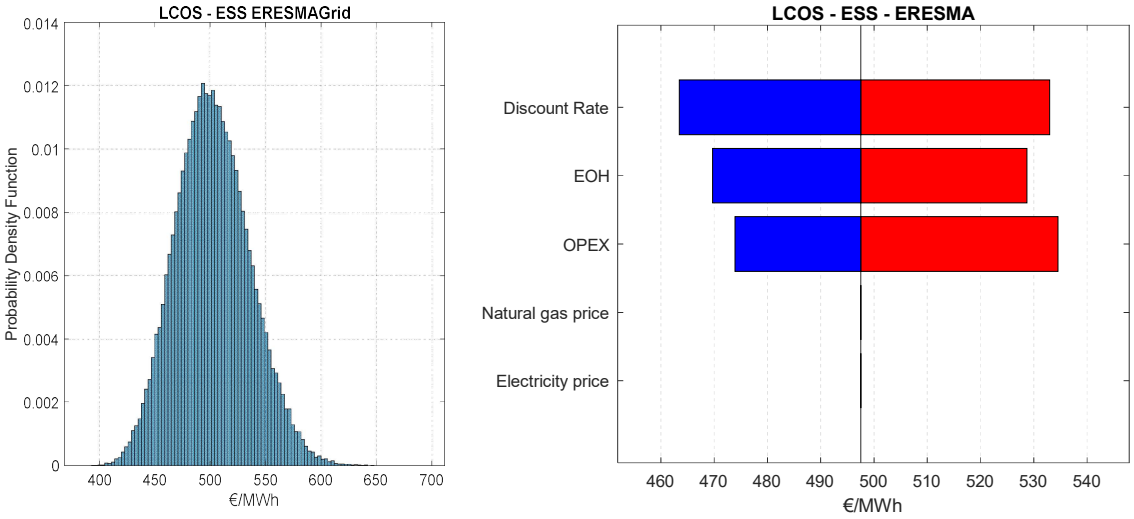

Figure 3.31. Probability density function (left) and tornado diagram (right) for the LCOS of the ESS of ERESMAGrid according to the Monte Carlo analysis.

Table 3.16. Variation and propagation coefficients for the ESS of ERESMAGrid.

Stochastic input parameter	μ	δ [-]	μ_{LCOS} [€/MWh]	δ_{LCOS} [-]	C_{LCOS} [-]
Charged energy [kWh/year]	9012	0.04	498.14	0.04	1.00
OPEX [€/kWh year]	20.51	0.76	501.66	0.04	0.05
Discount rate [%]	5	0.25	497.74	0.04	0.17

Finally, Table 3.16 shows the synthesis of results. In this case, the highest δ of input parameters corresponds to the *OPEX*, while the highest propagation coefficient is associated with the *EOH*. Nevertheless, the *LCOS* coefficient of variation values are almost the same for the three input variables. Referring to the *c* indicator, the

propagation of the *EOH* is about five times the one of the discount rate and twenty times that of the *OPEX*.

LCOE and *LCOEx* distribution for the ERESMAGrid

The pdf and the tornado diagram of the *LCOE* for the ERESMAGrid are reported in Figure 3.32. As the microgrid is pure electrical, in this case the *LCOEx* is equivalent to the *LCOE*. The pdf considers all the input parameters uncertain and shows a triangular-like distribution, where the most probable variable is € 184/MWh and the mean value is € 208/MWh. These values are significantly higher than the average price of the electricity purchased from the external grid (equal to € 140/MWh). In this case it must be highlighted that a significant amount of the load is satisfied by the external power grid and the capacity of the power generation plants of the microgrid is small. This fact helps to reduce the overall *LCOE* value, as all the generation technologies have a higher average *LCOE*. As visible on the plots, the minimum (5th percentile) value for the *LCOE* is € 150/MWh, while the maximum (95th percentile) achieves € 279/MWh. Nevertheless, it can be observed that the *LCOE* is lower than € 264/MWh in the 90% of cases.

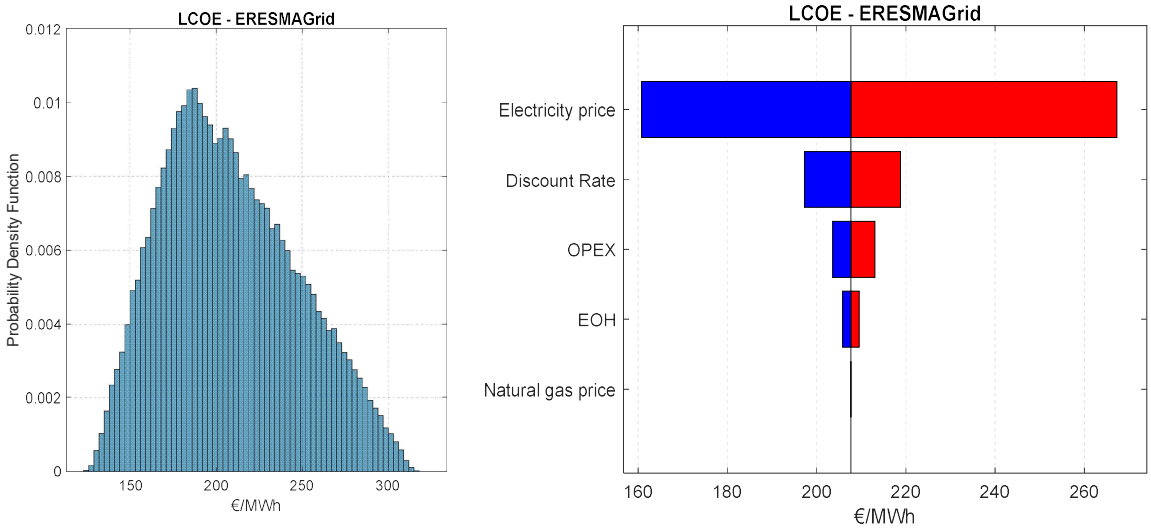

Figure 3.32. Probability density function (left) and tornado diagram (right) for the LCOE of the whole ERESMAGrid according to the MC analysis.

According to the tornado diagram for the microgrid (Figure 3.32 right), it is evident that the electricity price is the input parameter which affects *LCOE* the most, as the power grid supplies the majority of the load.

3.6 Summary and chapter conclusions

In the described case studies the main indicators (*LCOE*, *LCOH*, *LCOC*, *LCOS*, *LCOEx*) used to evaluate the cost of the energy and the associated profitability of investments in the energy sector have been evaluated by a Monte Carlo simulation approach. The *LCOEn* indicator is a robust metric to analyze not only single electrical generation technologies but also pure electric systems, such as microgrids, nanogrids and energy communities. In all these cases, it is useful to compare *LCOE* with the electricity purchase price to evaluate the possibility for the system to reach grid parity. Analogously, for pure thermal systems, such as boilers, solar collectors and heat pumps, the use of *LCOEx* should be preferred to *LCOH* and *LCOC* indicators since it takes into account real operating conditions, in terms of temperature at which thermal energy is supplied. Moreover, *LCOEx* is the only indicator which has to be adopted for the evaluation of multi-vector energy systems, such as reversible heat pumps, CHP and CCHP units, polygeneration microgrids, nanogrids and energy communities.

Finally, some specific considerations regarding the analyzed case studies are reported here below:

a) SPM, SEB and ERESMAGrid are test-bed facilities also designed for research and teaching purposes, and thus, not completely optimized to achieve the lowest *LCOE* and *LCOEx* values. It has been observed that for such microgrids and nanogrids, the *LCOEx* strongly depends on the electricity purchased from the external power grid as well as on the supplied fuels.
b) The obtained *LCOE* and *LCOEx* values have been obtained making some assumptions and not considering internalities and positive externalities associated to the operation of the facilities.

c) The generation and storage technologies integrated in the ERESMAGrid show high *LCOE* values and then, it is difficult for them to achieve grid parity individually. Their high *LCOE* values are mainly due to high *CAPEX* values associated with their small size, and low *EOH*. Conversely, the overall *LCOE* of the microgrid achieves lower values than those of the single technologies. This is due to the effect of the low purchase electricity price, which actually has the highest impact on the *LCOE* of the microgrid.

d) The results of the *LCOE* for PV plants in SPM, SEB and ERESMAGrid are in the range of typical values, however, the worst results have been observed for the PV Test plant of ERESMAGrid, as it is characterized by higher costs and lower performance. It must be noticed that for PV plants in ERESMAGrid the results have been obtained considering the effect of the storage system, which increases their *EOH* (as no surplus injection to the external power grid is allowed in this facility) but still includes some curtailments (i.e. even considering the *EOH* with the ESS, these *EOH* are not the maximum that could be achieved if the PV plant were connected directly to the power grid). On the other hand, the *LCOE* of the wind micro turbine is significantly higher than the average for this technology, due to the very low value and high volatility of its *EOH* caused by the unfavorable installation site conditions.

e) The *LCOS* of storage systems in SPM and ERESMAGrid presents typical values but way higher than the average purchase electricity price, making them not competitive yet. However, the results could change if internalities are considered, such as the provision of ancillary services, the increase of the resilience of the microgrid, etc.

f) For CHP and CCHP plants the typical indicators, namely *LCOE*, *LCOH* and *LCOC*, assume overestimated values. Consequently, it is better to use the *LCOEx* indicator for investment analyses related to projects dealing with these technologies.

3.7 References

1. Haldar A, Mahadevan S (2000) Probability, Reliability and Statistical Methods in Engineering Design. Wiley, New York, NY

2. Liu J, Liu H, Jiang C, et al (2018) A new measurement for structural uncertainty propagation based on pseudo-probability distribution. Applied Mathematical Modelling 63:744–760. https://doi.org/10.1016/j.apm.2018.07.017

3. Madsen HO, Krek S, Lind NC (1986) Methods of structural safety. Prentice-Hall, Englewood Cliffs, NJ

4. Solari G (1997) Wind-excited response of structures with uncertain parameters. Probabilistic Engineering Mechanics 12:75–87. https://doi.org/10.1016/S0266-8920(96)00027-6

5. Tubino F, Pagnini L, Piccardo G (2020) Uncertainty propagation in the serviceability assessment of footbridges. Structure and Infrastructure Engineering 16:123–137. https://doi.org/10.1080/15732479.2019.1618879

6. Gruppi di autoconsumatori e comunità di energia rinnovabile GSE (Italian technical rules for the renewable energy collective self-consumer and renewable energy community).https://www.gse.it/servizi-per-te/autoconsumo/gruppi-di-autoconsumatori-e-comunita-di-energia-rinnovabile/documenti. Accessed 20 Oct 2021

7. Warwick Wind Trials - Briefings and reports. https://warwickwindtrials.org.uk/2.html. Accessed 28 Nov 2021

8. Shaw S, Rosen A, Beavers D, Korn D (2008) Status Report on Small Wind Energy Projects Supported by the Massachusetts. Renewable Energy Trust, The Cadmous Group Inc.

9. Kc A, Whale J, Urmee T (2019) Urban wind conditions and small wind turbines in the built environment: A review. Renewable Energy 131:268–283. https://doi.org/10.1016/j.renene.2018.07.050

10. Orlando A, Pagnini L, Repetto MP (2021) Structural response and fatigue assessment of a small vertical axis wind turbine under stationary and non-stationary excitation. Renewable Energy 170:251–266. https://doi.org/10.1016/j.renene.2021.01.123

11. Pagnini L, Piccardo G, Repetto MP (2018) Full scale behavior of a small size vertical axis wind turbine. Renewable Energy 127:41–55. https://doi.org/10.1016/j.renene.2018.04.032

12. de la Puente-Gil Á, González-Martínez A, Borge-Diez D, et al (2019) True power consumption labeling and mapping of the health system of the Castilla y León region

in Spain by clustering techniques. Energy Procedia 157:1164–1181. https://doi.org/10.1016/j.egypro.2018.11.283

13. Nik VM, Sasic Kalagasidis A, Kjellström E (2012) Statistical methods for assessing and analysing the building performance in respect to the future climate. Building and Environment 53:107–118. https://doi.org/10.1016/j.buildenv.2012.01.015

14. Ma W, Fang S, Liu G, Zhou R (2017) Modeling of district load forecasting for distributed energy system. Applied Energy 204:181–205. https://doi.org/10.1016/j.apenergy.2017.07.009

15. Bracco S, Delfino F, Ferro G, et al (2018) Energy planning of sustainable districts: Towards the exploitation of small size intermittent renewables in urban areas. Applied Energy 228:2288–2297. https://doi.org/10.1016/j.apenergy.2018.07.074

16. Ortiz J, Guarino F, Salom J, et al (2014) Stochastic model for electrical loads in Mediterranean residential buildings: Validation and applications. Energy and Buildings 80:23–36. https://doi.org/10.1016/j.enbuild.2014.04.053

17. Tran TTD, Smith AD (2018) Incorporating performance-based global sensitivity and uncertainty analysis into LCOE calculations for emerging renewable energy technologies. Applied Energy 216:157–171. https://doi.org/10.1016/j.apenergy.2018.02.024

18. Sansavini G, Piccinelli R, Golea LR, Zio E (2014) A stochastic framework for uncertainty analysis in electric power transmission systems with wind generation. Renewable Energy 64:71–81. https://doi.org/10.1016/j.renene.2013.11.002

19. Weron R (2014) Electricity price forecasting: A review of the state-of-the-art with a look into the future. International Journal of Forecasting 30:1030–1081. https://doi.org/10.1016/j.ijforecast.2014.08.008

20. Muniain P, Ziel F (2020) Probabilistic forecasting in day-ahead electricity markets: Simulating peak and off-peak prices. International Journal of Forecasting 36:1193–1210. https://doi.org/10.1016/j.ijforecast.2019.11.006

21. de Simón-Martín M, Bracco S, Rosales-Asensio E, et al (2020) Electricity Spot Prices Forecasting for MIBEL by using Deep Learning: a comparison between NAR, NARX and LSTM networks. In: 2020 IEEE International Conference on Environment and Electrical Engineering and 2020 IEEE Industrial and Commercial Power Systems Europe (EEEIC / I CPS Europe). pp 1–6

22. Wang Y, Liu L, Wu C (2020) Forecasting commodity prices out-of-sample: Can technical indicators help? International Journal of Forecasting 36:666–683. https://doi.org/10.1016/j.ijforecast.2019.08.004

23. García-Gusano D, Espegren K, Lind A, Kirkengen M (2016) The role of the discount rates in energy systems optimisation models. Renewable and Sustainable Energy Reviews 59:56–72. https://doi.org/10.1016/j.rser.2015.12.359

24. Copiello S, Gabrielli L, Bonifaci P (2017) Evaluation of energy retrofit in buildings under conditions of uncertainty: The prominence of the discount rate. Energy 137:104–117. https://doi.org/10.1016/j.energy.2017.06.159

25. Lee C-Y, Ahn J (2020) Stochastic Modeling of the Levelized Cost of Electricity for Solar PV. Energies 13:3017. https://doi.org/10.3390/en13113017

26. Bracco S, Delfino F, Laiolo P, Morini A (2018) Planning & Open-Air Demonstrating Smart City Sustainable Districts. Sustainability 10:4636. https://doi.org/10.3390/su10124636

27. University of Genoa Savona Campus Webpage. In: Savona Campus Webpage. https://campus-savona.unige.it/en/. Accessed 15 Nov 2021

28. University of Genoa Energia 2020 project. In: Energia 2020 project. http://www.energia2020.unige.it/en/home/. Accessed 15 Nov 2021

29. Bracco S, Delfino F, Piazza G, de Simón-Martín M (2020) V2G technology to mitigate PV uncertainties. In: 2020 Fifteenth International Conference on Ecological Vehicles and Renewable Energies (EVER). pp 1–6

30. Bracco S, Delfino F, Foiadelli F, Longo M (2017) Smart microgrid monitoring: Evaluation of key performance indicators for a PV plant connected to a LV microgrid. In: 2017 IEEE PES Innovative Smart Grid Technologies Conference Europe (ISGT-Europe). pp 1–6

31. Bracco S, Delfino F, Trucco A, Zin S (2018) Electrical storage systems based on Sodium/Nickel chloride batteries: A mathematical model for the cell electrical parameter evaluation validated on a real smart microgrid application. Journal of Power Sources 399:372–382. https://doi.org/10.1016/j.jpowsour.2018.07.115

32. Delfino F, Procopio R, Rossi M, et al (2018) Microgrid Design and Operation. Toward Smart Energy in Cities, Primera Edición. Artech House, Norwood, MA

33. de Simón-Martín M, Bracco S, Rossi M, et al (2019) A flexible test-bed pilot facility for the analysis and simulation of Smart Microgrids. In: 2019 IEEE International Conference on Environment and Electrical Engineering and 2019 IEEE Industrial and Commercial Power Systems Europe (EEEIC / I CPS Europe). pp 1–6

34. de Simón-Martín M, Puente-Gil Á de la, Blanes-Peiró JJ, et al (2020) Smart Charging of Electric Vehicles to Minimize Renewable Power Curtailment in Polygeneration Prosumer Buildings. In: 2020 Fifteenth International Conference on Ecological Vehicles and Renewable Energies (EVER). pp 1–8

35. de Simón-Martín M, Diez-Suárez A-M, Álvarez-de Prado L, et al (2017) Development of a GIS Tool for High Precision PV Degradation Monitoring and Supervision: Feasibility Analysis in Large and Small PV Plants. Sustainability 9:965. https://doi.org/10.3390/su9060965

36. ERESMA Research Group ERESMA Webpage. In: ERESMA. https://eresma.unileon.es/. Accessed 12 Nov 2021

Levelized Cost of Energy in Sustainable Energy Communities

A systematic approach for multi-vector energy systems

CHAPTER 4 – Conclusions

Conclusions

4.1. Introduction

This final chapter summarizes the main conclusions, referred to the theoretical framework described in chapters 1 and 2, and to the results of the analyzed case studies reported in chapter 3. Finally, the most relevant future research lines in this field are depicted.

4.2. Conclusions on the theoretical framework

The “Energy Community” concept is being revisited by the latest regulations as an effective and sustainable way to integrate distributed renewable energy sources. In the European Union, it is proposed that energy communities must not be limited to isolated rural locations or islands, but extended to urban and industrial areas with the aim to achieve the target of 55% of CO_2 emissions reduction by 2030, set in the Clean Energy Package for all European Citizens. In this context, it has been defined and regulated both the “Renewable Energy Community” (REC) and the “Citizen Energy Community” (CEC) concepts. Both are based on the open and voluntary participation of natural persons, small and medium enterprises and local authorities with the primary purpose to provide environmental, economic and social benefits for their shareholders and the local areas where they operate.

Spain and Italy are part of the leading group in Europe for the regulation and deployment of energy communities, as their public authorities are conscious of their relevance to facilitate the integration of RES, and the reduction of fossil fuels. Although with some technical differences, both countries have properly defined energy communities and are promoting them in the latest times, specially RECs as a key agent for the ecological transition. The point is to eliminate one of the main barriers for its implementation, the regulation uncertainty, as the needed technologies are now mature enough to be economically competitive with traditional systems.

Technically speaking, both RECs and CECs are in some cases based on the implementation of microgrids (or, in some cases, nanogrids) characterized by the presence of energy prosumers and smart loads. Loads and generators can be of different energy nature (electrical, thermal or cooling) and both manageable or non-manageable. Moreover, they are coupled to either the electrical power grid or district thermal networks, interchange energy with them and participate to ancillary services and flexibility markets. This, added to the capability to operate in islanded mode, conducts to highlight the key role that plays the control strategy (i.e., the Energy Management System or EMS) and the associated infrastructure (smart meters, communication lines, datacenters, SCADAs, etc.). Multi-vector energy systems and, in particular, polygeneration microgrids constitute complex systems where electrical and thermal devices interact to provide energy to all the microgrid users minimizing the costs and maximizing the efficient exploitation of renewable sources. Finally, it must be highlighted their interaction with other services, such as transport (e.g., electric mobility) or clean water supply (e.g., drinking water systems).

Moreover, not only the technical feasibility of energy communities must be analyzed, but also their economic sustainability. Promoters look for the maximum profitability and an energy community is not only seen by them as a technical solution for a sustainable provision of energy to its users, but also like an economic asset which provides benefits, or at least savings. Public authorities must take this fact into account in order to properly design incentive policies to promote the deployment of energy communities.

Among the many economic metrics to analyze the feasibility of an energy project, the *LCOEn* (and its variants: *LCOE*, *LCOH*, *LCOC*, *LCOS* and *LCOEx*) results to be adequate as it considers the full life-cycle costs (fixed and variable) per unit of the supplied energy, considering the discount effect in time, and thus, allowing the comparison among different energy options independently of size, costs structure and useful life. It is a widely known indicator, specially for comparing generation technologies and for the evaluation of their grid parity. In this case, the definition of this metric has been extended, in a systematic approach to the case of polygeneration and multi-vector energy systems.

The *LCOEn* includes the total annual discounted costs (including capital expenditures, operation and maintenance, fuel costs, internalities and externalities) and discounted revenues or possible yearly benefits, incomes or avoided costs that may reduce the costs.

The *LCOEn* of multi-vector energy systems (hybrid generation plus storage systems, polygeneration systems, microgrids, nanogrids, etc.) can be expressed as a linear combination of the *LCOEn* of the constituent elements multiplied by a participation factor. However, each individual *LCOEn* must be normalized to take into account the possible different useful lifespans of each device. In the case a device must be replaced because its lifespan is lower than the time horizon considered for the whole investment, both the replacement costs (which may include the decommissioning costs of the asset and the reduced capital value of the new one) and the residual value of the asset, due to its remaining lifespan at the end of the expected life of the whole project, have to be properly assumed.

Furthermore, it must be noted the effect of storage systems as they increase costs but also allow to increase the EOH of the generators, i.e., to reduce the curtailed energy from renewable power plants. For this reason, it is useful to evaluate not only *LCOE* for the single technology, but *LCOE* for the whole system composed of the energy storage coupled with the renewable power plant.

Finally, the *LCOEx* indicator is the only one which must be used to evaluate the investments dealing with thermal energy vector or multi-vector energy systems. In the first case, *LCOEx* takes into account the real operating conditions of generation technologies by considering “the value” of the produced thermal energy in terms of supply temperature. For CHP and CCHP plants, *LCOEx* allows to properly evaluate the combined effects of multi-vector energy outcomes (electrical and thermal/cooling energy) while the use of *LCOE*, *LCOH* and *LCOC* would lead to overestimates. Furthermore, *LCOEx* is also the only indicator which can really provide a correct evaluation of a Polygeneration system such as microgrid or an energy community.

4.3. Conclusions on the results of the case studies

The application of the proposed methodology to three real case studies has drawn interesting conclusions. It must be reminded that the proposed indicators have been calculated by taking some conservative assumptions, not considering internalities and externalities, due to the difficulty to quantify them homogenously.

The Smart Polygeneration Microgrid and the Smart Energy Building at the Savona Campus (Italy), represent the cases of a microgrid and a nanogrid which actually satisfy the energy needs of a real community. However, both systems are also test-bed facilities focused on research and teaching purposes, and thus, they are not completely optimized to minimize the *LCOE* or *LCOEx* values. It has been observed that for such systems, the *LCOEx* strongly depends on the electricity and the fuel (natural gas) consumed and their purchase prices. The results of the *LCOE* for the PV plants in SPM and SEB and the *LCOS* of the ESS are in the range of typical values, although the latter is significantly higher than the average purchase electricity price, making the storage system non-competitive. Unfortunately, parameters on which the *LCOE* estimate depends are affected by errors in prediction and inherent randomness. Regarding PV plants, *LCOE* is strongly affected by the discount rate as well as by the EOH, which, in turn, is especially related to the availability of the resource. On the other hand, the most sensible parameter for the ESS is the *EOH* which has a complex relationship with the *LCOE* of generation plants as it affects both to the energy supplied by the device and its useful lifespan (the more energy discharged from the battery, the lowest the lifespan). For the CHP and CCHP plants of the SPM, both the *LCOE*, *LCOH* and *LCOC* assume overestimated values as these indicators cannot consider properly the coupled effects of the combined operation. Then, the *LCOEx* reflects better the overall performance of the aforesaid technologies and can be compared with the one of other plants or alternatives. Both the CHP, CCHP and boilers in the SPM are affected by the purchase price of the natural gas, as expected, closely followed by their *EOH*. However, in the case

of the heat pumps, the *EOH* has a major impact in the distribution of the *LCOEx* than the electricity price.

The analysis of SEB indicators has highlighted trends very similar to the ones observed for SPM. Nevertheless, it results remarkable that for the solar collectors, the *EOH* has a major impact on the *LCOEx* than the discount rate, in contrast to what observed for the solar PV plants. On the other hand, almost no differences in the propagation coefficients of the input parameters have been observed comparing the air heat pumps of the SPM and the geothermal heat pump of the SEB. Furthermore, similar results have been obtained for the *LCOEx* of the geothermal heat pump and the domestic hot water heat pump of the building.

The third case study is focused in the ERESMAGrid, a pure electrical microgrid located in the University Campus of Vegazana of the University of León, in Spain. It has two power plants, a micro wind turbine and a $LiFePO_4$ battery bank, which reduce the power demand of the School of Mining Engineering, although this still largely depends on the electricity purchased from the external power grid. The results for this system show a high dependency on the electricity price that, at the moment, contributes to reduce its overall *LCOE* (as the *LCOE* of the individual generation and storage technologies is much higher). As all the generators are based on RES, the scattering of the results is highly influenced by the operation parameters, i.e., the *EOH* and the *OPEX*, and the uncertainty of the discount rate also plays a significant role for each integrated generation and storage technology. In all cases, except for the *EOH*, the coefficient of propagation of the variables is significantly lower than 1, which means that the high uncertainty of the input parameters is mitigated in the *LCOE* results. Consequently, the operation team of the microgrid must take specific care when operating each generation and storage unit, also monitoring electricity purchase price variation, with the aim of minimizing the *LCOE* of the overall microgrid.

4.4. Future research lines

The deployment of the energy community concept defined by EU for urban and industrial areas is still at its first stages. Some issues have still to be solved from the

technical and regulatory point of view, such as the definition of the proximity constraint for RECs and the complete implementation of the CEC framework. Moreover, in the near future it will be interesting to further investigate the correlation between microgrids and energy communities, according to the evolution of the EU scenario and also more in general terms. Several efforts are being made by the Academia and the Industry in this direction and positive results will be seen soon.

The *LCOEn*, and more specifically, the *LCOEx*, should be extended as a reference indicator of the sustainability and competitiveness of the multi-vector energy systems in general, and of the energy communities in particular. The authors would like to develop systematic investigations of case studies located in different parts of the world to create an open-source database on the results and input parameters. Furthermore, they would like to make an *LCOEn* and *LCOEx* software tool available to researchers, industrial partners and promoters for the evaluation of investments in the energy community sector.

Levelized Cost of Energy in Sustainable Energy Communities

A systematic approach for multi-vector energy systems

Abbreviations

Abbreviation	Definition
µWTG	Micro Wind Turbine Generator
AC	Alternate Current
AM	Air Mass
ARERA	Italian Regulatory Authority for Energy, Networks and Environment
ASM	Ancillary Service Market
BMS	Building Management System
BoS	Balance of System
CAPEX	Capital expenditures
CCHP	Combined Cooling, Heat and Power
cdf	Cumulative density function
CEC	Citizen Energy Community
CHP	Combined Heat and Power
COEn	Cost of Energy
CSP	Concentrating Solar Power
DC	Direct Current
DHW	Domestic Hot Water
DNI	Direct Normal Irradiance
DOE	U.S. Department of Energy
DPP	Discounted Payback Period
DSO	Distribution System Operator
EC	Energy Community
EEA	European Environment Agency
EMD	Energy Market Directive
EMS	Energy Management System
EnSS	Energy Storage System
EOH	Equivalent Operating Hours
ERESMA	Energy Resources Smart Management (Research Group)
ESS	Electricity Storage System
EU	European Union
EV	Electrical Vehicle

FiT	Feed-in-Tariff
FMA	Financial Model Approach
GHG	Greenhouse gas emissions
GSE	Gestore dei Servizi Energetici (Italian national energy service manager)
HAWT	Horizontal Axis Wind Turbine
HSS	Heat Storage System
HV	High Voltage
ICT	Internet and Communication Technologies
IDAE	Instituto para la Diversificación y Ahorro de Energía (Spanish energy authority)
IEC	International Electrotechnical Commission
IoT	Internet of Things
IOU	Investor-owned utility
IRR	Internal Rate of Return
LCOC	Levelized Cost of Cooling
LCOE	Levelized Cost of Electricity
LCOEn	Levelized Cost of Energy
LCOEx	Levelized Cost of Exergy
LCOH	Levelized Cost of Heat
LCOS	Levelized Cost of Storage
LROE	Levelized Revenue of Electricity
LV	Low Voltage
MACRS	Modified Accelerated Cost Recovery System
MC	Monte Carlo simulation method
MILP	Mixed Integer Linear Programming
MPC	Model Predictive Control
MPPT	Maximum Power Point Tracking
MV	Medium Voltage
NPV	Net Present Value
O&M	Operation and Maintenance
OPEX	Operation Expenditures
PCC	Point of Common Coupling
pdf	Probability density function
POU	Publicly owned utility
PPA	Power Purchase Agreement
PV	Solar photovoltaics
PVPC	Precio Voluntario para el Pequeño Consumidor (Spanish regulated electricity tariff)
R&D	Research and Development
REC	Renewable Energy Community
RED	Renewable Energy Directive
RES	Renewable Energy Source
SCADA	Supervisory Control and Data Acquisition
SEB	Smart Energy Building

sLCOEn	Simplified Levelized Cost of Energy
SME	Small and Medium Enterprise
SoC	State of Charge
SPM	Smart Polygeneration Microgrid
SPP	Simple Payback Period
STC	Standard Test Conditions
TSE	Taylor Series Expansion method
U.S.	United States
V2B	Vehicle to Building
V2G	Vehicle to grid
V2H	Vehicle to Home
VAWT	Vertical Axis Wind Turbine
VHV	Very High Voltage
WACC	Weighted Average Cost of Capital
WAP	Weighted Average energy wholesale price
WTG	Wind Turbine Generator
ZEB	Zero Energy Building

Levelized Cost of Energy in Sustainable Energy Communities

A systematic approach for multi-vector energy systems

Nomenclature

Symbol	Definition	Units
μ	Mean value of normal distribution	-
C	Cooling energy	kWh
c	Propagation coefficient	-
CF	Capacity Factor	-
CRF	Capital Recovery Factor	-
d	Discount rate	%
d_{nom}	Nominal discount rate	%
D_{PV}	Present value of depreciation	%
d_{real}	Real discount rate	%
E	Electricity	kWh
E(x)	Mean value function	
E^{CH}	Energy charged in the ESS	kWh
E^{DCH}	Energy discharged from the ESS	kWh
En	Energy	kWh
EOH	Equivalent Operating Hours	h
Ex	Exergy	kWh
f	Participation factor	-
f'	Normalized participation factor	-
f''	Normalized participation factor referred to the energy supplied to the microgrid	-
H	Heat	kWh
H^{CH}	Energy charged in the HSS	kWh
H^{DCH}	Energy discharged from the HSS	kWh
J	Total number of generation units	units
K	Total number of energy storage units	units
k	Inflation rate	%
M	Total number of exergy sources of a generator	-
n	Project lifespan	Years
NC	Net cost: costs - revenues	Currency units

n_{ESS}	Lifespan of the ESS	Years
n_G	Lifespan of the generator	Years
p	Energy wholesale price	currency/kWh or currency/MWh
P	Rated power	kW
RV	Residual value	Currency units
t	Time	Several
T	Tax rate	%
T_a	Ambient temperature	K
T_C	Cold source temperature	K
T_H	Hot source temperature	K
T_s	Temperature of the supplied thermal energy	K
WAP	Weighted Average energy wholesale price	currency/kWh or currency/MWh
α^{co}	Separated cost coefficient for cooling energy	-
α^{E}	Separated cost coefficient for electricity	-
α^{th}	Separated cost coefficient for heat	-
β	Reduction costs factor	%
δ	Coefficient of variation	-
σ	Standard deviation	-
γ^{co}	Penalty factor for cooling energy	-
γ^{th}	Penalty factor for heat	-